TiO_2 Nanomaterials: Human Exposure and Environmental Release

by

Alex Alan Weir

A Thesis Presented in Partial Fulfillment
of the Requirements for the Degree
Master of Science

Approved July 2011 by the
Graduate Supervisory Committee

Paul Westerhoff, Chair
Kiril Hristovski
Pierre Herckes

ARIZONA STATE UNIVERSITY

August 2011

ABSTRACT

Titanium dioxide (TiO_2) nanomaterial use is becoming more prevalent as is the likelihood of human exposure and environmental release. The goal of this thesis is to develop analytical techniques to quantify the level of TiO_2 in complex matrices to support environmental, health, and safety research of TiO_2 nanomaterials.

A pharmacokinetic model showed that the inhalation of TiO_2 nanomaterials caused the highest amount to be absorbed and distributed throughout the body. Smaller nanomaterials (< 5nm) accumulated in the kidneys before clearance. Nanoparticles of 25 nm diameter accumulated in the liver and spleen and were cleared from the body slower than smaller nanomaterials.

A digestion method using nitric acid, hydrofluoric acid, and hydrogen peroxide was found to digest organic materials and TiO_2 with a recovery of >80%. The samples were measured by inductively coupled plasma-mass spectrometry (ICP-MS) and the method detection limit was 600 ng of Ti.

An intratracheal instillation study of TiO_2 nanomaterials in rats found anatase TiO_2 nanoparticles in the caudal lung lobe of rats 1 day post instillation at a concentration of 1.2 µg/mg dry tissue, the highest deposition rate of any TiO_2 nanomaterial. For all TiO_2 nanomaterial

morphologies the concentrations in the caudal lobes were significantly higher than those in the cranial lobes.

In a study of TiO_2 concentration in food products, white colored foods or foods with a hard outer shell had higher concentrations of TiO_2. Hostess Powdered Donettes were found to have the highest Ti mass per serving with 200 mg Ti. As much as 3.8% of the total TiO_2 mass was able to pass through a 0.45 µm indicating that some of the TiO_2 is likely nanosized.

In a study of TiO_2 concentrations in personal care products and paints, the concentration of TiO_2 was as high as 117 µg/mg in Benjamin Moore white paint and 70 µg/mg in a Neutrogena sunscreen. Greater than 6% of Ti in one sunscreen was able to pass through a 0.45 µm filter. The nanosized TiO_2 in food products and personal care products may release as much as 16 mg of nanosized TiO_2 per individual per day to wastewater.

DEDICATION

This work is dedicated to my Mom and Dad who gave me the two most important things in this world: roots and wings. My parents encouraged me to be successful from an early age and supported me in all my endeavors.

ACKNOWLEDGEMENTS

This thesis could not have been completed without the help and support of many colleagues. First, I want to thank Paul Westerhoff for being my advisor during the completion of my Master's program, for giving me guidance, and for always being full of new ideas. I want to thank my committee members Kiril Hristovski and Pierre Herckes who helped me become comfortable and confident in my lab work and were always available to discuss ideas and new techniques.

I want to thank David Ladner for helping me understand the dynamics of a research lab. I want to thank Marisa Masles and Gwyneth Gordon for their support with the Arizona State University analytical instruments. I want to thank Kent Pinkerton and Rona Silva for UC-Davis for providing an opportunity for a great collaboration. Finally, I want to thank the National Institute of Health who funded the Nano Go collaboration, making this all possible.

TABLE OF CONTENTS

CHAPTER Page

CHAPTER Page

CHAPTER Page

LIST OF TABLES

LIST OF FIGURES

ACRONYMS

ADME	Absorption, Distribution, Metabolism, and Excretion
BSA	Bovine Serum Albumin
CFR	Code of Federal Regulations
CPS	Counts Per Second
EPA	Environmental Protection Agency
FDA	Food and Drug Administration
FFF	Field Flow Fractionation
GALT	Gastrointestinal Associated Lymphatic Tissue
GI	Gastrointestinal
HEPA	High Efficiency Particulate Air
ICP-OES	Inductively Coupled Plasma Optical Emission Spectrometry
ICP-MS	Inductively Coupled Plasma Mass Spectrometry
IDL	Instrument Detection Limit
LD_{50}	Lethal Dose-50% of Organisms
MDL	Method Detection Limit
NIOSH	National Institute of Occupational Safety and Health
NOM	Natural Organic Matter
PALS	Phase Analysis Light Scattering
PCP	Personal Care Product
PEL	Permissible Exposure Limit

PPE	Personal Protective Equipment
PSP	Poorly Soluble Particle
REL	Recommended Exposure Limit
ROS	Reactive Oxygen Species
SEM	Scanning Electron Microscopy
SPE	Solid Phase Extraction
SPF	Sun Protection Factor
TEM	Transmission Electron Microscopy
TiO_2	Titanium Dioxide
UV	Ultraviolet
WWTP	Wastewater Treatment Plant

CHAPTER 1: INTRODUCTION

1.1 NANOTECHNOLOGY BACKGROUND INFORMATION

A nanomaterial is generally defined to have at least one dimension that measures less than 100 nm. Nanomaterials often have novel physicochemical properties different than their bulk material counterparts due to their small nature and large surface area to volume ratio. Nanotechnology has developed in the last two decades as a discipline concerned with deriving advantages from the special properties of nanomaterials. [1] Nanotechnology was a $10 billion industry in 2010 and forecasters predict that the industry will grow to $1 trillion by 2015. [2] Nanomaterials can be naturally occurring or manmade and can be carbon based or created from metals and metal oxides like titanium dioxide (TiO_2).

The opportunities that nanotechnologies create span a wide range of disciplines. Nanomaterials have been touted as a means to create molecular machines, provide clean water to those without access, and revolutionize the health care industry. [3-6] Though the applications of nanotechnology seem limitless, many experts warn that a more thorough investigation needs to be conducted into the health and environmental risks associated with nanomaterials. As David Warheit, chairman of the task force on “Health and Environmental Safety of Nanomaterials” for the European Centre for Ecotoxicology and Toxicology of Chemicals put it,

“The number of implication studies has not caught up with the number of application studies.” [7] The need for more implication studies continues to grow as the uses of nanomaterials continue to grow. This is especially true for one of the most commonly use nanomaterials, TiO_2.

1.2 TITANIUM DIOXIDE NANOMATERIALS

As a bulk material, TiO_2 is primarily used as a pigment because of its brightness, high refractive index, and resistance to discoloration. Nearly 70% of all TiO_2 produced is uses as a pigment in paints, but it is also used as a pigment in glazes, enamels, plastics, paper, fibers, foods, pharmaceuticals, cosmetics, and toothpastes. [8] However, recently more attention is being given to the applications of TiO_2 as a nanomaterial. In 2005 the global production of nanoscale TiO_2 was estimated to be 2000 metric tons worth $70 million. [9] By 2010 the production had increased to 5000 metric tons and is expected to continue to increase till 2025. [10]

Production of TiO_2 materials produces a range of primary particles sizes. Most applications of TiO_2 would benefit more from smaller primary particle sizes, and the percentage of TiO_2 that is produced to be closer to the nanosized range is expected to increase exponentially. [11] This shift in production to materials with a smaller primary particle size is the increase of TiO_2 “nanomaterial” production. TiO_2 nanomaterial is an ill-defined term that is often interchanged with TiO_2 nanoparticle. TiO_2 nanoparticles are generally synthesized to have a crystalline structure.

When TiO_2 nanoparticles are created they can be amorphous or from into some mix of three different crystal structures: anatase, rutile, and brookite. Each of these crystal structures has its own unique properties. [12] The most common procedure for synthesizing TiO_2 nanoparticles utilizes the hydrolysis of titanium (Ti) salts in an acidic solution. [13] The structure, size, and shape of the TiO_2 nanoparticles can be controlled by using chemical vapor condensation or nucleation from sol gel. [14, 15] TiO_2 can also be formed into nanowires or nanotubes. [16, 17] Thus, nanomaterial is an umbrella term that actually encompasses nanoparticles, nanowires, nanotubes, or other morphology all with different sizes, shapes, and structures.

1.3 APPLICATIONS OF TITANIUM DIOXIDE NANOMATERIALS

1.3.1 UV protection and opacity. One unique property of TiO_2 nanomaterials is an increased ability to disperse light which makes them an ideal ingredient in sunscreens and cosmetics to protect the skin against harmful ultraviolet (UV) rays. [9, 18, 19] A large portion of the nanosized TiO_2 produced ends up as personal care products like sunscreen and cosmetic creams. As stated before, bulk TiO_2 is often used as a bright white pigment. However, TiO_2 nanomaterials tend to be good opacifiers and are used in paints and coatings.[20, 21]

1.3.2 Water treatment and remediation. The photocatalytic properties of TiO_2 nanomaterials are often used in water treatment

applications. The high surface area per unit mass creates a larger catalytic surface for the production of hydroxyl radicals that are strong oxidizing agents. [22] When UV light is used to activate the nanoparticles, efficient removal of aromatic organic compounds can be achieved. They also provide an absorptive surface for the removal of heavy metals. Other advantages of using TiO_2 for water treatment applications are its low cost, resistance to corrosion, and overall stability. [3, 4]

TiO_2 nanoparticles have been used as a solid phase extraction (SPE) packing material for the remediation of surface waters. Using TiO_2 nanoparticles as a packing material can effectively preconcentrate and extract heavy metals from river water and seawater. [23] This has been effectively accomplished in batch and column experiments at the natural pH of coastal waters. [24]

1.3.3 Antimicrobial applications. Pure TiO_2 nanoparticles or TiO_2 nanoparticles doped with other materials such as iron or silver exhibit antimicrobial properties. The nanoparticle composites have been shown to be effective at disinfecting airborne bacteria for hospitals and have been incorporated into textiles for antimicrobial clothing. [25, 26] The photocatalytic antimicrobial activity of TiO_2 nanoparticle composites have led them to be used in coatings to create self-cleaning surfaces. [27, 28] These coatings have found applications in self-cleaning windows and anti-fogging glass. [8]

1.3.4 Health care applications. TiO_2 nanomaterials are being evaluated for many different uses in the health care industry. A platinum TiO_2 nanocomposite has been shown to be effective in the treatment of cancer cells. [29] TiO_2 nanotubes applied to bandages have been shown to enhance blood clotting rates by forming a sort of scaffold for blood clots to form against. [30] TiO_2 nanoparticles have been generated *in situ* in polyurethane membranes to be used as bandages that not only enhance clotting, but keep bacteria out while allowing gas permeability and water vapor transmission. [31]

1.3.5 Other novel applications. TiO_2 nanomaterials continue to be studied so that they can be utilized in new and exciting ways. TiO_2 nanomaterials are being evaluated for their capacity for energy storage and conversion. [1] TiO_2 nanomaterials may also prove to be a low cost environmentally friendly means to split water for hydrogen production in the future. [32] The potential applications for TiO_2 nanomaterials are numerous and cover a wide variety of disciplines.

1.4 TITANIUM DIOXIDE NANOMATERIAL RISK

As a bulk material, TiO_2 is inert and insoluble which results in a relatively high median lethal dose (LD_{50}) for rats of 12,000 mg/kg body weight by oral administration. [33] However, TiO_2 nanomaterials interact with tissues differently than the bulk material making them more toxic. A nanomaterial risk framework must be established to judge the

environmental, health, safety risk of any engineering nanomaterial. [34] The risk depends on both the hazard potential and external exposure likelihood. [10]

1.4.1 Risk to human health. Chronic effects have been observed from TiO_2 nanoparticle exposure. Workers in the TiO_2 nanoparticle production industry in six European countries were more likely to develop lung cancer compared to the general population. [35] Though this trend was not confirmed in the United States or Canada, there was enough concern for the National Institute for Occupational Health and Safety (NIOSH) to propose a draft permissible exposure level (PEL) of 1.5 mg/m^3 and a recommended exposure level (REL) of 0.1 mg/m^3. The PEL for TIO_2 nanoparticles is 15 times lower than the PEL for TiO_2 microparticles. [9]

Many exposure and toxicity tests are conducted on rodents rather than human subjects. Two separate studies found that a TiO_2 nanoparticle dose of 5 g/kg body weight did not cause obvious acute toxicity in rats. However, there were acute effects on individual tissues in the rats. [33, 36] The instillation or inhalation of large doses of TiO_2 nanoparticles have been shown to strongly affect lung function. [37] Other localized toxic effects are detailed in Table 1.1.

Table 1.1

Toxic Effects of TiO_2 Nanoparticles on Rat Tissues

Target Organ	Effect
Blood Brain Barrier	Cationic TiO_2 nanoparticles can have an immediate toxic effect at the blood brain barrier [38]
Brain Microglia	P25 TiO_2 can cause sustained production of reactive oxygen species [39]
Central Nervous System	TiO_2 nanoparticles can cause increased segmented neutrophils and lymphocytes, protein carbonyl levels, and interstitial fibrosis [40]
DNA	TiO_2 nanoparticles are able to penetrate the nucleus membrane and interact with the DNA of cells [40]
Intestinal Cells	TiO_2 nanoparticles can cause a rise in intracellular free-calcium [41]
Kidney	TiO_2 nanoparticles caused increased levels of uric acid, blood urea nitrogen, and creatine [40]
Kidney	TiO_2 nanoparticles can cause swelling of the renal glomerulus [33]
Liver	80 nm TiO_2 nanoparticles cause hepatic lesions of the liver [33]
Lung	Inflammatory response when TiO_2 nanoparticles are not recognized by microphages [22]
Lung	TiO_2 nanoparticles cause a decreased pulmonary diffusion capacity for carbon monoxide [42]
Lung	Chronic TiO_2 nanoparticle aerosol exposure leads to an increased risk of lung cancer [43]
Septic Brain	TiO_2 nanoparticles enhance the inflammatory response [44]
U937 Cells	TiO_2 nanoparticles resulting from the degradation of Ti implants induced cell death by apoptotic and necrotic modifications [45]
Overall	Animal studies have given sufficient evidence that TiO_2 nanoparticles are a Group 2B carcinogen [35]

1.4.2 Ecotoxicology. The risks to human health come from both intentional and unintentional exposure to TiO_2 nanomaterials. Many studies have been conducted on intentional exposure such as sunscreen application and unintentional exposure such as inhalation of nanoparticles

in an improperly controlled production facility. Less is known about how nanomaterials behave once they are released to the environment. TiO_2 nanomaterials in consumer products like sunscreen are washed off and end up in wastewater. It has been shown that wastewater treatment plants (WWTPs) are capable of removing the majority of TiO_2 nanomaterials from influent sewage. [46] However, TiO_2 particles measuring between 4 and 30 nm were still found in the treated effluent. [47] These nanomaterials are then released to the surface waters where they can interact with living organisms. One study monitoring TiO_2 nanomaterials found the highest concentrations in river water to be directly downstream of a WWTP. [48] TiO_2 nanomaterials that are absorbed in the treatment plants may still end up in the environment if the biomass is land applied and it later leaches out of the soil. Though the release of TiO_2 nanomaterials to the environment has been shown, it is difficult to quantify how much is released. Since it is impossible to measure every single source of TiO_2 nanomaterials, amounts are often modeled to better predict how TiO_2 nanomaterials may affect the environment. [49]

Once in the environment, even less is known about how organisms are affected by TiO_2 nanomaterials. Phytotoxicity studies have shown that TiO_2 nanoparticles inhibited growth of some plants by reducing the hydraulic conductivity while others have shown that the particles may improve growth by enhancing photosynthesis in leaves and nitrogen fixing in roots. [50] It has been shown that fish absorb TiO_2 nanoparticles

through their gills. Once into the bloodstream, TiO2 nanoparticles can translocate to various organs in the body. [51] Concentrations as low as 16 mg/L of nanosized TiO_2 have been shown to inhibit the growth of algae in natural waters. [52] TiO_2 has been shown to bioaccumulate, with higher concentrations in *Daphnia magna* at 21 days than at 3 days. [53] However, several studies have agreed that TiO_2 tends to be a less hazardous to organisms than other nanomaterials such as multi-wall carbon nanotubes, nano cerium oxide, and nano zinc oxide. [6, 10]

The goal of toxicology and ecotoxicology studies is to attempt to identify characteristics of the nanomaterials that make them particularly toxic. It had been generally accepted that primary particle size was a large factor in assessing toxicity, with smaller particles tending to be more toxic. However, recent studies have shown that particle size is only a single (and perhaps minor) factor influencing the toxicity of nanoparticles. [34] The reason it is still so difficult to assess the risk of certain nanomaterials is that nanotoxicology studies rarely have enough reliable information on the physicochemical characteristics of the nanoparticles tested. Thus, it is impossible to determine a discernable correlation between any single parameter and toxic effect. [52] The results of many past nanotoxicology studies have been deemed unreliable because they did not adequately characterize the studied nanomaterials. [37] The number of applications for TiO_2 nanomaterials continues to grow while health and environmental studies attempt to catch up.

1.5 MOTIVATION FOR RESEARCH

Human exposure to TiO_2 nanomaterials is only going to increase as the number of applications utilizing TiO_2 grows and usage increases. Similarly more nanosized TiO_2 will ultimately be released to the environment. Large knowledge gaps exist regarding the fate of TiO_2 nanomaterials once they have been used for their designed purpose or after unintentional releases. The goal of this thesis is to develop analytical techniques to quantify the level of TiO_2 in complex matrices to support research of the environmental, health, and safety ramification of TiO_2 nanomaterials.

1.6 THESIS ORGANIZATION AND OBJECTIVES

This thesis is divided into a number of closely related projects all pertaining to TiO_2 nanomaterials. Each project is presented here as a separate chapter (Chapters 2-7) seeking to complete a specific objective, and a chapter synthesizing the findings from all of the projects and providing conclusions, recommendations, and future research goals (Chapter 8).

1.6.1 Objective 1: Create a model for the behavior of TiO_2 nanomaterials absorbed into the body. One way to better understand the fate of TiO_2 nanomaterials in the human body is to develop an absorption, distribution, metabolism, and excretion (ADME) model. ADME models are often used to better understand the effects of pharmaceuticals

on the human body. The data that are used as inputs to these models typically come from rodent studies. The rodent studies can be used to simulate effects of exposure to humans. These studies will be combined in an attempt to create a complete model from the absorption of TiO_2 nanomaterials till their excretion from the body. Then a hypothetical exposure dosage of TiO_2 nanomaterials will be added as an input to determine distribution though the body and likely concentrations in organs.

1.6.2 Objective 2: Develop a digestion method to quantify the total amount of TiO_2 in organic matrices. In order to verify TiO_2 concentrations in tissues after exposure studies or to find out how much TiO_2 is contained in consumer products that may release to the environment, a digestion method must be developed that can quantify TiO_2 in various types of samples. The method must be able to detect trace quantities of TiO_2 and be capable of efficiently digesting large amounts of TiO_2, all in a timely manner so that large quantities of samples can be analyzed. The method should also be able to digest any organic material that may cause interferences during analysis.

1.6.3 Objective 3: Measure the total TiO_2 content in rat lungs instilled with various TiO_2 nanomaterials. Different types of TiO_2 nanomaterials can deposit in the lung and be cleared to different degrees. In a collaboration study with the University of California at Davis, rats exposed to TiO_2 nanomaterials by means of intratracheal instillation were analyzed for effects. The animals were exposed to two crystal structures

of TiO_2 nanoparticles and TiO_2 nanobelts. Then the animals were sacrificed so that the TiO_2 could be quantified to measure the TiO_2 concentration per lung mass. The TiO_2 concentration provided information about which types of nanomaterials deposit into the lung with a greater efficiency and how long it takes for the nanomaterials to clear from the lung.

1.6.4 Objective 4: Measure the total TiO_2 in food products and separate the nanosized fraction for further analysis. While many products list TiO_2 as an ingredient, it is possible that it may be contained in other products and remains unlisted. It was the objective of the project to obtain a number of different food products and determine the total TiO_2 content. Then, to determine the percentage of the total TiO_2 content that was in the nanoscale size range by filtration. This was done to know how much nanosized TiO_2 would have been ingested by a person consuming such food products. TiO_2 eventually ends up in wastewater, and the data provided a better understanding of how much nanosized TiO_2 is released into the environment.

1.6.5 Objective 5: Measure the total TiO_2 in personal care products and separate the nanosized fraction for further analysis. Like food products, it is possible that TiO_2 may be contained in personal careproducts and remain unlisted. The objective of the project was to obtain a number of different personal care products and determine the total TiO_2 content. Then, to determine the percentage of the total TiO_2

content that was in the nanoscale size range by filtration. This was done to know how much nanosized TiO_2 a person would have been exposed to. TiO_2 eventually ends up in wastewater, and the data provided a better understanding of how much nanosized TiO_2 may be released into the environment.

1.6.6 Objective 6: Measure the total TiO_2 in paint products.

TiO_2 is likely to be found within paints, but how much may vary by brand and type. The objective of this project was to obtain a number of different paint products and determine the total TiO_2 content. This was done to know how much total TiO_2 exists within pain to predict how much might be nanosized. Eventually the paint weathers and TiO_2 is released to the environment. Combining these six objectives gave a better idea of how much TiO_2 a person may be exposed to and how much would be released to wastewater and the environment.

CHAPTER 2: PHARMACOKINETIC MODELING OF TITANIUM DIOXIDE NANOMATERIALS

2.1 PROBLEM STATEMENT

Many nanomaterials—TiO_2 included—may potentially be hazardous, but the direct risk to human health depends on the probability of exposure occurring. [1] To better gauge the risk to human health, a quantitative risk assessment should be completed. A quantitative risk assessment is defined as "the estimation of the severity and likelihood of adverse responses associated with exposure to a hazardous agent" and should include a hazard identification, exposure assessment, dose-response assessment, and risk characterization. [43] One way to complete an exposure assessment and dose-response assessment is to use a physiologically based pharmacokinetic model. These types of models have been used to study the absorption, distribution, metabolism, and excretion (ADME) of pharmaceuticals, but can be applied to nanomaterial kinetics in the body with certain modifications to account for differences between nanomaterials and pharmaceuticals. [54] It is the objective of this project to develop a pharmacokinetic ADME model for TiO_2 nanomaterials that can predict tissue concentrations based on an exposure level.

2.2 INTRODUCTION

2.2.1 Exposure. An exposure assessment is a critical first step in modeling nanomaterial kinetics and characterizing risks to human health. Nanomaterial exposure may be intentional or unintentional. Intentional exposure to nanomaterials may result from medical applications such as drug delivery or imaging. Unintentional exposures may come from nanomaterials in food, cosmetics, or air and water pollution. [54] While pollution, personal care products, and nanomaterials in foodstuffs pose some exposure risk to the general population, the population groups most susceptible to nanomaterial exposure are those people who work with nanomaterials regularly for their careers. One of these key populations is the researchers who study nanomaterials at private labs, universities, and in the research and development divisions of private enterprises. [55] A study in a research lab found that the airborne concentrations peaked to a concentration of $3x10^3$ TiO_2 particles/cm^3 within a minute of nanoparticle production or use and remained at nearly the same level for 30 minutes. [56]

Another at-risk population is the people who work in the engineered nanomaterial production industry. These workers have a significant risk of a cytotoxicity response especially to particles in the size range of 10-30 nm. [57] The most at-risk workers are those who perform nanomaterial handling duties such as bagging, reactor cleaning, bag dumping, pouring, and transferring as these duties produce the most dust in the nanosize

range. [58] The ventilation schemes near these processes affect the nanomaterial concentrations. [55] Concentrations were often measured as high as $5.0x10^5$ TiO_2 particles/cm^3. [58] For spherical TiO_2 nanoparticles with an average diameter of 50 nm, this corresponds to a mass concentration of 0.14 mg/m^3, above the NIOSH REL. A sudden release of TiO_2 nanomaterials to the air could raise the concentration much higher. One study found the acceptable workplace concentration of TiO_2 nanoparticles to be 1.2 mg/m^3 in respirable dust which is close to the NIOSH PEL. [22] The producers of P25 TiO_2 nanoparticles, Evonik DeGussa, claim to keep TiO_2 nanoparticle concentrations under 0.5 mg/m^3. [9] These values can be compared to a general background particle concentration in a lab which is roughly 0.009 mg/m^3. [56] Particle levels outside of these production facilities were measured as high as $1.3x10^4$ particles/m^3, 94% of which had diameters <100 nm. [9] While this level is higher than ambient levels, it is negligible compared to levels inside of the plant, suggesting that the most susceptible population are the nanomaterial industry workers. The only likely high exposure scenario for the general public would be if there was an accident where an unintentional release of nanomaterials from a plant or during transport occurred. [9]

In order to reduce exposure to nanomaterials, engineering controls and personal protective equipment can be used. Automated processes, fume hoods, and high efficiency particulate air (HEPA) filters can reduce

exposure risk. Respirators and masks may help, but have not been proven to effectively remove all nanomaterials. [56, 59] It is also important to understand how nanomaterials will behave once airborne. Particles tend to aggregate in the air, shifting the average particle diameter to a larger size over time. [58] It was found that the most important mechanism driving nanoparticle aggregation is collisions of nanoparticles with other nanoparticles and background aerosols. [60] Thus, the most critical risk of exposure to smaller sized nanomaterials is to those workers who are near nanomaterial dusts when they are first created.

2.2.2 Toxicity study extrapolation. Many exposure and toxicity tests are conducted on rodents rather than human subjects. A scientifically reasonable approach must be used to extrapolate rodent data to humans. This can be done by allometric relationships between species or by lung dosimetry models. Allometric models are the simpler way and are based on the ratios of different metrics between humans and rodents. Examples of these factors are tissue weight, tissue surface area, respirations rates, and nanomaterial deposition fractions. [22, 43] In the absence of other data an equal response is assumed for a normalized dose in both species. [43]

2.3 ABSORPTION

Once a subject has been exposed to TiO_2 nanomaterials, they must be absorbed into the body to have any effect. Absorption is the process of

how a material moves from the external site of exposure to an internal biological space. [54] The primary routes for exposure are inhalation, ingestion, injection, and absorption by the skin. The most important exposure route is inhalation for two reasons. One reason is that nanomaterial aerosols generally have higher concentrations of nanomaterials than anything that would likely be ingested or applied to the skin. Ingestion and dermal exposure are also more likely from intentional exposure (i.e. oral drug delivery or sunscreen application), which is better understood than unintentional exposure. [61] The second reason is because of the large surface area of the lungs and the minimal anatomical barriers once nanomaterials reach the alveoli. [62] This chapter focuses primarily on inhalation kinetics. A short review of ingestion and dermal exposure is provided along with the reasons that the routes are less relevant to exposure than inhalation.

2.3.1 Gastrointestinal absorption. Nanomaterials may be ingested accidently or intentionally. These particles can be absorbed by the mucosal lining and epithelial barrier in the gastrointestinal associate lymphatic tissues (GALT) in as little as 60 minutes. [1] A modeled concentration of 10 μg/mL TiO_2 nanomaterials in the intestines can cross the epithelial lining by transcytosis, but will only result in low concentrations after crossing. [41] Positive particles tend to be absorbed better, and smaller particles move more easily through barriers. [61] Wang [33] showed that TiO_2 nanoparticles orally administered to a rat could

move from the GALT to the liver, spleen, kidneys, and lung. However, Jani [63] showed that micro-scale TiO_2 particles of 500 nm could also move to the liver, spleen, and lung with no distribution to the heart or kidney. This means that there is little remarkable difference between TiO_2 nanoparticles compared to regular TiO_2 particles except that the nanoparticles were able to move to the kidney of a rat as well. Despite the translocation of TiO_2 nanomaterials from the gastrointestinal tract, no negative effects on any rats have been shown as they have been with inhalation studies. [61]

2.3.2 Dermal absorption. The European NANODERM 3 year study of TiO_2 nanomaterial based sunscreens used *in vitro* and *in vivo* techniques to assess whether the particles can penetrate the skin. The results were inconclusive with some studies reporting penetration from the surface into deeper epidermal layers and others reporting no penetration. The study ultimately concluded TiO_2 nanomaterial based sunscreens were safe. [64] The skin condition could factor into dermal penetration of TiO_2 nanomaterials. The nanomaterials may be more likely to penetrate deeper into the skin at creases, cracks, or hair follicles as well as more readily into damaged skin. [61] One study found penetration was greater when applied to hairier skin. [64] There is no clear evidence that TiO_2 nanomaterials that enter the skin are able to enter the systemic circulatory system. [40] The reason skin is difficult to penetrate is because of a 10 μm thick barrier of strongly keratinized dead cells. The total area of the skin is

roughly 1.6 m^2. This can be compared to the 140 m^2 surface area of the lungs and the 0.5 μm thick barrier between the airspace in the alveoli and the blood flow to illustrate that the lungs are a more likely absorptive site for nanomaterials.

2.3.3 Other absorption sites and exposure routes. TiO_2 nanomaterials in the body may come from wear and tear of prosthetics in the body. Originally the materials are biocompatible, but at the nano-size they can cause inflammatory responses and have been shown to move to the liver, kidney, and colon. TiO_2 nanomaterials may be transported from a mother to a fetus by trans-placenta absorption. [61] Specifically, the TiO_2 nanomaterials were able to affect the brains of the mouse fetuses after being administered to their mothers. This is because the blood-brain barrier is not fully developed while in the womb. [65] TiO_2 nanomaterials in water spray can be inhaled or absorbed through the eye. [9] However, this is likely only relevant to those who use concentrated nanomaterial solutions in a lab or industrial setting since the highest TiO_2 nanomaterial concentration directly downstream from paint run-off was only measured to be 4 μg/L. [66] Other exposure routes such as intravaginal and intravenous exist. [54] However, these exposure routes are less likely and less studied than inhalation and pulmonary absorption. The different absorption routes into the body are displayed in Figure 2.1.

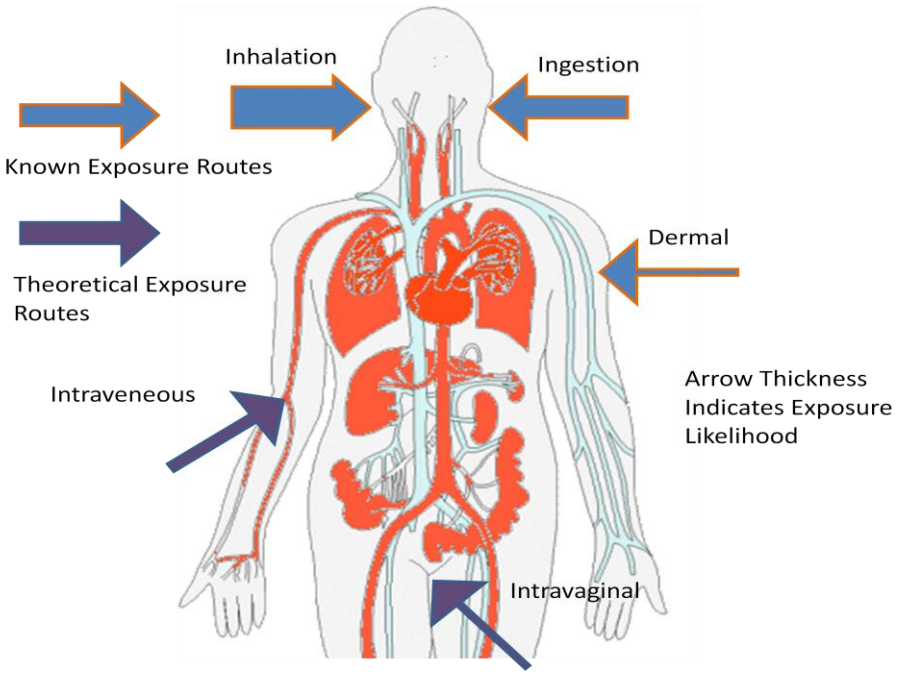

Figure 2.1 Known and theorized nanomaterial exposure routes.

2.3.4 Deposition of TiO_2 nanoparticles in the lung. Before TiO_2 nanomaterials can be absorbed to the blood from the alveoli, they must first be deposited there. An inhalable dust can enter the respiratory tract, but a respirable dust will travel all the way to the alveolar region. [9] TiO_2 nanomaterials are respirable because they will travel to the alveoli. This is important because the epithelial barrier is thinner in the alveolar region. It has been shown that up to 80% of nanomaterials may deposit in the lungs. Particles >100 nm are much less likely to deposit. [61] One study found that 1 nm diameter TiO_2 nanoparticles nearly all deposited before the alveoli, while one third of 5 nm diameter particles made it to the alveoli, and roughly half of 20 nm diameter particles reach the alveoli. [9] The deposition rate will also depend on the subject. Subjects with asthma

or pulmonary disease and patients who were exercising had higher deposition efficiencies. [42, 67] Deposition rates are covered in more detail in Chapter 4. While deposition fractions might change, Kuempel [43] showed that the relationship between external exposure and internal dose is linear.

2.3.5 Pulmonary absorption. After nanomaterials are deposited in the lung, they may absorb from the airspace side into the internal biological space. This is relevant because capillaries carrying blood are close to the surface of the alveoli where they exchange gases. TiO_2 nanomaterials are absorbed to the blood primarily by phagocytosis by macrophages or by endocytosis by epithelial and endothelial cells. [40] TiO_2 nanomaterials exposed to pulmonary macrophages and red blood cells are taken up by diffusion or adhesive interactions. Once within cells, they are not membrane bound which greatly enhances their toxic potential. [68] It was found that after low concentrations of TiO_2 nanomaterials were absorbed, the epithelial integrity was not disrupted when measured by trans-epithelial electrical resistance. [41] However, when the epithelial tissue is damaged beforehand, TiO_2 nanomaterials can absorb into the blood stream more rapidly. [69] TiO_2 nanomaterials may also absorb into the body by transient passage. [62] This has been shown when stimuli caused by the nanomaterials causes the epithelial cells to shrink which can create gaps between cells that TiO_2 nanomaterials can transverse. [70] These mechanisms may work outside of the alveoli in the

airways as well. After rats inhaled a TiO_2 nanoparticle aerosol with a median diameter of 22 nm, particles were found on the luminal side of airways and alveoli, within all major lung tissue compartments and cells, and within capillaries. This absorption may occur rapidly. One study found that within 1 hour, 24% of respired TiO_2 nanomaterials were found beyond the epithelial border. 24 hours later the distribution through the lung remained the same. [68] Nanomaterials that are difficult to clear may remain in the lung for long periods of time. This accumulation of nanomaterials can provide a persistent source of nanomaterial absorption over time. [71]

2.3.6 Olfactory nerve absorption. While most absorption in the lungs takes place in the alveoli, the olfactory nerve is another key location where absorption can take place. Nanomaterials can deposit on the olfactory mucosa and migrate along the olfactory nerve into the olfactory bulb where they are able to interact with the brain. [72] This is important because the restrictive brain-blood barrier generally prevents nanomaterials from entering the brain. The olfactory nerve bypasses the blood-brain barrier allowing nanomaterial interaction with the central nervous system. [61] Larger nanomaterials tend to be better absorbed by the olfactory bulb. [40] This is likely because only 10% of 10 nm diameter nanomaterials are expected to deposit in the nasopharyngeal region. [73] However, micro-sized particles (>100 nm) were unable to be absorbed by the olfactory nerve into the brain. [74]

2.4 DISTRIBUTION

2.4.1 Systematic distribution. The distribution of nanomaterials describes how they move through different tissues and through the circulatory system to other organs. Translocation is a term often used to describe the combined absorption and distribution of nanomaterials. Once out of the lung, TiO_2 nanomaterials may distribute to different systems and organs. One key system is the lymphatic system. Lymphatic vessels are found all through the body except in the cartilage, the eye, and the central nervous system. TiO_2 nanomaterials can traverse the body by the lymphatic fluid. [54] Uptake of anatase TiO_2 nanomaterials increased linearly in the lung over time and exponentially in the lymph nodes over time. [57] This increase can continue for a long period of time after exposure has ended. A 25 mg/m^3 airborne dose of TiO_2 nanomaterials led to a concentration of nanomaterials in the lymph nodes that continued to increase for more than 300 days after the exposure ended. [72] Another study confirmed that the lymph node concentration continued to increase for 1 year after a 10 mg/m^3 dose and peaked at 26 weeks for a 2 mg/m^3 dose. [75] This is caused by the persistence of TiO_2 nanomaterials in the lung that continue to absorb into the lymph nodes even after exposure has ended. Not only can distribution within the lymph nodes increase for over a half a year, it can also occur very rapidly. Small nanomaterials (<5 nm) moved to the mediastinal lymph nodes with 3 minutes and then on into the kidneys within 30 minutes. [62]

Once into the circulatory system TiO_2 nanomaterials can reach other organs as well. Small nanomaterials (<5 nm) were not observed in the liver or bile, but accumulated in the kidneys and were quickly cleared. Larger nanomaterials (27 nm) moved to the lymph nodes in 20 minutes and into the blood after 30 minutes. None of these particles were found in the urine, but tended to accumulate in the liver, lungs, and lymph nodes. Nanomaterials larger than 34 nm mostly were retained in the lungs. [62] This study demonstrates the dependence of distribution on nanomaterial diameter. Another factor is the surface charge of the nanomaterial. Positive surface charges tend to be more restrictive for nanomaterial distribution. [62] To observe distribution trends, nanomaterials are sometimes injected directly into the blood stream. When 2000 μg of 15 nm TiO_2 nanomaterials were injected into a rat nearly the entire mass eventually concentrated in the liver along with 20 μg in the kidney, 10 μg in the lungs, and 5 μg in the spleen and blood. [76] A 5 mg/kg body weight intravenous dose of 20-30 nm TiO_2 nanomaterials led to a 134 μg/g concentration in the liver, a 79 μg/g concentration in the spleen, a 8.8 μg/g concentration in the lung, and a 0.67 μg/g concentration in the kidney after one day. The concentration of Ti in the liver remained nearly constant over 28 days, decreased slightly over 28 days in the spleen, and was returned to control levels by 14 days in the lung and kidney. [36] Another intravenous study found that 80 nm TiO_2 nanomaterials mostly accumulated in the liver, while 25 nm TiO_2 n nanomaterials accumulated

in the spleen, liver, and lungs. [40] A 5g/kg body weight oral dose of 50 nm TiO_2 nanomaterials showed that the majority of the nanomaterials went to the liver. [23] No study showed a measurable concentration of TiO_2 nanomaterials in the brain from pulmonary absorption or intravenous exposure.

2.4.2 Olfactory nerve distribution. As described previously, nanomaterials can bypass the restrictive blood-brain barrier by the olfactory nerve. After exposure to 10 nm diameter TiO_2 nanomaterials, the particles that deposited remained in the olfactory bulb. After exposure to 80 nm diameter TiO_2 nanomaterials, the particles were in the olfactory bulb within 2 days and inside the brain within 30 days. [33] A dose of 5 g/kg body weight of 50 nm TiO_2 nanomaterials to rats resulted in 100 µg/g concentration in the brain, specifically the cortex and hippocampus regions. The same dose of 120 nm TiO_2 particles did not result in a Ti concentration in the brain significantly different than the control animals. [23] The distribution into the brain and the inflammatory response is affected by the crystalline structure of the nanomaterial as well. Anatase TiO_2 nanoparticles were shown to have a greater inflammatory response than rutile TiO_2 nanoparticles. [73] The cited studies show that there are many different distribution profiles of TiO_2 nanomaterials. While particle diameter has a significant effect on distribution; other factors like surface charge, surface coating, and crystalline structure have been shown to affect distribution as well.

2.5 METABOLISM

Metabolism of nanomaterials broadly means a process within the body that will change the nanomaterials' properties. Few journal articles on nanomaterial metabolism have been published. Inorganic materials are generally stable and hard to metabolize rapidly. [54] It is difficult for the body to metabolize inert nanomaterials; however, organic coatings on nanomaterials and metal oxides can be metabolized. [61] It has been shown that TiO_2 can be dissolved by macrophagic activity in the liver and can be considered an easily eliminated compound, unlike asbestos or carbon nanotubes. [76] Dissolution is a key factor in the metabolism and clearance of nanomaterials. Though nanomaterials may be more difficult to clear for other reasons, they will dissolve faster than micro-sized particles. Even if the dissolution takes weeks or months, it will still increase the clearance of nanomaterials. [40]

2.6 EXCRETION

2.6.1 Pulmonary Clearance. Excretion refers the way the body eliminates nanomaterials out of the biological space. In the lungs—as well as the gastrointestinal tract—there are competing processes: absorption vs. clearance. [54] The lungs are cleared of deposited, unabsorbed nanomaterials by two processes. In the upper region, the mucocilliary escalator moves particles upward. In the alveolar region, nanomaterials are cleared by macrophage phagocytosis. [77] Both processes move

particles toward the larynx where they enter into the gastrointestinal tract. From here they can possibly be found in feces despite no oral administration. [78] One study observed that dissolution of TiO_2 nanomaterials was not observed in the lungs and all clearance was primarily by the physical and mechanical processes. [79]

Transportation of nanomaterials by macrophages can be a slow process and may not be able to clear all the particles. [40] One way to measure lung clearance is by finding the half-life of particles absorbed into the lung. A 23 mg/m^3 dose of 20 nm and 250 nm TiO_2 particles was administered to rats. The half-life for the 20 nm TiO_2 nanomaterials was 501 days, while the half-life for the 250 nm TiO_2 nanomaterials was only 174 days. [79] This can be compared to a 6 μm diameter particle which would generally be cleared within 1-2 days. [80] Dosage also has a factor on clearance rates. The half-life times were 63 days, 132 days, and 395 days for doses of 0.5 mg/L, 2 mg/L, and 10 mg/L TiO_2 nanomaterials respectively. This prolongation of particle clearance for higher doses is indicative of pulmonary overload. [75] If a particle larger than 200 nm reaches the lower regions of the lungs, it is generally responded to by macrophages within a few hours. However, smaller nanomaterials are often “hidden” from the macrophages for long periods of time that increase the clearance time. [80]

2.6.2 Systematic Clearance. Once into the circulatory system, excretion mainly occurs by the liver and kidneys, with small nanomaterials

(<5.5 nm) being almost completely cleared by the kidneys into the urine. [54, 62] Intravenously introduced TiO_2 nanomaterials cleared from the kidney, blood, and spleen within 72 hours. One month later 30% of the peak concentration of nanomaterials had cleared from the liver into the bile. [76] The clearance times for the circulatory systems are generally much faster than the lungs if there is not a persistent source remaining in the lungs. Other excretion routes such as by sweat or breast milk have been theorized, but not yet proven. [54, 61]

2.6.3 Accumulation. If nanomaterials are unable to clear, they may accumulate in the organs. The retained dose is a result of biopersistence of a compound and is a function of deposition rates and clearance rates. [79] Lipid soluble nanomaterials may deposit in the lung surfactant where they can be retained for months or even years. [59] These lipid soluble nanomaterials may also be retained in the intestinal fluid unless they are biodegraded or cleared by chemical dissolution. [40] High accumulation is likely to occur where nanomaterials are administered, especially the lungs and the gastrointestinal tract. There is virtually no accumulation in the brain and low accumulation in the kidneys and muscles. However, because the muscles are larger than the kidneys, they may have a high absolute mass despite a low concentration. [54] By accumulation processes, one can see how if nanomaterials are not cleared, they can build up over long periods of time and cause chronic health problems.

2.7 MODEL DEVELOPMENT

The data gathered from TiO_2 nanomaterial ADME studies mentioned above were combined to create a model capable of modeling how two different sized of nanoparticles will move throughout the body based on different exposure types and exposure levels. The ADME model was created from inhalation, ingestion, and injection studies that recorded the concentrations of TiO_2 nanomaterials in different tissues after the animals were sacrificed. The organs that were consistently studied were the lymph nodes, liver, kidneys, spleen, and brain. [23, 33, 36, 73, 79] The model dose was scaled linearly to the dose used in the studies in order to predict the tissue concentrations. When available, the model is based upon different times post dosage. The inputs and calculations used for the model can be seen in Figure

2.7.1 Hypothetical exposure scenarios. To better illustrate the effect particles size has on the pharmacokinetics of TiO_2 nanomaterials, two hypothetical exposure scenarios were created. The duration, airborne concentration, and size of the TiO_2 nanomaterials were varied to simulate possible workplace environments. The two exposure scenarios are shown in Table 2.1. The first scenario is a moderate nanoparticle concentration of 5 nm diameter particles for a 4 week period of 8 hour work days. The second scenario is a high nanoparticle concentration of 25 nm diameter particles for just 3 work days. The final concentrations in the tissues resulting from inhalation are shown in Tables 2.2 and 2.3. A similar

dosage (mass per body weight) of 25 nm diameter TiO_2 nanoparticles was modeled as being ingested and injected. The results are shown in Table 2.4.

Table 2.1

Hypothetical Exposure Scenarios

Hypothetical Exposure	Dose # 1	Dose # 2
Nanoparticle Level	Moderate	High
Airborne Concentration	2 mg/m3	2.5 mg/m3
Nanoparticle Diameter	5 nm	25 nm
Worker Status	Healthy	Healthy
Exposure Length	4 weeks	3 days
Subject Weight	70 kg	70 kg
Blood Volume	5 L	5 L

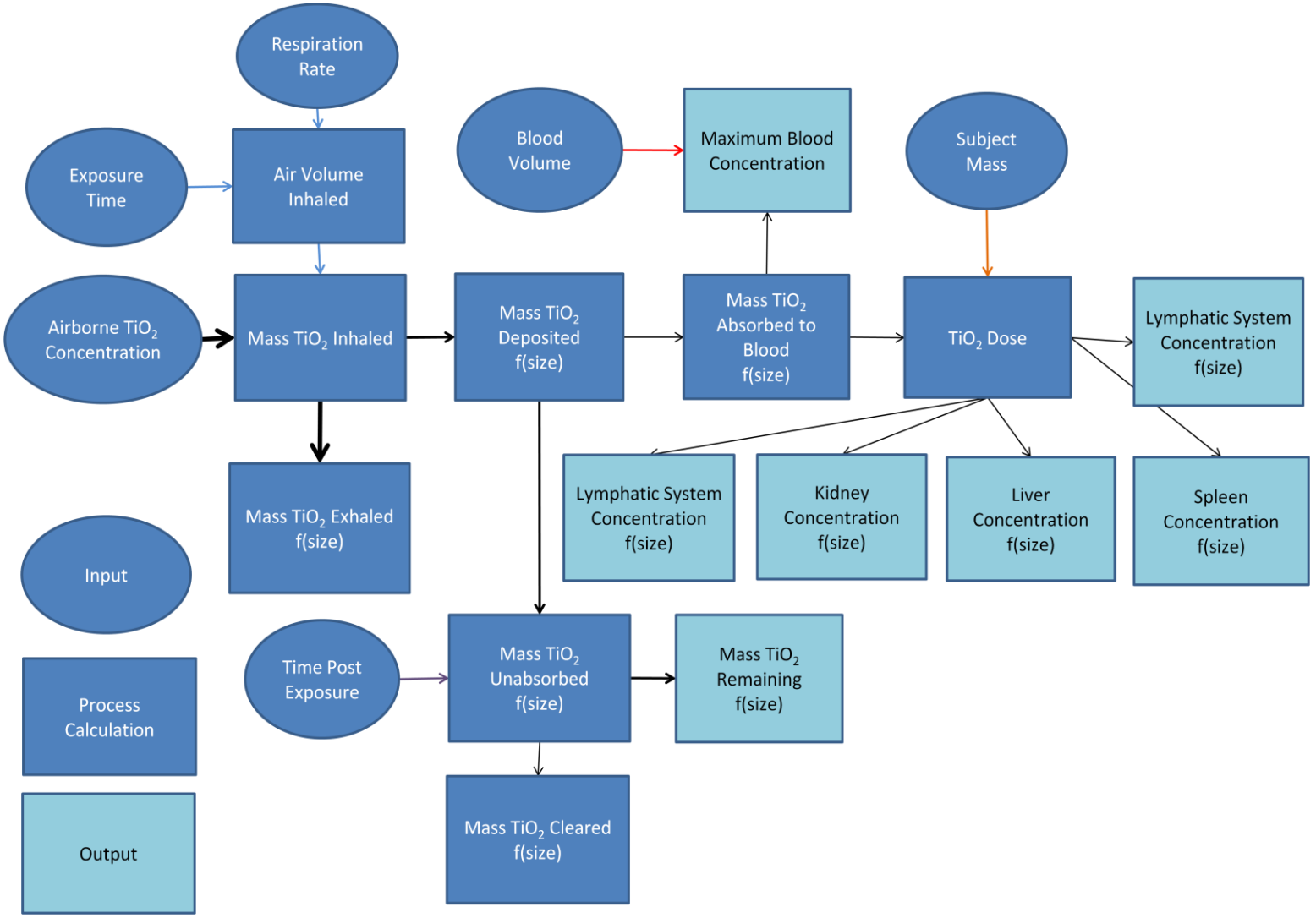

Figure 2.2 ADME Inhalation Model Flowchart: Ovals indicate inputs, green boxes indicate outputs, black lines are TiO_2 moving through the body, and the line thickness indicates relative TiO_2 mass.

Table 2.2

Modeled Inhalation Tissue Concentrations: Hypothetical Dose #1

INHALATION		
Input	**Value**	**Unit**
Mass Deposited in Alveoli	128	mg
Inhalation Dose	1.8	mg/kg
Mass Absorbed to Blood (10 min)	35.8	mg
Mass Absorbed to Blood (30 min)	64	mg
Maximum Blood Concentration	12.8	ug/mL
Lymph Node Concentration (10 min)	0.7	mg/g
Lymph Node Concentration (30 min)	1.3	mg/g
Mass Cleared by Urine	9.3	mg
Maximum Kidney Concentration	66.3	ug/g
Brain Concentration	Negligible	ug/g
Liver Concentration	Negligible	ug/g
Spleen Concentration	Negligible	ug/g

Table 2.3

Modeled Inhalation Tissue Concentrations: Hypothetical Dose #2

INHALATION		
Input	**Value**	**Unit**
Particle Mass Inhaled	72	mg
Mass Deposited in Alveoli	36	mg
Inhalation Dose	0.5	mg/kg
Mass Absorbed to Blood	8.6	mg
Maximum Blood Concentration	17.3	ug/mL
Mass in Lymphatic System (100 days)	1.1	mg
Kidney Concentration (1 day)	0.02	ug/g
Kidney Concentration (14 days)	0.005	ug/g
Kidney Concentration (28 days)	0.005	ug/g
Liver Concentration (1 day)	3.3	ug/g
Liver Concentration (14 days)	2.5	ug/g
Liver Concentration (28 days)	2.8	ug/g
Spleen Concentration (1 day)	1.9	ug/g
Spleen Concentration (14 days)	1.1	ug/g
Spleen Concentration (28 days)	0.8	ug/g
Brain Concentration (1 day)	1.2	ng/g
Days Post Exposure	501	days
Mass Remaining in Lungs	18	mg

Table 2.4

Modeled Ingestion and Injection Tissue Concentrations: Hypothetical Dose #2

	INGESTION		INJECTION	
Input	**Value**	**Unit**	**Value**	**Unit**
Ingestion Dose	5.0	mg/kg	5.0	mg/kg
Mass Absorbed to Blood	2.8	mg	350	Mg
Maximum Blood Concentration	0.6	ug/mL	70	ug/mL
Kidney Concentration (1 day)	-		0.67	ug/g
Kidney Concentration (14 days)	0.375	ng/g	0.20	ug/g
Kidney Concentration (28 days)	-		0.20	ug/g
Liver Concentration (1 day)	-		134	ug/g
Liver Concentration (14 days)	0.107	ng/g	99	ug/g
Liver Concentration (28 days)	-		111	ug/g
Spleen Concentration (1 day)	-		79	ug/g
Spleen Concentration (14 days)	0.580	ng/g	49	ug/g
Spleen Concentration (28 days)	-		33	ug/g
Brain Concentration (1 day)	0.15	ng/g	0.10	ng/g

2.7.2 Clearance rates. It is important to understand how TiO_2 nanomaterials remaining in the lung can act as a persistent source of absorption into the body. Small nanoparticles can have an especially long half-life in the lung before they are cleared. The clearance of TiO_2 nanomaterials can decrease linearly or decay exponentially depending on the initial dosage. The mass deposited decrease from the lungs, modeled as an exponential decay for each of the two exposure scenarios can be seen in Figure 2.2 and Figure 2.3 which show the clearance of TiO_2 nanoparticles over time.

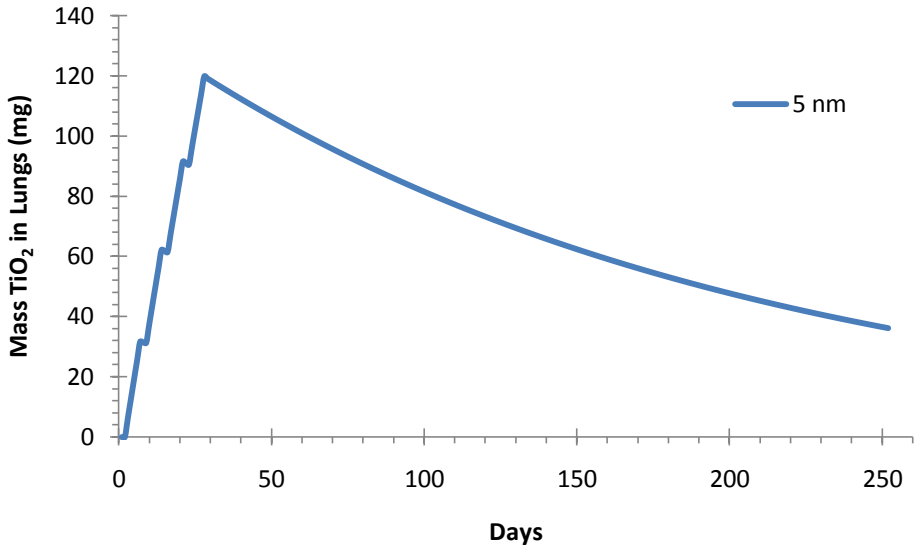

Figure 2.3 TiO_2 nanoparticle lung clearance for exposure scenario #1

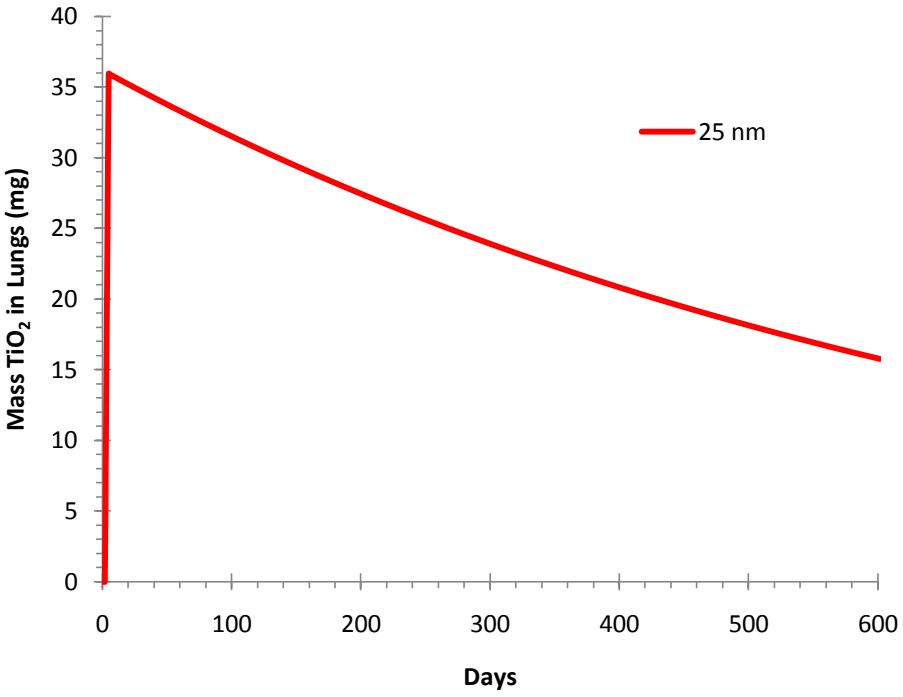

Figure 2.4 TiO_2 nanoparticle lung clearance for exposure scenario #2

2.8 DISCUSSION

TiO_2 nanomaterials are already used in applications in many different industries, and their use increases every year. The most susceptible people are those who regularly are exposed to TiO_2 nanomaterials in their workplace. To judge how TiO_2 nanomaterials are taken up and distributed by the body, pharmacokinetic ADME models can be applied. The most important absorption route in the body is pulmonary absorption. The importance of pulmonary absorption is reflected by the TiO_2 nanomaterial tissue concentrations from inhalation being 4 orderes of magnitude higher than the tissue concentrations from ingestion. Though ingested and dermally applied nanomaterials are not as relevant from a human health standpoint, there are still environmentally relevant as a waste after being excreted or washed off.

From the lungs TiO_2 nanomaterials can be distributed to the lymphatic system, brain, liver, kidney, and spleen. The distribution throughout the body depends largely on nanomaterial diameter, but also on other factors like surface charge as well. TiO_2 nanomaterials may be metabolized in the liver, primarily by dissolution by the macrophages. The nanomaterials are cleared from the lungs by the mucocilliary escalator and phagocytosis by macrophages. They are cleared from the circulatory system primarily by the liver and kidneys depending on particle size. TiO_2 nanomaterials will primarily end up in feces if ingested or cleared from the lungs to the esophagus. Those nanomaterials cleared by the kidneys will

end up in urine. If particles are not excreted they can accumulate in organs and remain there for months or years. Studies of TiO_2 toxicity and ADME are complicated by the many factors that must be accounted for when studying nanomaterials. This chapter has demonstrated some of the kinetic behaviors of TiO_2 nanomaterials in the body, but it is important to remember many knowledge gaps still exist and the risk to human health created by TiO_2 nanomaterials warrants further study.

2.9 SUMMARY

- Inhalation is the most important exposure route for human health implications of TiO_2 nanomaterials.
- TiO_2 nanomaterials are more slowly cleared from the lungs than larger particles and have greater toxic effects with the half-life being as high as 501 days.
- TiO_2 nanomaterials may distribute to the lymphatic system, brain, kidneys, liver, and spleen. Modeled liver concentrations were generally highest, as much as 3.3 µg/g after inhalation.
- Primary particle size plays an important role in the ADME of particles as dose crystal structure, surface coating, and charge.
- Extremely small TiO_2 nanomaterials (< 5nm diameter) are excreted by the kidneys through the urine.
- Larger TiO_2 nanomaterials (~25 nm) are more likely to be excreted in bile from the liver.

CHAPTER 3: TITANIUM DIOXIDE QUANTIFICATION METHOD DEVELOPMENT

3.1 INTRODUCTION

Spectrometric methods can be used to determine trace metals, including Ti from TiO_2 bulk and nanomaterials, in environmentally and biologically relevant matrices. Two popular methods are inductively coupled plasma mass spectrometry (ICP-MS) and inductively coupled plasma optical emission spectrometry (ICP-OES). In both methods, the sample is nebulized and a small part of the sample enters a plasma torch where it is atomized and conveyed to a spectrometer. ICP-MS instruments use the mass to charge ratio of the ions to differentiate species, ICP-OES instruments use the different optical emissions of elements to differentiate. The two spectrometric methods have become popular because they allow for multi-elemental analysis of both major and trace elements and are capable of rapidly processing a large number of samples requiring only a minimal sample volume. [81, 82] ICP-MS and ICP-OES methods have been shown to be more accurate than photometrical methods. [83]

A key sample preparation step for inductively couple plasma spectrometry is the conversion of solid samples to a representative solution so that the entirety of the element in question is atomized in the plasma. [84] Direct injection of unprepared samples into the spectrometer

has proven inefficient because samples may have a high viscosity or be insoluble. [85] Matrix constituents such as a high concentration of suspended solids can suppress the torch plasma which can also cause incomplete atomization and ionization of the elements. [84] A digestion procedure can be used “to reduce interferences by organic matter and convert metals associated with particulate matter to a form…that can be determined by inductively coupled plasma spectrometry.” [86]

A number of different methods have been devised to adequately digest samples before an inductively coupled plasma spectrometry analysis. Digestion procedures generally involve adding acids and/or a catalyst to a sample. Different combinations and proportions of nitric acid, hydrochloric acid, sulfuric acid, perchloric acid, phosphoric acid, hydrofluoric acid, and hydrogen peroxide have all been evaluated for the digestion of organic and inorganic metals containing trace metals including Ti. [81, 82, 84-90] *Standard Methods* recommends that if possible, it is ideal to use only very pure nitric acid to prevent spectrometric interferences; but the digestion of TiO_2 requires a stronger digestion method. [86] It has been shown that either a mix of hydrogen peroxide, nitric acid, and sulfuric acid or hydrogen peroxide, nitric acid, and hydrofluoric acid can sufficiently digest TiO_2. [81, 87, 89] Using reference standards, the recovery of Ti after digestion has been shown to be 95 percent or greater. [84, 85, 87, 88, 90] The spectrometry results were

further verified by X-ray fluorescence and spectrophotometric methods. [84, 90]

Microwaves and hot plates are two common standard methods used to heat samples after acids are added in order to accelerate the digestion. Heating temperature and heating time have both been shown to have large effects on digestion efficiency. [88, 91] Ashing has been used for the digestion of samples; however, studies have shown that ashing before digestion had little effect on the digestion efficiency of TiO_2 and can cause losses. [88]

For Ti analysis both ICP-MS and ICP-OES have been shown to be sufficient for a variety of sample types. [89, 92] The ICP-MS generally has a lower instrument detection limit (IDL) and is used for ultra trace metals analysis. [86, 93] No other technique can currently approach the sensitivity of an ICP-MS instrument for multielemental analysis. The power of ICP-MS is reflected in the fact that the use of ICP-MS continues to grow while the use of ICP-OES has reached a steady state. [94] ICP-MS also has the ability to determine isotope fractionation of elements. [89] However, an ICP-MS instrument is more expensive to purchase and more complex to operate and maintain than an ICP-OES instrument. [92] ICP-OES instruments can handle a higher amount of total dissolved solids in each sample as well requiring less sample preparation than samples analyzed by an ICP-MS instrument. Thus, there is a tradeoff between ease of use and capability in the instruments.

3.2 PROBLEM STATEMENT

The objective of this project was to develop a quantification method consisting of a digestion procedure and analysis procedure capable of accurately measuring TiO_2 at widely varying concentrations. The digestion procedure had to be capable of digesting large numbers of samples using the resources available at Arizona State University. The digestion method had to efficiently digest all Ti so that complete ionization of the Ti can occur in the plasma. The digestion method had to digest any organics or solids that could cause interferences during analysis or damage to the instruments. The analysis procedure had to optimize the use of the inductively coupled plasma spectrometry instruments available at Arizona State University. An IDL was established for each ICP instrument to determine which can quantify titanium at lower concentrations. Then a method detection limit (MDL) was established for the digestion and analysis.

3.3 MATERIALS AND METHODOLOGY

3.3.1 Choice of digestion reagents. As described in the introduction, there are various acid combinations that can be used to adequately digest TiO_2 for analysis. One proven digestion method uses a combination of nitric and sulfuric acid to digest the TiO_2. While this method may provide a good recovery of Ti, it was not optimal for ICP-MS analysis because the sulfur oxide species (S-O) has a mass to charge

ratio (m/z) of 48 which interferes with the primary Ti isotope which is also 48. Using sulfuric acid as a digestion reagent would have made quantification of trace concentrations of Ti impossible by ICP-MS. ICP-OES could still be used, but the detection limit of ICP-OES was not thought to be as low as ICP-MS. Another popular method used by geologists is a combination of nitric acid, hydrochloric acid, and hydrofluoric acid. However, the chlorides from the hydrochloric acid can complex with elements in the water that may be analyzed during environmental monitoring. These complexes can cause precipitation of solids in the solution or cause interferences for analysis.

Packer et al. found that a combination of nitric acid, hydrogen peroxide, and hydrofluoric acid was able to digest Ti in ceramic materials. [89] Nitric acid, hydrogen peroxide, and hydrofluoric acid were chosen to be evaluated as reagents for the digestion of TiO_2. The reagents were all Ultrapure acids purchased from JT Baker. The percentage acid and Ti levels for the reagents are shown in table A.1. It should be mentioned that hydrofluoric acid is extremely hazardous. [95] However, with caution and the use of proper personal protection equipment (PPE) and an adequate fume hood, the hazard of using hydrofluoric acid can be minimized.

3.3.2 Digestion procedure. Two digestion procedures were evaluated, a hot plate digestion method and a microwave digestion method. In the hot plate method, sample was added to a 150 mL polytetrafluoroethylene (PTFE or Teflon) beaker along with 10 mL of

hydrogen peroxide and 2 mL of nitric acid. The beakers were heated at 120° C for 4 hours to digest the organics. The beakers were removed from the hot plate and allowed to cool. Then 8 mL of nitric acid and 2 mL of hydrofluoric acid was added. The beakers were heated on a hot plate at 120° C to digest the TiO_2 and evaporate the acids. When 0.1 to 0.5 mL of solution remained, the beakers were removed from the hot plate and allowed to cool. Then the beakers were rinsed >3 times with a solution of 2% nitric acid in nanopure (resistivity = 18.3 MΩ*cm) water into a 25 mL volumetric flask before being stored for analysis.

In the microwave digestion method, sample was added to a 55 mL microwave digestion vessel along with 8 mL of nitric acid and 2 mL of hydrofluoric acid. The vessels were digested using a Microwave Assisted Reaction System (MARS) Express instrument. The microwave digestion program can be seen in Table 3.1. After cooling, the sample was rinsed >3 times using approximately 20 mL of a 2% nitric acid solution into a Teflon beaker. 2 mL of hydrogen peroxide was added to each beaker to digest any remaining organics. The beaker was then heated on a hot plate at 180°C until between 0.1 and 0.5 mL of solution remained. The beakers were removed from the hot plate and allowed to cool. The beakers were rinsed >3 times with a 2% nitric acid solution into a 25 mL volumetric flask before being stored for analysis.

Table 3.1

MARS Express Microwave Digestion Parameters

Power	Ramp Time	Temperature	Hold Time
1200 W	15:00	150°C	0:00
1200 W	15:00	180°C	20:00

In both digestion procedure, the solution was evaporated and diluted to ensure that the maximum concentration of HF in the final sample was 2%. The actual concentration is likely much lower because the HF is more likely to evaporate upon heating than HNO_3. This was done to ensure that there is no etching of the glassware on the spectrometers from the hydrofluoric acid.

The digestions were evaluated for the recovery of a known amount of TiO_2 and ability to digest organics sufficiently for analysis. A solution with a known amount of TiO_2 was digested to evaluate the Ti recovery efficiency. A piece of tripe was digested with the TiO_2 solution to simulate an organic sample. Tripe was chosen because it is an exceptionally tough tissue and a method that could digest tripe should be robust enough for any tissue sample. The digestion method was applied to a number of method blank samples, containing only the reagents and no sample, in order to measure the amount of Ti contamination that is likely to occur. The data was used to find the digestion MDL after the IDLs were established for each instrument. Whole milk was used to evaluate the

ability of the digestion procedure to digest samples with a high organic content.

3.3.3 TiO_2 stock preparation. The digestion methods were evaluated using a TiO_2 nanoparticle solution. The nanoparticles used were P25 TiO_2 purchased from the Evonik DeGussa Corporation that consist of a 81%/19% anatase/rutile TiO_2 crystal structure mix with an average primary particles size of 24 nm. [96] A stock solution was prepared by adding the desired weight of P25 to nanopure water and sonicating for 30 minutes in a Bronson 2510 bath sonicator at a 40 kHz frequency. A serial dilution of the stock was done to create various concentrations for the digestion evaluation.

3.3.4 ICP analysis. Analysis was conducted by ICP-OES and ICP-MS to compare the two instruments. Ti standards were prepared in 2% nitric acid to match the matrix of the samples. The concentrations for the Ti standards were chosen in the range where the concentration and CPS are related linearly to create a linear calibration curve. Samples with concentrations above the highest standard concentration were diluted so that they fell within the calibration curve. Quality control blank checks and external calibration verification checks were run regularly throughout the analysis. An internal standard was used to account for fluctuations in the plasma temperature. Scandium was used as the internal standard because it has an ionization energy close to Ti. Instrument detection limits were determined according to the method prescribed by the

Environmental Protection Agency in the Code of Federal Regulations (CFR) Title 40: Part 136 Appendix B. [97] The instrument with the lower detection limit for Ti was further optimized for sensitivity and repeatability.

The ICP-MS instrument evaluated was a Thermo X Series 2 quadrupole. The instrument was equipped with a standard quartz torch assembly, a concentric nebulizer, a double-pass spray chamber, and a CETAC ASX-520 autosampler. The instrument was tuned with a solution containing lithium, indium and uranium at a concentration of 10 µg/L. A 2% nitric acid solution was used as a rinse between all samples. The operating parameters for the ICP-MS instrument are shown in Table 3.2. A performance report was conducted on the instrument to evaluate the sensitivity and stability of the signal. The requirements for a passing performance report are shown in Appendix A Table A.2. Ti isotope mass to charge ratios of 46, 47, 48, 49, and 50 were all evaluated. The typical detection limit provided by the manufacturer listed Ti minimum detection as 0.01 µg/L.

The ICP-OES instrument evaluated was a Thermo iCAP 6200 ICP Spectrometer. The instrument was equipped with a standard quartz torch assembly, a concentric nebulizer, a cyclonic spray chamber, and a CETAC ASX-520 autosampler. A 2% nitric acid solution was used as a rinse between all samples. The operating parameters for the ICP-OES are shown in Table 3.2. The wavelengths of 3234 Å and 3349 Å were both monitored for optical emissions due to the presence of Ti. The

typical detection limits provided by the manufacturer listed Ti minimum detection as 0.01 to 0.1 µg/L.

Table 3.2

Operating Condition for the ICP-MS and ICP-OES Instruments

	ICP-MS	**ICP-OES**
Instrument	Thermo X-Series 2	Thermo iCAP 6200
RF Power	1350 W	1150 W
Nebulizer Flow	0.87 L/min	1 L/min
Auxiliary Flow	0.7 L/min	0.5 L/min
Sample Flow	0.4 mL/min	2 mL/min
Equilibration Time	1.5 ms	-
Background Correction	450 CPS	220 CPS
Measurement Process	Peak Height	Peak Height
Integration Time	3 s	5 s
Uptake Delay	60	60
Rinse Delay	30	30
Number of Replicates	3	3

3.3.5 Cleaning. Between digestions, all glassware, Teflon, and microwave digestion vials were filled with a 10% nitric acid solution and sonicated for 10 minutes. The labware was then rinsed 3 times with nanopure water and dried. Cones in the ICP-MS and ICP-OES instruments were cleaned regularly. Sample tubes for the autosampler were disposable and only used for one sample.

3.4 RESULTS

3.4.1 Digestion of organics. 5 mL of whole milk was digested by the microwave digestion and hot plate digestion methods. The microwave digestion method produced a clear sample. The hot plate digestion

method produced a dark sample that still had visible solids. The samples are shown in Figure 3.1. Running the hot plate digestion samples through the ICP-MS and ICP-OES instruments caused the sensitivity on both instruments to decrease so much that both instruments required extensive maintenance. All sample tubing had to be replaced. Running the microwave digestion samples through the ICP-MS and ICP-OES instruments had no effect on the sensitivity. This was verified by running another performance report after analysis of the digestion samples. The performance report passed.

Figure 3.1. Whole milk digested by hot plate digestion (right), microwave digestion (center), and microwave digestion with hydrogen peroxide (left). All samples shown were blanks, with no TiO_2 added.

3.4.2 Digestion of TiO_2. 10 mL of a 1 mg/L P25 TiO_2 nanoparticle solution was digested in triplicate with a piece of tripe by the microwave digestion and hot plate digestion methods. Both methods produced a clear sample that had no effect on the spectrometers. The microwave digestion had a recovery of 95.3 +/- 6.5%. The hot plate digestion had a recovery of 94.2 +/- 13.5 %. Because the microwave digestion method gave a good recovery and slightly more consistent results, the method was evaluated for higher concentrations of TiO_2 to ensure that the method was robust enough to digest larger quantities of Ti. 10 mL of both a 10 mg/L and a 100 mg/L P25 TiO_2 nanoparticle solution were digested in triplicate with a piece of tripe by the microwave digestion method. The results are shown in Table 3.3.

Table 3.3

Microwave Digestion Ti Recovery

Sample Concentration	Recovery (%)	% Std. Dev. (n=3)
1 ppm	95.3	6.5
10 ppm	99.2	14.8
100 ppm	86.3	0.7

3.4.3 Instrument method detection limit. The IDL was determined for the ICP-MS and ICP-OES instruments. A 2 µg/L Ti standard and a 5 µg/L Ti standard were prepared. Each standard was analyzed 10 times on both of the instruments. The IDL was then calculated for each instrument by the EPA method using equation:

$$MDL = \sigma (n) * t (n-1, 0.01)$$

Where σ (n) is the standard deviation of the replicates, and t (n-1, 0.01) is a value from a t distribution based on the number of replicates. The IDLs are shown in Table 3.4. To further verify the sensitivity of each instrument, a calibration curve was created for each instrument using low concentrations of Ti (less than 10 µg/L). A linear trend line was added to each calibration to compare the R^2 values for each instrument. The calibration curves are shown in Figure 3.2 and Figure 3.3. The R^2 value for the ICP-MS instrument was 0.996 using the Ti isotope 49, the R^2 value for the ICP-OES instrument was 0.966 for the Ti emission wavelength 3234 Å. Other isotopes and wavelengths were evaluated as well. The ICP-MS calibration curve for 49 is shown because it had less interferences, the ICP-OES calibration curve is shown for 3234 Å is shown because it had the highest relative intensity of any Ti emission wavelength.

Table 3.4

Instrument Method Detection Limit

Test Concentration	ICP-MS (Ti 49)	ICP-OES (Ti 3234)
Stated MDL	10 ng/L	10-100 ng/L
2000 ng/L	81 ng/L	562 ng/L
5000 ng/L	164 ng/L	491 ng/L

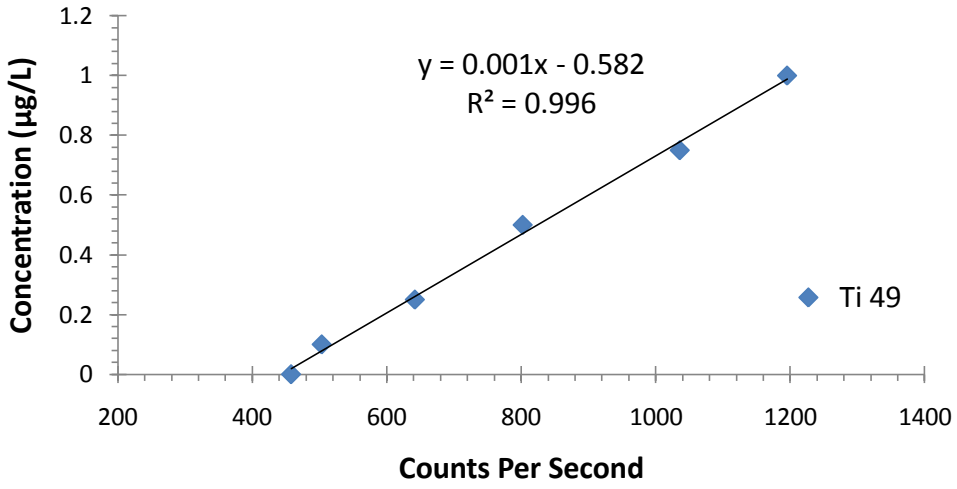

Figure 3.2. ICP-MS calibration curve

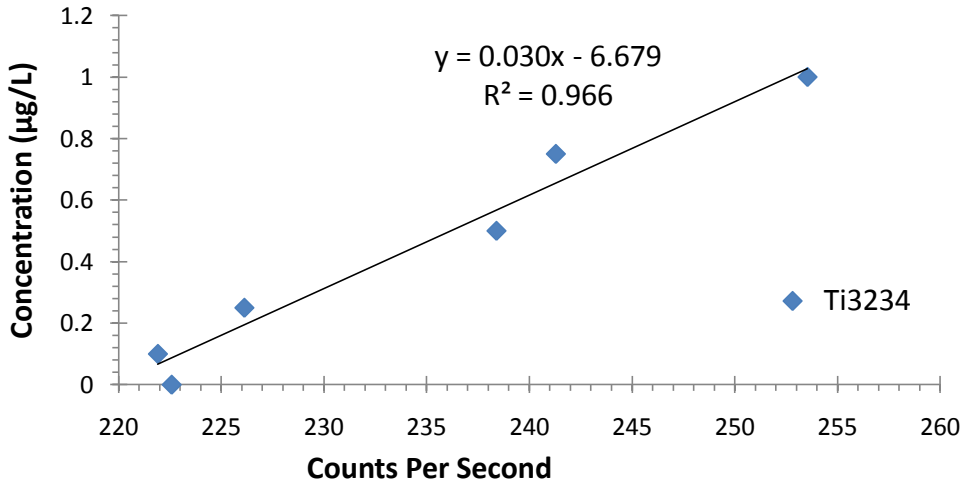

Figure 3.3 ICP-OES calibration curve.

3.4.4 Digestion method detection limit. Twelve method blanks were digested using the microwave digestion method and analyzed by ICP-MS. The results are shown in Figure 3.4. The blanks were digested and evaporated at different times over the course of 3 weeks. The

average amount of Ti for the 12 blanks was 496 ng with a maximum of 2.07 µg. Generally the samples had less than 500 ng of Ti after the complete digestion method. Only method blank #10 had over 2 µg of Ti which was over 3 times higher than the closest method blank. It was determined that the Teflon beaker had been improperly washed and blank #10 was considered to be an outlier. If method blank #10 is considered an outlier and ignored, the average for the remaining 11 blanks is 353 ng Ti with a maximum of 593 ng. Thus, any sample measuring below an absolute Ti mass of 600 ng would be considered to be below the digestion MDL. This corresponds to a TiO_2 MDL of 1 µg.

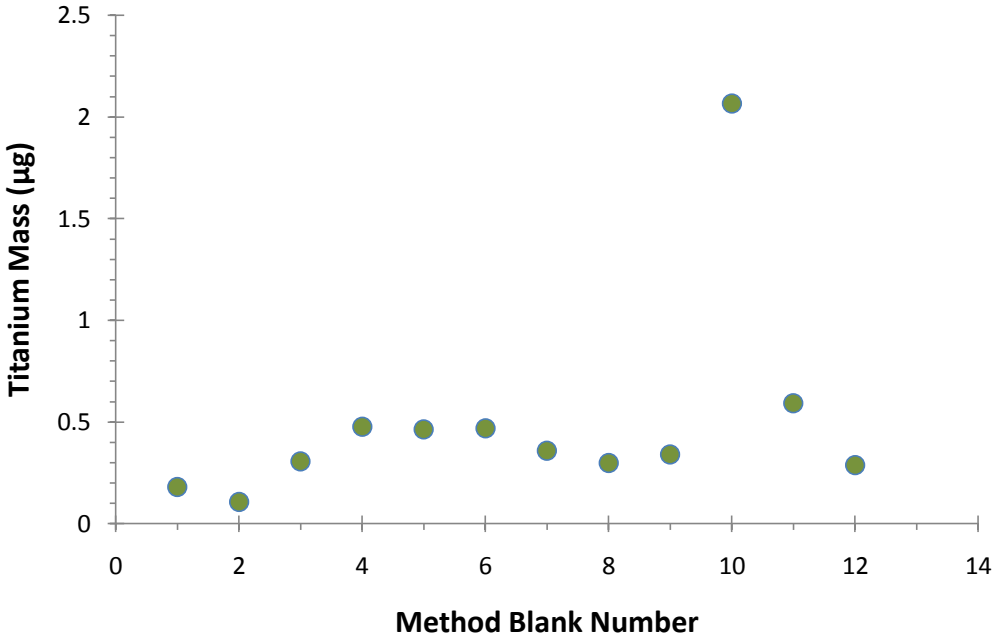

Figure 3.4. Digestion method detection limit of microwave digestion blanks.

3.5 DISCUSSION

3.5.1 Digestion method evaluation. The microwave digestion method proved to be a better method than the hot plate digestion method. The hot plate digestion method was totally incapable of handling high organic contents as proven by the milk digestion results. The microwave digestion method broke down the tissue and milk in the samples very well. After evaporation, if any color remained hydrogen peroxide was added and the sample was heated again. It is important that the samples be as free of organics and solids as possible to minimize the required maintenance time on the instrument. During an analysis using the ICP-MS instrument, as many as 150 microwave digested samples were run at one time and a performance report conducted after the sample set was finished indicated that the sensitivity of the instrument had not decreased at all.

The TiO_2 recovery for both methods was greater than 90%. When digesting higher concentrations of TiO_2 by the microwave digestion method, the recovery was still high and there was less than a 15% standard deviation in the triplicate samples. The recovery was not perfectly 100%, but any impurities in the TiO_2 P25 stock powder or heterogeneity of the nanoparticle solutions would cause the recovery to be less than 100%. However, the recoveries were generally in good agreement with those found in the literature.

For ultra-trace samples, the amount of Ti contamination was kept to a minimum by following proper cleaning procedures. The Ti concentration that corresponds to the digestion MDL was 24 µg/L which is well above the IDL for either instrument. The contamination likely occurred during the evaporation of the acids in the Teflon beakers. The samples may remain uncovered for up to 4 hours while the acids evaporated. During this time, Ti particles in the air may deposit in the sample. Each batch of rinse water used was analyzed and the Ti concentration was always near zero. For samples with Ti concentrations near the digestion MDL, increasing the total amount of sample digested or spiking in a known amount of Ti could provide more reliable data.

3.5.2 Instrument optimization. The ICP-MS IDL was significantly lower than the ICP-OES instrument. The better sensitivity of the ICP-MS instrument is reflected in the calibration curve. The linear trend line for the ICP-MS had a higher R^2 fit value than the ICP-OES instrument. When looking at how many counts per second (CPS) the instrument recorded, the 1 µg/L standard had a CPS value that was three time higher than the blank standard. For the ICP-OES instrument, the 1 µg/L standard only had a CPS value that was roughly 15% higher than the blank standard. The larger increase of CPS values in comparison to the background further demonstrates the sensitivity of the ICP-MS instrument.

The ICP-MS instrument had multiple Ti mass lines that could be monitored. The ICP-OES instrument had multiple Ti emission lines that

could be monitored. For the ICP-OES instrument, Ti emission wavelength 3234 Å had a higher relative intensity than wavelength 3349 Å and better sensitivity at low concentrations. For the ICP-MS instrument, Ti 48 m/z was the most abundant isotope. However, due to interferences from sulfur oxide and phosphorus oxide species that occur in organic samples, an accurate quantification of Ti could not be achieved. Similar interferences occurred with the Ti 47 m/z isotope. These interferences can be seen in Figure 3.5. When analyzing the complete mass spectrum, phosphorus can clearly be detected as shown by Figure 3.6. No quantification of the Ti 46 m/z isotope could be determined due to high interferences from the scandium 45 m/z isotope. For the two remaining mass isotopes, Ti 49 m/z and Ti 50 m/z, the Ti 49 m/z isotope was more abundant. Ti 49 m/z on the ICP-MS instrument was designated as the best option for analysis because of the lower instrument detection limit and lack of interferences despite the lower responses resulting in higher MDLs.

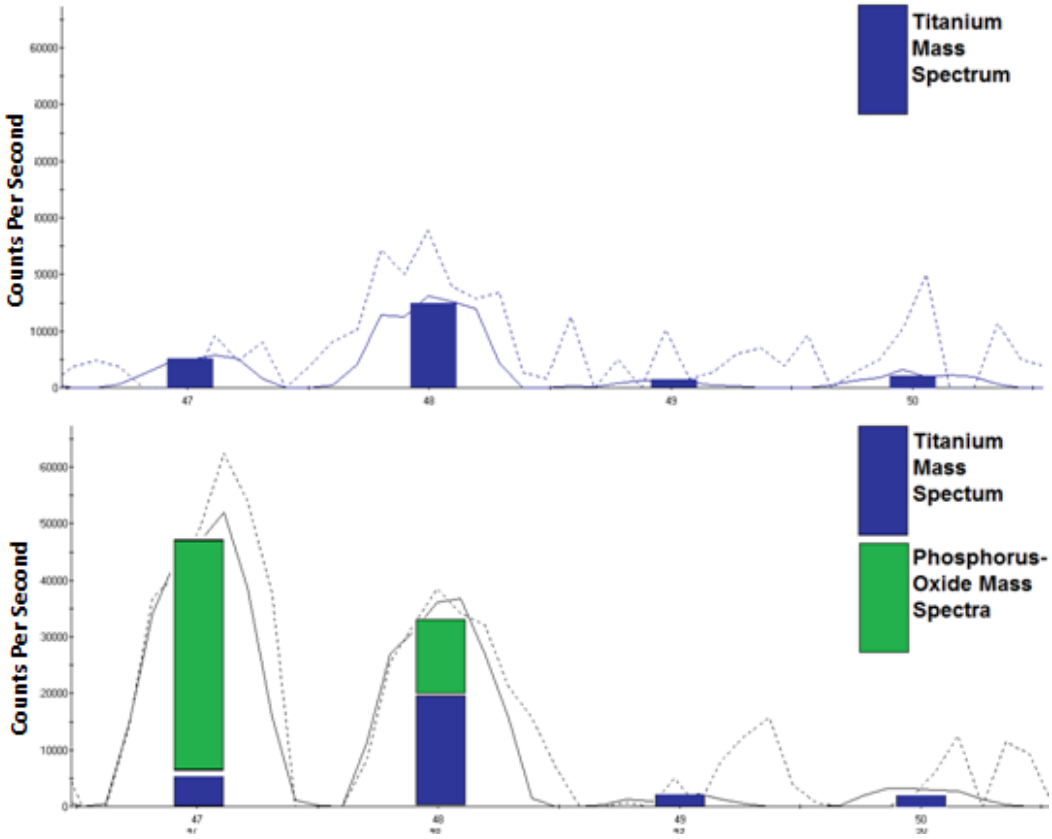

Figure 3.5. Mass spectra for two samples with similar amounts of Ti. One sample (above) had no organic content, while the second sample (below) had digested rat lung tissue which contained phosphorus.

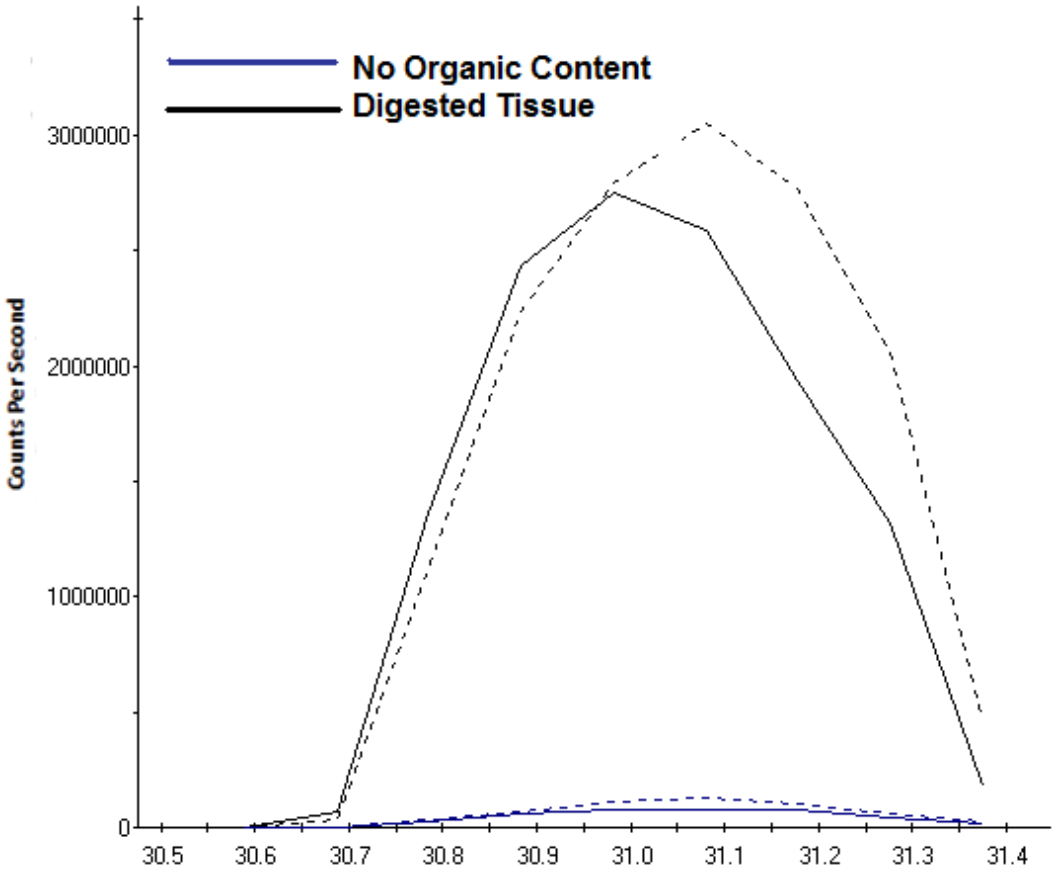

Figure 3.6. Phosphorus comparison between a digested rat lung sample with organics and a sample without organic material.

3.6 SUMMARY

- The digestion method degraded organic material enough that the samples could be analyzed by ICP without damaging the instruments.
- The digestion method had greater than 86% recovery of Ti.
- ICP-MS was the best choice for quantifying Ti because the detection limit of 164 ng/L was lower than ICP-OES detection limit.

- Ti isotope 49 m/z is the best isotope to monitor because it has the least interferences from other species like P-O and S-O complexes.
- The MDL for the digestion method was 1 µg TiO_2.

CHAPTER 4: TITANIUM DIOXIDE NANOMATERIAL MORPHOLOGY EFFECT ON DEPOSITION AND CLEARANCE IN RAT LUNGS

4.1 INTRODUCTION

4.1.1 Pulmonary deposition of TiO_2 nanomaterials. A review of literature regarding the deposition rates of TiO_2 nanomaterials stated that nanoparticles between 20-40 nm in diameter may deposit in the alveoli with 30-60% efficiency.[9, 61] Nanomaterials deposit by different mechanisms than larger particles because of their small size. Nanomaterials tend to deposit due to diffusion rather than inertial impaction, gravitational sedimentation, or interception like larger particles. [80] In terms of total mass, one rat inhalation study has shown that a 0.11 mg/m^3 TiO_2 aerosol containing 22 nm agglomerates resulted in a deposition of 4-5 µg per rat in just one hour of exposure. [68] It is important to distinguish between primary particle size and agglomerate size in the aerosol. One study generated an aerosol from 20-30 nm primary sized TiO_2 nanomaterials, but found that only a 0.5% mass fraction of the agglomerates had a diameter measuring less than 100 nm. As a result only 6.3% of the total aerosol deposited in the lung, a similar deposition rate to larger pigmentary TiO_2 particles. [98] While size is an important factor influencing nanomaterial deposition, the morphology of the lung, the respiratory conditions, and the physicochemical properties of the particles also influence deposition. [80]

4.1.2 Biopersistence of TiO_2 nanomaterials. TiO_2 particulates as a dust are categorized as a poorly soluble particulate (PSP), meaning they are unlikely to dissolve within the body. [75] It has been recommended that toxicology studies of PSP materials monitor post-exposure periods for at least 3 months because of the biopersistence of the materials in the lung. [99] TiO_2 nanomaterials may be retained for even longer than larger TiO_2 particulates because they can penetrate into lung tissues making macrophage clearance more difficult. [100] This longer clearance of nanomaterials is demonstrated in a study that showed the amount of TiO_2 nanomaterials in the avelolar space was not significantly different than fine TiO_2, but the total retention was greater for the nanosize TiO_2 because the particles had translocated into the pulmonary interstitium and persisted there. [79]

One measurement of biopersistence is half-life, or the time it takes for half of the total burden to be cleared. When rats were exposed to a nebulized solution of P25 TiO_2 nanoparticles at a high concentration (10 mg/m^3), the TiO_2 had a half-life of 395 days. [99] Another study of P25 showed similar results; after one year the original burden had decreased 57% in rats and 45% in mice. [75] Other studies with TiO_2 of similar primary particle size showed much faster clearance. One study demonstrated a decline of 51% after just 5 weeks and another showed 24% clearance in just 2 weeks. However, both determined that the particles had formed large agglomerates (200-300 nm diameter) in the

aerosol. [98, 101] Just as agglomeration affected the deposition rate, so too does it affect the clearance rate. The agglomeration size for deposition and clearance may be even more important than the primary particle size. [102] The dosage also affects the clearance rate. Higher dosages can result in a linear decrease of the lung burden, while lower dosages tend to have an exponential decay. [75]

4.1.3 Differences in TiO_2 nanoparticle morphology. Though many toxicology studies use P25 TiO_2 as a standard material, it is not representative of all types of TiO_2 nanomaterials. The crystal structure and particle shape are important factors as well. Exposure to anatase TiO_2 nanoparticles has been shown to produce significantly more pulmonary inflammation and lung tissue damage than rutile TiO_2 nanoparticles of the same size. [103] It has been theorized that anatase TiO_2 nanoparticles are more toxic because the crystal structure allows for a greater interaction between the DNA in the cells and the nanoparticles. [104] The anatase TiO_2 nanoparticles have been shown to be more readily taken up by cells. [102] The greater uptake can cause an increased retention time within the lung. This means that anatase nanoparticles can have a different toxicity level and different deposition and clearance rates than rutile nanoparticles. Alteration of TiO_2 nanomaterials to create a fiber structure like a nanobelt can cause an even greater increase in toxicity. TiO_2 nanobelts have been shown to be highly toxic, much like asbestos fibers. [105] TiO_2 nanobelts may have different deposition and clearance

rates as well because of their length. All TiO_2 nanoparticles are likely to have a higher deposition rate and increased cytotoxicity than larger TiO_2 microparticles like E171 that is used as a food additive.

4.2 PROBLEM STATEMENT

The morphology of TiO_2 nanomaterials has been shown to have an effect on deposition and clearance in the lung. This project intended to study how three different morphologies of TiO_2 nanomaterials—anatase nanoparticles, rutile nanoparticles, and nanobelts—affect the deposition into the lungs of rats after intratracheal instillation, and the clearance rate of the particles 1 day and 1 week after instillation by collaborators at UC-Davis. The rat lungs were digested to measure the total Ti in the lung. The digestion results were compared to the fraction of cells lavaged from within the lungs that have visible TiO_2 particles found inside the cell membrane.

4.3 MATERIALS AND METHODOLOGY

4.3.1 TiO_2 nanomaterials. Three types of TiO_2 nanomaterials were evaluated for their deposition and clearance in rat lungs. P25 TiO_2 nanoparticles were supplied by the Evonik DeGussa Corporation that consist of a 81%/19% anatase/rutile TiO_2 crystal structure mix with an average primary particle size of 24 nm. The P25 is referred to as “Rutile.” Another TiO_2 nanoparticle with a 100% anatase crystal structure and a 26 nm primary particle size was produced at Rochester University. This pure

anatase nanoparticle is referred to as “Anatase”. TiO_2 nanobelts were also evaluated, but no characterization data was provided.

4.3.2 Animals. The rats used in the instillation study were male Sprague-Dawley rats. The rats were 6-8 weeks of age upon being received and 8-10 weeks of age during instillation. The rats were received by the University of California-Davis from Hilltop Labs in Scottsdale, PA. All studies of the animals while they were alive were conducted at University of California-Davis.

4.3.3 Dispersion method. The nanoparticles were dispersed in a dispersion media composed of a phosphate buffered solution of glucose with dipalmitoyl phosphatidyl chlorine at 10 µg/mL and albumin at 0.6 mg/mL. The dispersion was probe sonicated on ice for 30 minutes. The total energy input was approximately 3700 J.

4.3.4 Intratracheal instillation. Suspensions were created at concentrations of 0, 20, 70, and 200 µg TiO_2 per 250 µL of each type of nanomaterial. The rats were lightly anesthetized using isoflurane in an airtight chamber before intratracheal instillation with 250 µL of suspension. The rats were then monitored until their scheduled necropsy date.

4.3.5 Broncoalveolar lavage. The rats were sacrificed either 1 day or 7 days post-instillation. The ribs were cut to expose the lungs and 5 separate aliquots of 5 mL of sterile saline solution were pushed through the trachea and recovered. The total 25 mL of saline solution were

retained for cell count analysis, cell type analysis, and biochemical analysis (results not shown here). After broncoalveolar lavage, the lung tissue was harvested and frozen.

4.3.6 Digestion. The right caudal and right cranial lung lobes of the animals exposed to the highest dosages of nanoparticles (200 µg/ 250 µL) were shipped on dry ice to Arizona State University for quantification of total TiO_2. Each lobe was digested individually. Since the moisture content of the rat lungs is variable, the lungs were dried overnight in the microwave vessels at 80°C to assess Ti concentrations per dry mass. It was found that after 8 hours the weight of the lung mass no longer decreased. The microwave vessels were weighed before and after the lungs were dried to find the dry mass. The lungs were then microwave digested at 180°C according to the settings listed in Table 3.1 with 2 mL HF and 8 mL HNO_3 to break down the tissue and the TiO_2. This method is described in detail in Chapter 3. There was one difference in the method used for the rat lungs rather than the tripe. The rat tissue dry mass was so small (20-50 mg typically) that no hydrogen peroxide was needed after microwave digestion during the acid evaporation to further digest the organics (See Appendix D, Photo D.5). Ti was quantified using the same ICP-MS analysis procedure detailed in Chapter 3. A study using a similar method of microwave digestion for Ti quantification of rat lungs with HF and HNO_3 demonstrated a 102% +/- 4.8 recovery. [87] Method blanks were run every 12 samples.

4.3.7 TiO_2 nanomaterial cell inclusion counts. The lavaged fluid was analyzed by microscopy to determine what fraction of the cells had observable TiO_2 nanoparticles within the cell membranes. 500 cells from each animal were observed to determine whether TiO_2 nanoparticles had entered the cells or not. The cell counts were then compared to the Ti concentrations to determine the correlation. All microscopy work and cell inclusion counts were conducted at UC-Davis

4.4 RESULTS

4.4.1 Digestion results. Lobes from 66 animals were digested. Lobes were only examined from the animals exposed to the highest dosage of each nanomaterial, which was 200 µg/250 µL. Since each animal was instilled with 250 µL, the maximum mass in the lungs would be 200 µg if all the TiO_2 deposited. The total Ti in each lung lobe sample varied greatly from animal to animal. The largest amount of Ti was found in the caudal lobe of animal P1148. The animal had been exposed to anatase TiO_2 nanoparticles and 51.9 µg of Ti remained in the lung 1 day post-instillation. The largest amount of Ti found in a cranial lobe was found in animal P1110. The animal had been exposed to rutile TiO_2 nanoparticles and 8.1 µg of Ti remained in the lung 7 days post-instillation. However, the values varied greatly with some animals appearing to have virtually no Ti in either lobe. The method blank average was 0.29 µg +/- 0.12 µg (n=12) of Ti per sample and was consistently low. The larger

caudal lobes tended to have more total Ti than the cranial lobes. The results are shown in Figure 4.1.

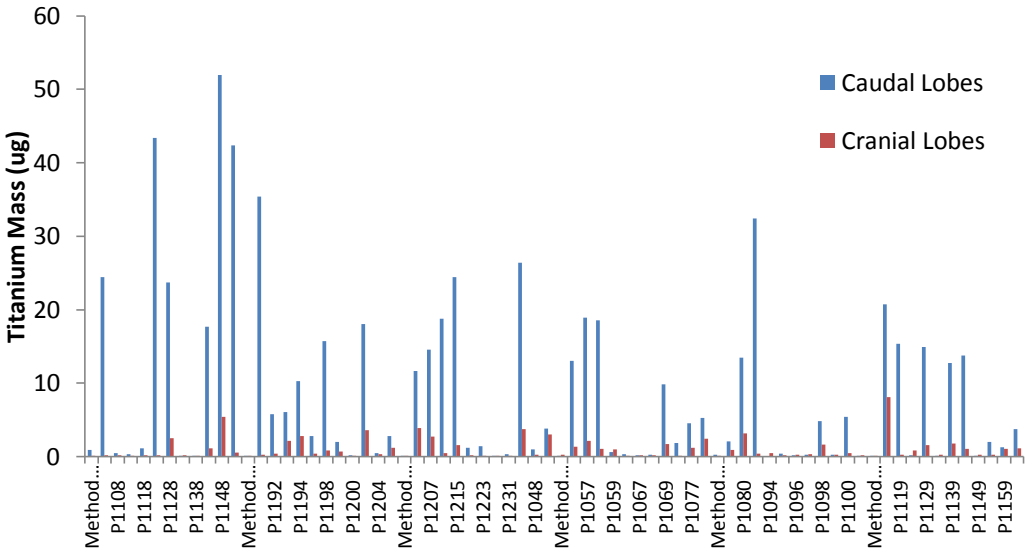

Figure 4.1. Total Ti mass in rat lungs determine by microwave digestion.

The Ti mass was used to calculate the mass of TiO_2 that was deposited and then normalized to the dry weight of each lung lobe. Again, the normalized TiO_2 in each lung lobe sample varied greatly from animal to animal. The highest normalized concentration of TiO_2 was found in the caudal lobe of animal P1148. The animal had been exposed to anatase TiO_2 nanoparticles and 3.46 µg TiO_2/mg dry tissue remained in the lung 1 day post-instillation. The highest normalized concentration of TiO_2 found in a cranial lobe was found in animal P1206. The animal had been exposed to TiO_2 nanobelts and 0.72 µg TiO_2/mg dry tissue remained in the lung 7 days post-instillation. The larger caudal lobes tended to have a

higher concentration of TiO_2, but the difference between caudal and cranial lobes was smaller than the total titanium mass difference between lobes. This is because the average mass of the caudal lobes was twice as much as the cranial lobes. The results are shown in Figure 4.2.

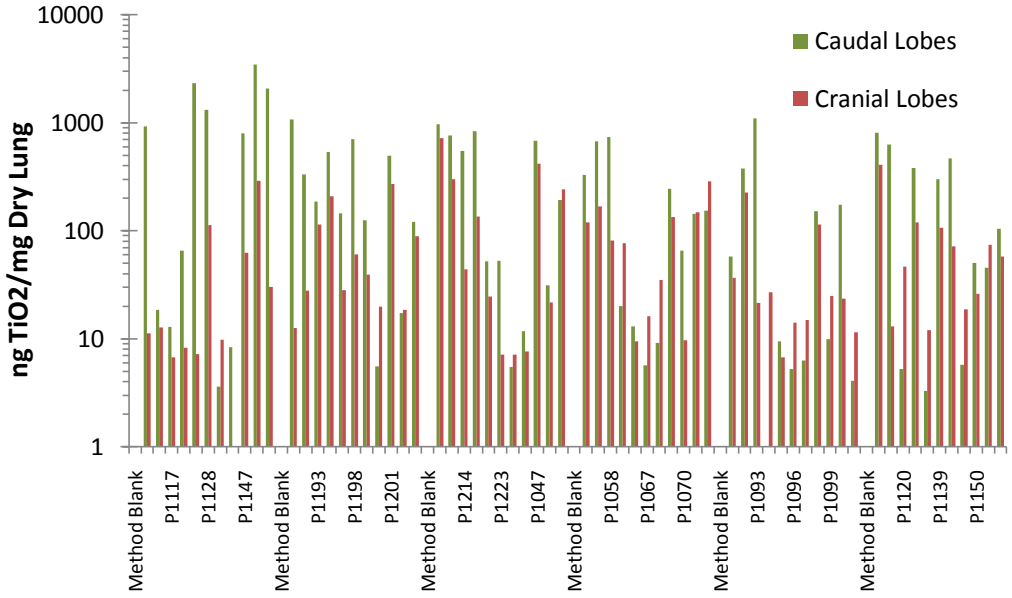

Figure 4.2. Normalized TiO_2 concentration in rat lungs.

4.4.2 TiO_2 nanomaterial comparison. Despite all animals being exposed to the same dosage of TiO_2 nanomaterials, certain morphologies were more likely to be found in the lung. In the caudal lobes, a greater mass of the anatase TiO_2 nanoparticles were detected meaning that they deposited to the highest degree. After 7 days the average mass of TiO_2 had lower than one day. The rutile TiO_2 nanoparticles and TiO_2 nanobelts deposited to approximately the same degree. The rutile and nanobelt TiO_2 mass remained relatively constant from day 1 to day 7. The average

titanium masses depositing in the caudal lobes for each TiO_2 nanomaterial morphology are shown in Figure 4.3.

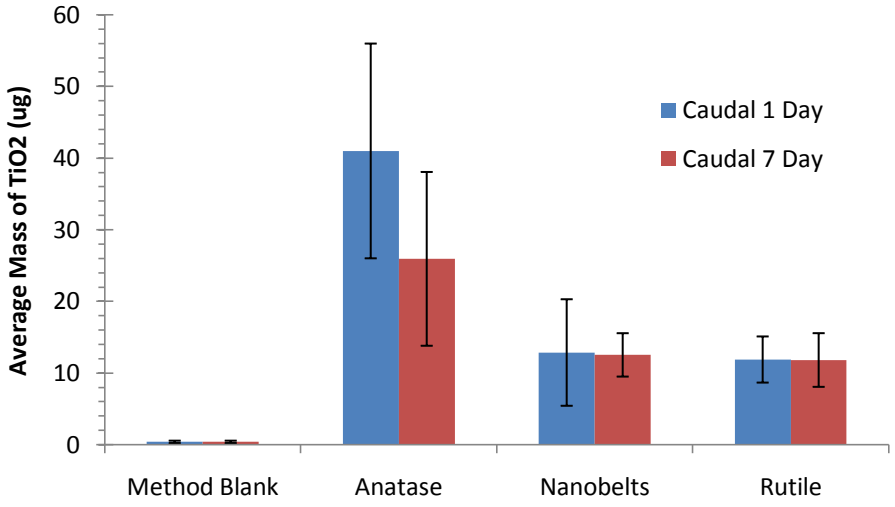

Figure 4.3. Average mass deposited in caudal lobe by nanomaterial type. Error bars represent the standard deviation of the TiO_2 mass for the sampled lung lobes.

In the cranial lobes, there was no significant difference in deposition between nanomaterial morphology. There was also no trend in clearance with the rutile nanoparticles and nanobelts actually having a higher mass remaining in the lung after 7 days compared to 1 day. The average titanium mass depositing in the cranial lobes for each TiO_2 nanomaterial morphology are shown in Figure 4.4.

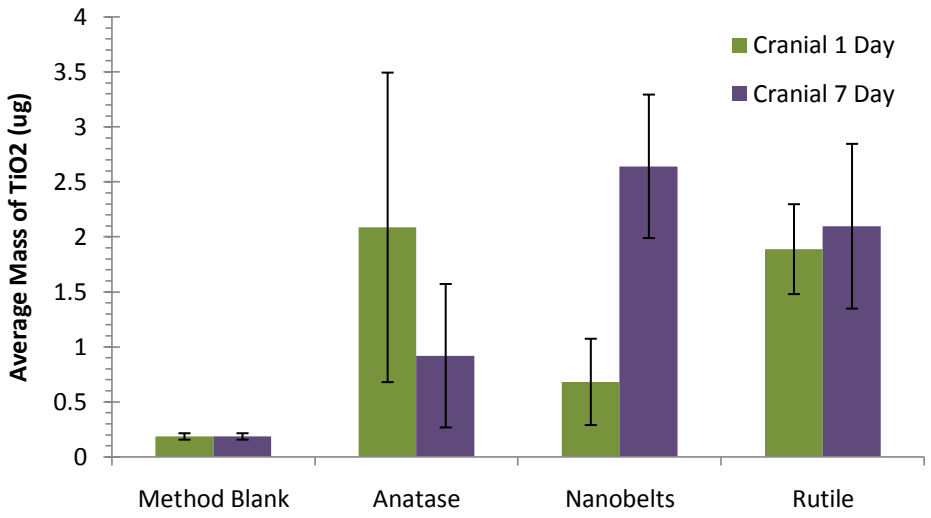

Figure 4.4. Average mass deposited in cranial lobe by nanomaterial type. Error bars represent the standard deviation of the TiO_2 mass for the sampled lung lobes.

The normalized TiO_2 concentration in the lungs followed the same trends as the total mass. The anatase TiO_2 nanoparticles had a higher concentration in the caudal lobes than either of the other two TiO_2 nanomaterial morphologies. The concentration decreased after 7 days for the anatase particles, increased for the nanobelts, and remained relatively constant for the rutile particles. The concentrations in the cranial lobes were much lower than the caudal lobes for all morphologies. The normalized TiO_2 concentrations deposited in the cranial lobes for each TiO_2 nanomaterial morphology are shown in Figure 4.5.

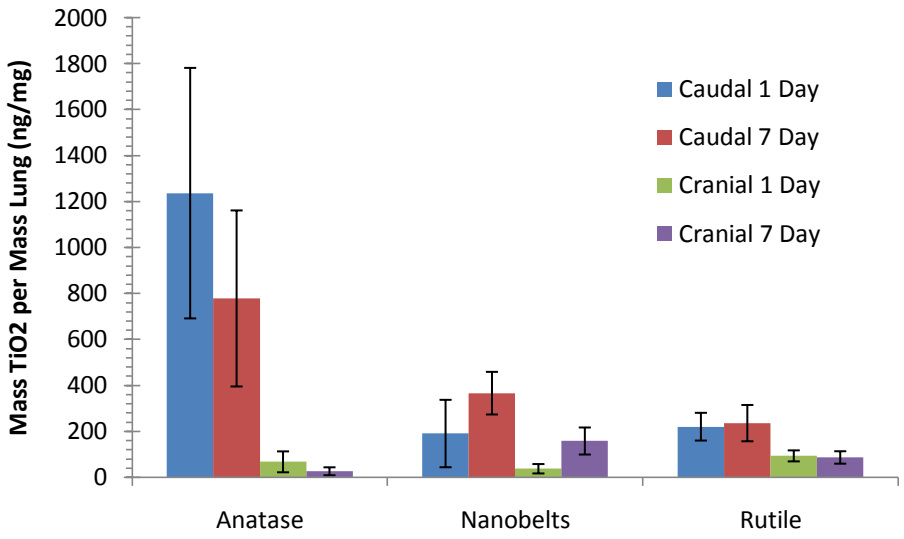

Figure 4.5. Normalized TiO_2 concentrations in both caudal and cranial lobes for all TiO_2 morphologies. Error bars represent the standard deviation of the TiO_2 concentration for sampled lung lobes.

4.4.3 Lung clearance significance. When comparing the caudal lobe TiO_2 concentrations from 1 day post instillation to 7 day post instillation, it was necessary to determine if the levels changed a significant amount. The 90% confidence interval was determine based on the standard deviation and sample size for each of the morphologies 1 day post instillation. No morphology had a difference 7 days post instillation that was outside of the 90% confidence interval. The same was seen for an 80% confidence interval. When applying a 70% confidence interval to the 1 day instillation concentration means, the nanobelt TiO_2 concentration was outside of the confidence interval. However the concentration actually had increased rather than decreased from day 1 to

day 7. The decrease of concentration of the anatase nanoparticles was only deemed significant outside of a 60% confidence interval. The TiO_2 mean 1 day concentration for each morphology can be seen with the confidence levels in Figure 4.6 along with the TiO_2 mean 7 day concentrations.

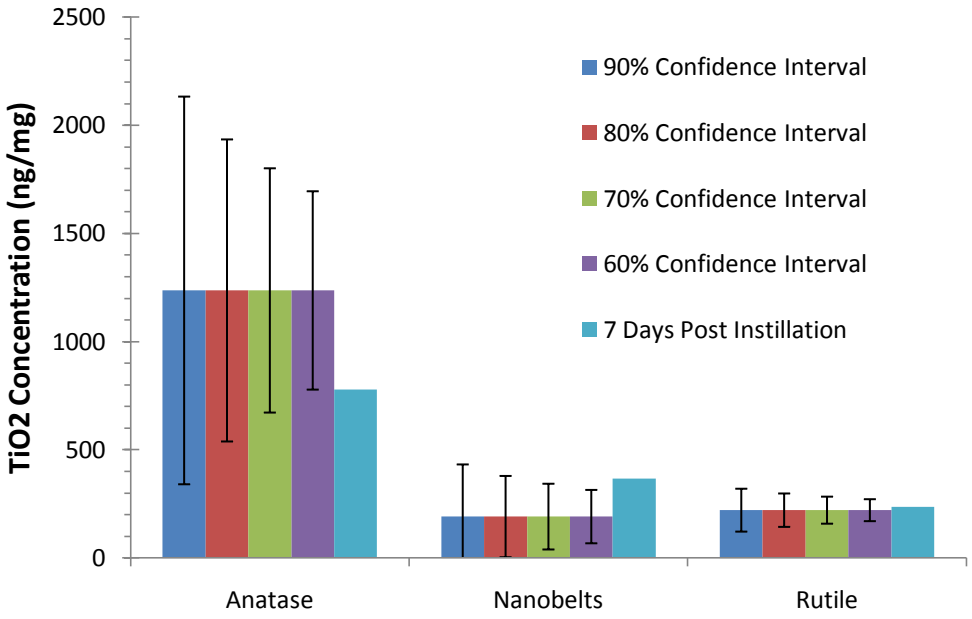

Figure 4.6 Caudal lobe mean TiO_2 concentrations for 1 day post instillation with various confidence levels as well as the 7 day post instillation.

4.4.4 Cell inclusion results. For each animal, the broncoalveolar lavage fluid was analyzed at UC-Davis to determine what fraction of the cells had TiO_2 nanoparticles within the cells. The resulting counts are in number of cells with visible particles per 500 cells. The data is for each animal rather than each lobe because the solution is lavaged through the whole lung. The nanobelts could not be clearly seen in the cells for all of

the animals so there are no cell count data for the animals exposed to the nanobelts. One successful image using cross polarized light of TiO_2 nanobelts within a cell is shown in Figure 4.9, however the same technique did not work for all of the samples. Of the animals exposed to the anatase and rutile nanoparticles, the number of cells with TIO_2 nanoparticles in the cells varied greatly from animal to animal. The highest number of cells with visible TiO_2 nanoparticles was animal P1110. The animal had been exposed to rutile TiO_2 nanoparticles and had 148 cells with visible particles from the lavage 7 day post-instillation. The animals exposed to the anatase TiO_2 nanoparticles that were lavaged after one day had the highest number of cells with visible particles. The number decreased at 7 days. The number of cells with rutile particles was less than the anatase and actually increased from day 1 to 7. The results for each animal are shown in Figure 4.7 and the average for each type of nanoparticle is shown in Figure 4.8.

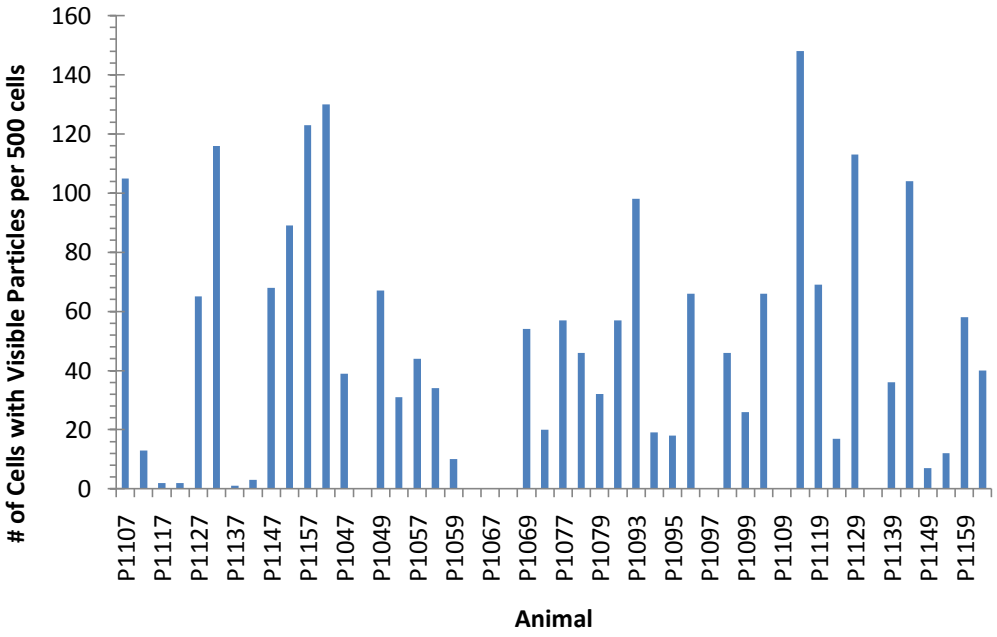

Figure 4.7. Number of cells with visible TiO_2 nanomaterials. Data provided by UC-Davis

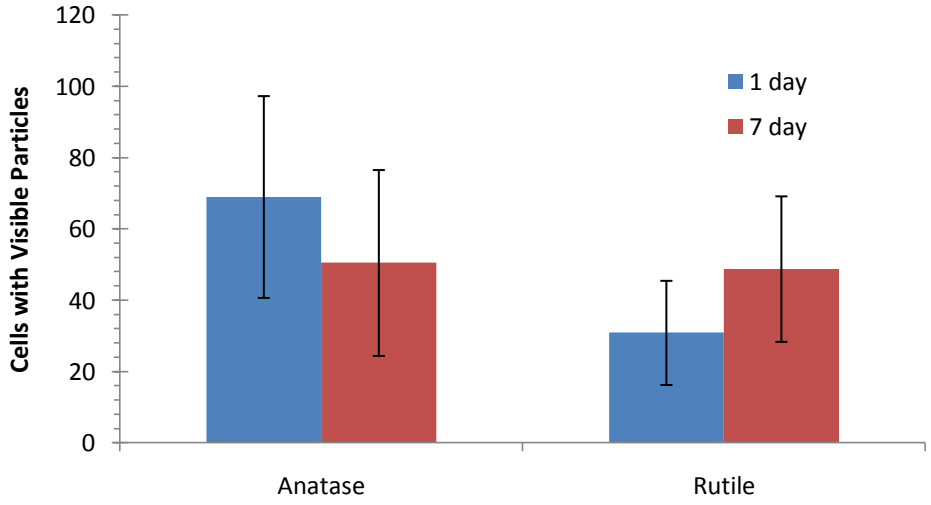

Figure 4.8 Average results for the number of cells with visible TiO_2 nanomaterials. Error bars represent the standard deviation of the cell counts. Data provided by UC-Davis.

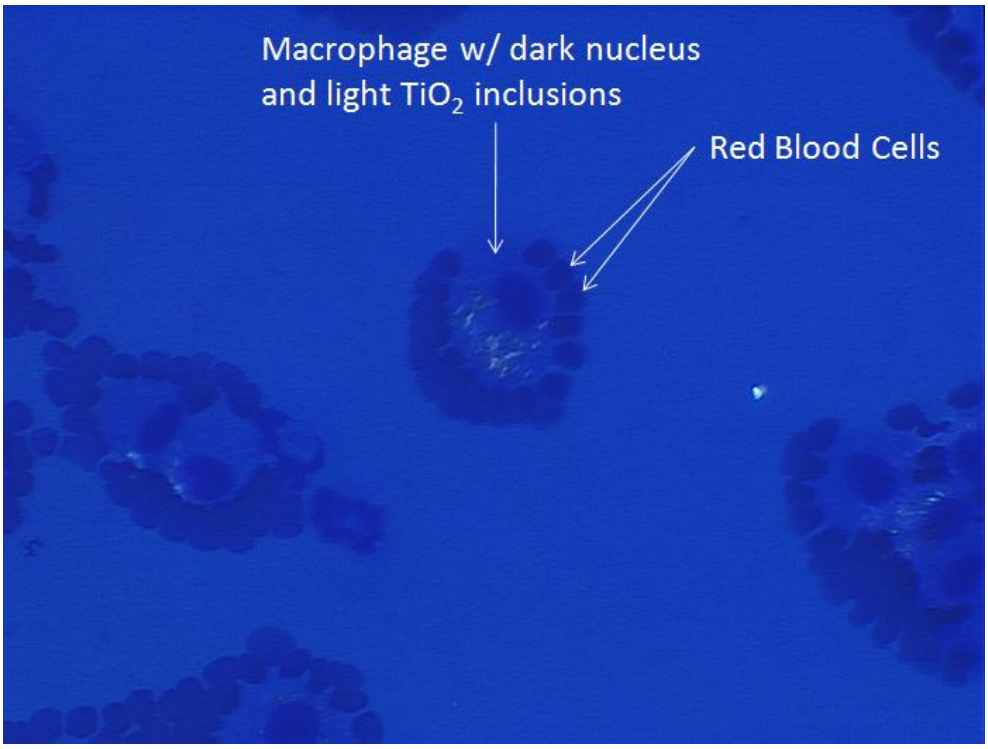

Figure 4.9. Animal P1229 broncoalveolar lavage cells with TiO_2 nanobelt inclusions. Shown at 40x. Image provided by UC-Davis.

The results of the cell count microscopy and the lung digestions were compared to determine if there was a good correlation between the two methods of determining the TiO_2 nanomaterial lung burden. There was a positive correlation between the two metrics. A linear regression line was applied to the data and the R^2 value was 0.376. A plot of the TiO_2 concentration compared to the cells with visible particle numbers is shown in Figure 4.10.

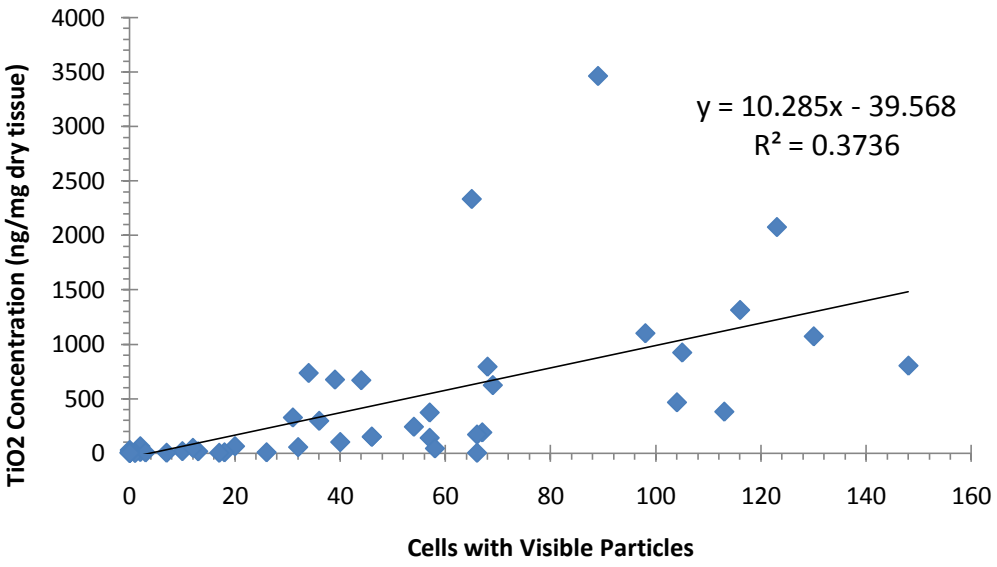

Figure 4.10 Correlation between cells containing visible TiO_2 particles and the TiO_2 concentration in the caudal lobes.

4.5 DISCUSSION

The study shows that with equal doses of TiO_2 nanomaterials, the anatase particles are more likely to deposit in the lung. The anatase nanoparticles appeared to clear from the lung from 1 day post-instillation to 7 days post-instillation. No clearance trend can be observed in any of the other nanomaterials. This is could be because the study did not last long enough. As stated in the introduction of this chapter, a toxicology study should observe the animals for at least 3 months post exposure. Thus, any difference from day 1 to day 7 could just as easily be attributed to inefficient instillation or differences between the animals rather than actual clearance from the lung. Most of the TiO_2 nanomaterials deposited

in the caudal lobe rather than the cranial lobe. When TiO_2 was observed in the cranial lobe it was also observed in the caudal lobe, however the converse was not necessarily true. The concentration data for the cranial lobes may have a larger degree of error than the caudal lobes because when the cranial lobes were dried, their mass was so small that even small errors in the weight can cause a high percentage of uncertainty. The average mass was only 24.7 mg.

A number of lungs had Ti concentrations so low it appeared that there was no exposure. Many of these were verified by the cell inclusion counts because no cells were observed with particles. This is likely because the instillation method does not always work. Sometimes rather than being instilled in the lungs, the solution is swallowed. There are other factors that can show why the correlation between the two lung burden metrics did not show a better correlation. Only 2 lobes of the lung were digested, but the lavage was from the total lungs. The instillation could have all gone into the left lobes which would cause there to be a large number of cells with visible particles, but a low concentration from the digestion of the right lobes. How the instilled solution was distributed through the lungs would change the Ti concentration determined by the right lobes for the same overall deposition rates. However, it was a good sign that there were no false positives from the digestion method; any lobes that measured significant TiO_2 concentrations had observable TiO_2 in the cells.

4.6 SUMMARY

- Anatase TiO_2 nanoparticles deposited in rat lungs to a greater degree than rutile nanoparticles or nanobelts with an average of 41 µg of Ti found in caudal lobes 1 day after exposure to anatase TiO_2. This was 218% higher than the second highest average concentration.
- The anatase TiO_2 nanoparticles were also found at the highest concentration in the caudal lobes with 1236 ng Ti/mg dry tissue as the average.
- TiO_2 nanoparticles concentration were found to be 58% higher in caudal lobes than in the cranial lobes for anatase TiO_2. Similar trends were observed for all morphologies.
- There was no significant evidence that there was less TiO_2 material in the lung 7 days after instillation when compared to 1 day after instillation for all morphologies. The Ti concentration had increased beyond the 80% confidence interval level for nanobelts from day 1 to day 7.
- The Ti lung concentrations from the digestion of the lungs showed an R^2 agreement of 0.376 with cell inclusion counts conducted with microscopy.

CHAPTER 5: NANOSCALE FRACTION OF TITANIUM DIOXIDE USED IN FOOD PRODUCTS

5.1 INTRODUCTION

TiO_2 is used in as an additive in foods for coloring because—as a microparticle—it has a bright white color. [106] A very low amount of Ti is naturally occurring in foods, especially vegetables, because of the high Ti content in the soils. Soybeans and shrimp with no additives were measured to have a Ti concentration of 3.23 µg/g and 2.52 µg/g respectively. [76] However, for the most part Ti and more specifically TiO_2 found in foods is included as an additive.

5.1.1 Pigmentary TiO_2 additives. TiO_2 is added as a whitening agent to foods like dressing, gum, icing, cookies, and candies in a primarily microparticle form that is known as E171. [107] TiO_2 is also sometimes used as an additive to create a barrier between layers of different colors in foods. [108] TiO_2 is an ideal pigment because it is stable to heat, light, oxygen, and pH making it unaffected by almost any food processing. [106] These same qualities make it resistant to degradation in the body. TiO_2 is used as an inert marker for studies of the digestibility of foods in animals. [81] The digestive system is exposed to exogenous, inorganic microparticles. The most common of these microparticles are TiO_2 and silicates.[109] A western diet may expose the gastrointestinal (GI) tract to as many as 10^{12} inorganic microparticles per day from food

additives. [110] TiO_2 used as a color additive may results in the ingestion of up to 112 mg of Ti per person per day. [109]

The Food and Drug Administration (FDA) regulates food safety in the United States. They have recognized synthetically prepared TiO_2 as a color additive in foods. The U.S. Code of Federal Regulations states that "any color additive intended solely for coloring purposes shall be labeled." [111] However, it has been shown that many foods that contain TiO_2 do not list TiO_2 as an ingredient, and those that did gave no indication of how much TiO_2 is included in the product. [108]

5.1.2 TiO_2 nanomaterials in food. Nanomaterials engineered specifically to be used as food additives are uncommon because at such a small size they lose their white coloring, but they are increasingly being used in other areas of the food production industry. [112] Nanotechnology has been applied in agriculture cultivation, food processing, food packaging, and water purification. [113] TiO_2 nanomaterials specifically have been used in the food industry for their photcatalytic antimicrobial properties. TiO_2 nanomaterials used with UV light have been shown to increase the quality and shelf life of food by reducing the bacteria. [114, 115] TiO_2 nanotubes and TiO_2 nanopowders have been used for food packaging and have been shown to cause an inactivation of *E. Coli, Salmonella,* and *Staph* bacteria. [116, 117] TiO_2 nanomaterials have been applied in films onto steel and glass surfaces used in the food processing industry to prevent biofilms from growing on the surfaces. [118, 119] As a

result of the increased use of nanotechnology in the food production industry, there is an increased likelihood that TiO_2 nanomaterials may ultimately end up in the food products from contact with packaging or coated surfaces. Other ways have been proposed that TiO_2 may enter into the food chain. TiO_2 nanoparticles with a diameter less than 5 nm can be taken up by plants and it has been hypothesized that they may biomagnify as they move up the food chain. [120] So while TiO_2 nanomaterials may not specifically be engineered to be food additives; they can still end up in food products.

Ingesting food products is the primary way that TiO_2 may enter the digestive system, but it is not the only way. [61] TiO_2 that is cleared from the lungs by the mucocilliary is often swallowed. TiO_2 may be accidently ingested by those in TiO_2 production facilities or by hand-to-mouth contact after using personal care products containing TiO_2. [112] New medical products are using TiO_2 nanomaterials that may reach the digestive system. [121] There are numerous ways that TIO_2 nanoparticles can enter the digestive system in addition to the ingestion of food.

5.1.3 Effects caused by ingestion of TiO_2 microparticles.

Though TiO_2 is not readily degradable by the body and up to 98% may pass through the digestive system and be recovered in the fecal matter, there can still be some slight absorption by the GI tract. [81] 500 nm particles orally exposed to rats were found in all major gastrointestinal associated lymphatic tissues (GALT) with limited translocation to the liver

and spleen. [63] Macrophages in the GALT actually become loaded with a dark pigment from aluminum, silicon, and titanium microparticles, with a significant amount coming from TiO_2 spheres with a diameter of 100-200 nm that are believed to have come from coloring additives. [122] Though microparticles like TiO_2 have a limited effect on macrophages; they can aggravate ongoing inflammatory responses in the GI tract. [110]

Crohn's disease can cause an inflammatory response in the GI tract. Similarly to how asthma patients are sensitive to microparticle exposure in the air, patients with Crohn's disease are sensitive to microparticles in food. [123] It has been shown that a diet low in microparticles like TiO_2 color additives can alleviate the symptoms of Crohn's disease. [124] It has been hypothesized that negatively charged TiO_2 particles in the gut may bind metal cations that are then coated with inflammatory bacterial anions. [123] TiO_2 microparticles may often be described as inert, but there are acute effects in the body, especially to those with preexisting inflammatory conditions in their GI tract.

5.1.4 Effects caused by of ingestion TiO_2 nanomaterials.

Similar to TiO_2 microparticles, TiO_2 nanomaterials are capable of being absorbed by the GI tract to a small degree. The reason more TiO_2 is not absorbed is that the absorption occurs primarily through the Peyer's Patches in the intestine. These patches only occupy a small fraction of the surface area in the intestine. [61] At high concentrations (> 10 µg/mL), TiO_2 nanomaterials in the intestines can cross the epithelial lining at low

levels. [41] From the GALT, orally administered TiO_2 nanoparticles of 25 and 80 nm diameter both translocated to the liver, kidney, and spleen, but with no obvious acute toxicity. [33] TiO_2 nanomaterials ingested by terrestrial isopods showed a decrease in activity of antioxidant enzymes, but no effects were observed on higher level endpoints like weight, feeding habits, or survival. [125] Addition of TiO_2 nanomaterials to the food of terrestrial invertebrates caused similar effects and was controlled by the duration of exposure rather than total dose, a trend that is different than soluble chemicals. [126]

5.1.5 Release of TiO_2 nanomaterials to the environment.

Ingested TiO_2 nanomaterials may cause some acute effects on humans and other organisms, but the majority of the ingested dose passes through the body and end up in fecal matter. [81] It has been shown that TiO_2 from human waste ends up in wastewater and eventually at WWTPs. [46, 47] From WWTPs TiO_2 nanomaterials can be released to the environment.

5.2 PROBLEM STATEMENT

TiO_2 nanomaterials may end up in food products from packaging and processing. However, they are not as prevalent as TiO_2 microparticles used in food products as a coloring additive. The size of pigmentary TiO_2 microparticles is not uniform, but rather a distribution of sizes. It is hypothesized that some of the particles included in pigmentary TiO_2 are in the nanoscale range. This research project intended to study a

number of foods with and without TiO_2 listed as an ingredient to determine if TiO_2 is present. The total TiO_2 was quantified to understand the total TiO_2 mass a person may be exposed to from a normal diet. The smallest particles were isolated and quantified to better understand the size distribution of TiO_2 used as a food coloring additive and if TiO_2 nanoparticles are included in pigmentary TiO_2.

5.3 MATERIALS AND METHODOLOGY

5.3.1 Food products. Eighty nine different food products were purchased in Arizona grocery stores in March 2011. Different types of products were chosen—many because they were white—including sauces, dairy products, confectionaries, candies, beverages, chocolates and gums. These products were more likely to have additives then foods with limited processing like fruits, vegetables, and unprocessed meat. Attempts were made to purchase at least 2 brands of each product, usually a name brand and a separate generic brand. Samples were transported to the laboratory and stored in a clean, dry cupboard or refrigerated and analyzed prior to expiration dates listed on the product labels. Information about the products, including the serving size and whether or not TiO_2 was listed on the label was recorded.

5.3.2 Digestion. For samples with serving sizes measured by mass, 500 mg of each food were weighed and added to a clean microwave digestion vessel. Foods were weighed as is rather than dried

because serving sizes are not based on dry weight. For samples with serving sizes measure by volume, 5 mL of each food or beverage were pipetted into a clean microwave digestion vessel. The foods were then microwave digested at 180°C according to the settings listed in Table 3.1 with 2 mL HF and 8 mL HNO_3 to break down the tissue and the TiO_2. This method is described in detail in Chapter 3. Some of the foods with a large amount of organics were not totally broken down by the initial 2 mL of hydrogen peroxide added after digestion. As the liquid was evaporated, if it became apparent that there was organic material remaining in the sample, it was cooled and then 2 mL of hydrogen peroxide was added and the sample was heated again. It is important to note that samples with high concentrations of Ti will turn orange with the addition of peroxide in an acidic environment. [83] (See Appendix D, Photo D.9) Ti was quantified using the same ICP-MS analysis procedure detailed in Chapter 3. All samples with Ti concentrations outside of the calibration range were diluted and re-analyzed. A study using a similar method of acid digestion for Ti quantification in food matrices demonstrated a precision of typically 1% or better. [81] Method blanks were run every 12 samples and the average for the blanks was 0.58 µg +/- 0.29 from 12 method blanks.

5.3.3. TiO_2 materials. The digestion method was evaluated for recovery of TiO_2 nanoparticles and TiO_2 microparticles in a food matrix. 50 mg of each material was spiked into 500 mg of chocolate. Chocolate was chosen because it is known to have a very low concentration of TiO_2

so an accurate recovery percentage can be determined. It is also relatively difficult to digest for a food. The microparticles used were E171 pigmentary TiO_2 purchased from Fiorio Colori Spa in Italy with an average primary particle size of 110 nm. The nanoparticles used were P25 TiO_2 purchased from the Evonik DeGussa Corporation with an average primary particles size of 24 nm. Each TiO_2 nano powder was analyzed by SEM to determine the primary particle size. The E171 TiO_2 particles were then dispersed in nanopure water with Bovine Serum Albumin (BSA). The P25 TIO_2 particles were dispersed in nanopure water and the solution was sonicated for 30 minutes according to the stock preparation method described in Appendix B. Solutions were analyzed using phase analysis light scattering (PALS) to identify the size distribution and find the average aggregate size after dispersion.

5.3.4 Separation method. In order to determine how much TiO_2 is in the nanosize range a separation method had to be created to separate smaller TiO_2 from larger TiO_2 and organic materials. 500 mg of a food sample was added to a beaker. The organic material from the food was broken down by adding 10 mL of hydrogen peroxide and 0.5 mL of HNO_3 and heating on a hot plate at 110°C. When the volume of liquid remaining in the sample was less than 1 mL, the beakers were removed from the hot plate and allowed to cool. The beaker sides and bottom were then rinsed with approximately 20 mL of nanopure water. The sample was filtered with a 0.45 µm nylon filter and added to a microwave vessel. To

determine the total TiO_2 that was able to pass the 0.45 µm filter the sample was then digested using the microwave digestion with HF and HNO_3. For microscopy analysis, after the sample was filtered with a 0.45 µm nylon filter, it was poured into a 25 mL volumetric flask and filled to the 25 mL mark with nanopure water. In this way the final concentration of the undigested TIO_2 particles that pass the 0.45 µm filter will be the same as the concentration of the digested TiO_2 particles that pass the 0.45 µm filter. A 0.45 µm filter was chosen because preliminary tests evaluating 0.45 µm filters and GF/F filters (data not shown here) found that a measurable amount of Ti was able to pass both filters. Since 0.45 µm filters have a smaller pore size than the 0.7 µm pore size of GF/F filter, the 0.45 µm filter was selected to remove any particles larger than 450 nm. The pH of the samples was determined before filtration to ensure that the nylon filter would not be damaged during filtration.

5.3.5 Microscopy. The control TiO_2 particles, E171 and P25 were analyzed by SEM to find the primary particle size. P25 Nanoparticles had a more consistent particle diameter of 20-30 nm. E171 had a wider variance in primary particle size with some being nanosized (< 100 nm) and others being as large as 250 nm in diameter. (See Figure 5.1)

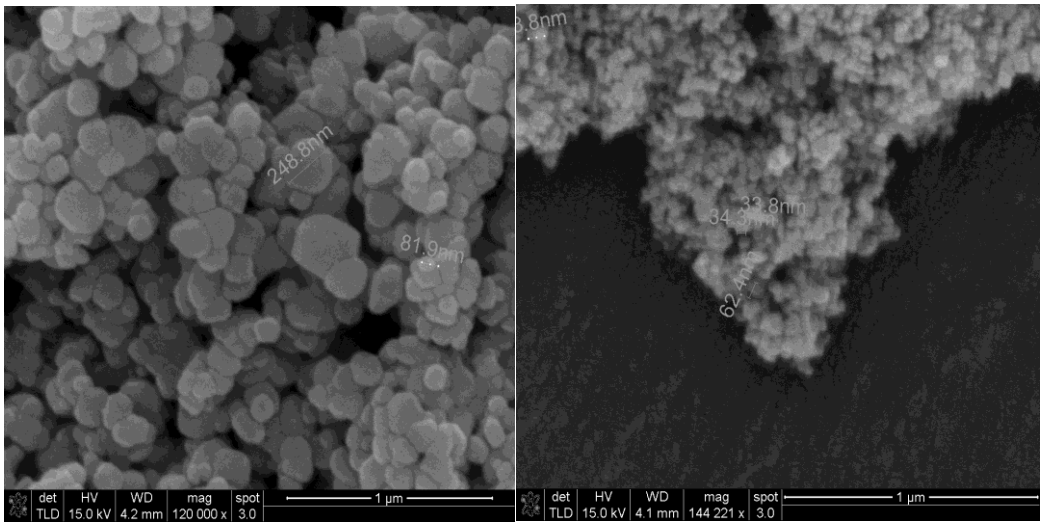

Figure 5.1. SEM images of E171 (left) and P25 (right) TiO_2 materials.

5.4 RESULTS

5.4.1 TiO_2 particle characterization. After dispersion in nanopure water the two TiO_2 control particle solutions were analyzed by PALS and the results are shown in Table 5.1. After dispersion the aggregate size of the P25 was still smaller than the primary size of the E171 and still nanosized (<100 nm).

Table 5.1

Primary Particle Size and Aggregate Size for TiO_2 Control Particles.

TiO_2 Particle	Primary Particle Size	DLS (in BSA)
E171	110 nm	380 nm
P25	24 nm	60 nm

5.4.2 TiO_2 recovery tests. The recovery of two different types of TiO_2 was each greater than 80%. The samples were run in triplicate and

the standard deviation was approximately 2.5%. The average Ti from the chocolate was less than 0.1% of the 50 mg P25 and E171 added to the samples. The recoveries are shown in Table 5.2.

Table 5.2

Digestion Recovery for P25 and E171 TiO_2.

TiO_2 Particle	P25 50 mg	E171 50 mg
Recovery	81 %	87 %
Standard Deviation (n=3)	+/- 2.7 %	+/- 2.3 %

5.4.3 Total TiO_2 in food. All eighty nine foods were digested and the concentration of Ti in the food was determined. 16 of the foods were digested in triplicate. The agreement amongst the triplicates was good, all within 30%. The blank average was 0.579 µg. The highest concentration in any food was Dickinson's Coconut Curd at 3.59 µg/mg. The rest of the Ti concentrations spanned 5 orders of magnitude with some foods having levels below the detection limit for the method. The 20 highest Ti concentrations in food are shown in Figure 5.2. The concentrations for all 89 foods are shown in Appendix A, Figure A.1.

The gum products consistently had some of the highest concentrations of Ti of any products. The 5 gums that were analyzed all were within the top 17 products in terms of Ti concentration all with greater than 0.12 µg Ti/mg. Of those 5 gum products, the cinnamon gum that had a red coating was the lowest. The white colored gums made up 4 of the

13 foods with the highest Ti concentration. It is important to note that all the gum products were the types of gum with a hard shell coating the gum-based center. Other candy products that had a hard outer shell also had high Ti concentrations. The candy products wither hard shells (M&Ms, M&Ms with peanuts, and Good and Plenty) all were in the top 10 for Ti concentration. When you combine the gums and candies into a more general hard shell candy category, 8 of the 17 products with the highest Ti concentrations would fall into the hard shell category.

Another group of food products that was well represented in the top 20 highest Ti concentrations were powder products that were mixed into foods. Two brands of Kool-Aid drink mix were in the top 14 for products with the highest concentration of Ti. Albertson's Vanilla Pudding and Jell-O Banana Pudding were ranked at 8th and 12th respectively. However, other powdered products like Carnation Instant Breakfast and Nestle Coffee Mate had much lower concentrations at 33rd and 61st highest with less than 0.015 µg Ti/mg for both products.

Chocolate products that did not have a hard outer shell had much lower concentrations compared to those with a shell. Hershey's Special Dark chocolate bar had the highest concentration for chocolate products without a shell at 0.0050 µg Ti/mg. This can be compared to M&Ms which had a Ti concentration of 1.25 µg Ti/mg. Dairy products like cheeses, mayonnaise, routinely had low concentrations of Ti with 10 of the 12 products with the lowest Ti concentrations were dairy products. The

highest of any dairy product was Albertson's American Single cheese with 0.0069 µg Ti/mg which ranked it 37th on the food product list.

There was generally not a significantly large difference between generic and name brand products. The largest came between Albertson's Mini Marshmallows at 0.307µg Ti/mg and Kraft Jet Puffed Marshmallows at 0.00255 µg Ti/mg. However, other comparison products ranked were nearly identical. For instance, Hershey's Chocolate Syrup and Albertson's Chocolate Syrup were measured at 0.0026 and 0.0025 µg Ti/mg respectively. Likewise Nestle Coffee Mate and Albertson's Coffee Creamer measured 0.040 and 0.036 µg Ti/mg respectively.

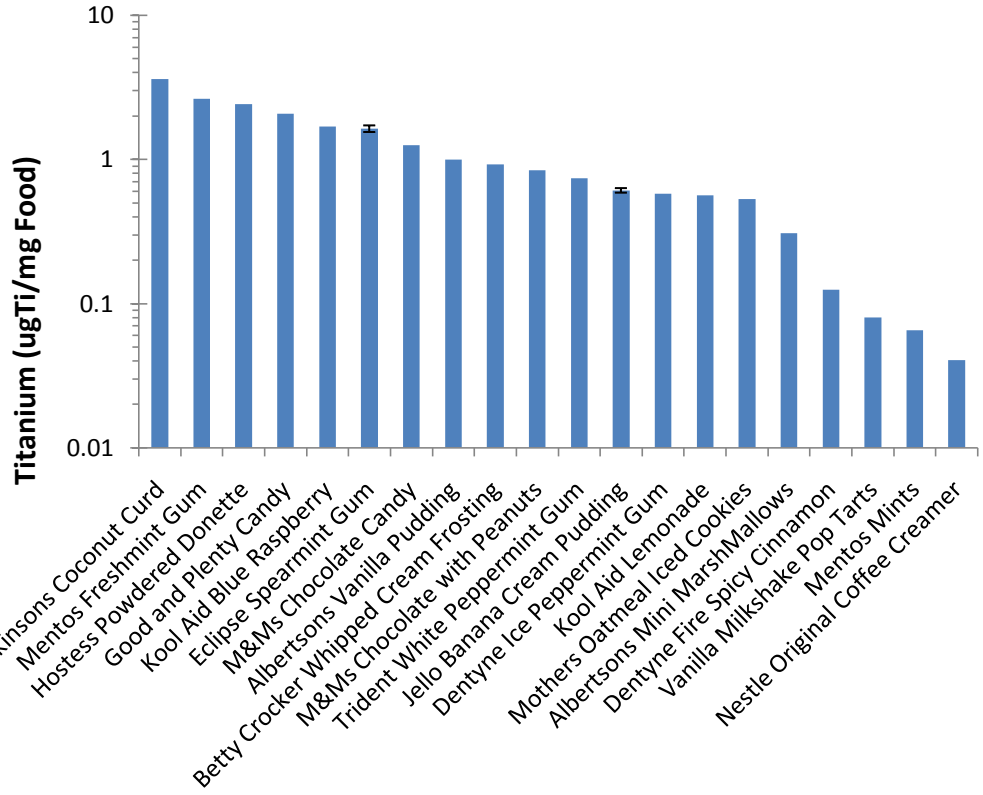

Figure 5.2. Normalized Ti concentration in food products. Error bars represent standard deviation from samples digested in triplicate.

Using the Ti concentrations, the amount of Ti consumed per serving was calculated. Because the serving sizes are different, the foods that had the highest concentration Ti did not necessarily have the largest amount of Ti per serving. The food with the highest Ti mass per serving was Hostess Powdered Donettes with 206 mg of Ti per serving. The 20 samples with the most Ti are shown in Figure 5.3. The samples highlighted in red had TiO_2 listed on the labels, all others omitted TiO_2

from the label. The Ti per serving for all the foods is shown in Appendix A, Figure A.2. Samples in green measured below the MDL.

The foods with the highest concentrations of Ti did not necessarily have the highest amount of Ti per serving. This was especially true for the gums which only had a serving size of 2 or 3 g depending on the brand. Since most other products had serving sizes ranging between 20 g and 60 g, the absolute Ti ingested in products with a larger serving size might be higher than a serving of gum despite gum having a greater concentration of Ti. The Ti mass per serving from the chocolate products were higher due to the high Ti concentrations in the shell products and the larger serving size of the products without a shell. The M&Ms and M&Ms with peanuts had the 4th and 5th highest mass of Ti per serving at 60.2 and 45. 3 mg per serving. The Hershey's Special Dark bar and Hershey's Dark Chocolate Bliss had the 23rd and 24th highest mass of Ti per serving at 0.22 mg and 0.19 mg respectively. All the beverages ranked in the lower half of the products evaluated. The Shamrock Farms Fat Free Milk was the highest of any beverage at 0.062 mg.

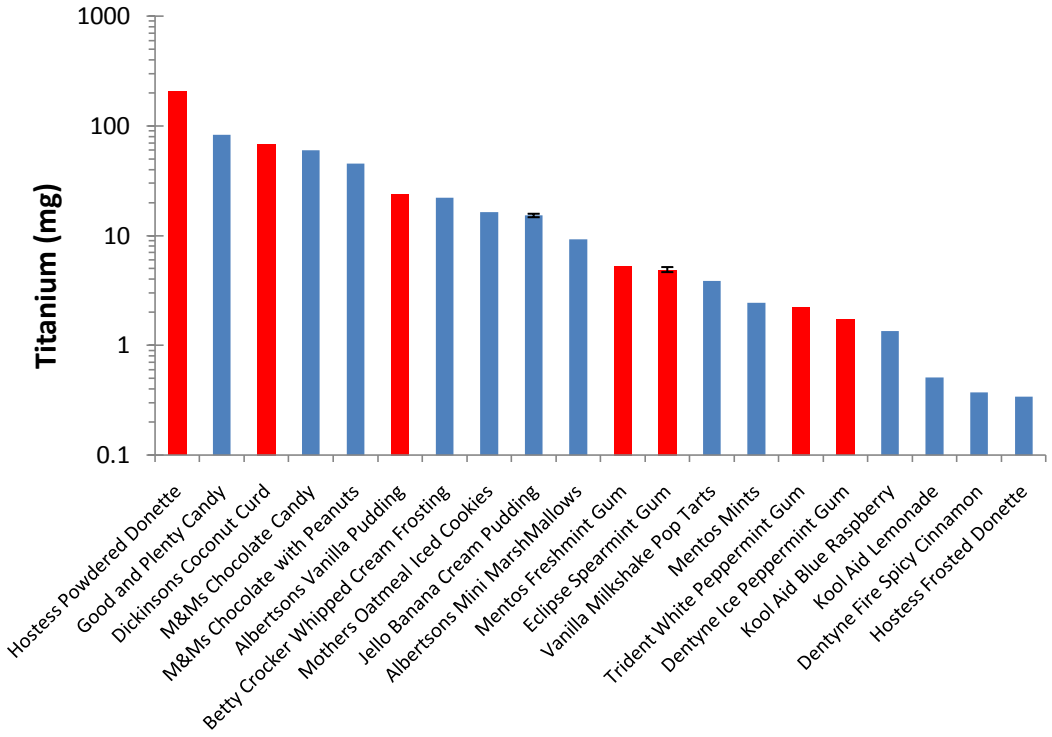

Figure 5.3. Ti mass per serving of food products. Foods displayed in red had TiO_2 listed as an ingredient. Error bars represent the standard deviation for foods digested in triplicate.

5.4.4 TiO_2 fraction to pass a 0.45 µm filter. The 12 food products with the highest concentration of Ti were filtered to determine what fraction of the total Ti was small enough to pass a 0.45 µm filter. Only the 11 foods with the highest concentration were chosen because preliminary studies (results not shown here) indicated that only a small percentage of the total Ti would pass through the filter. Filtering a sample with a moderate level of Ti might move the concentration below the MDL. The Dentyne Ice gum had the highest percentage of the total Ti pass through

the 0.45 µm filter at 3.86%. Four of the samples had less than 0.5% pass through the filter. The results for the filtration tests are shown in Figure 5.4.

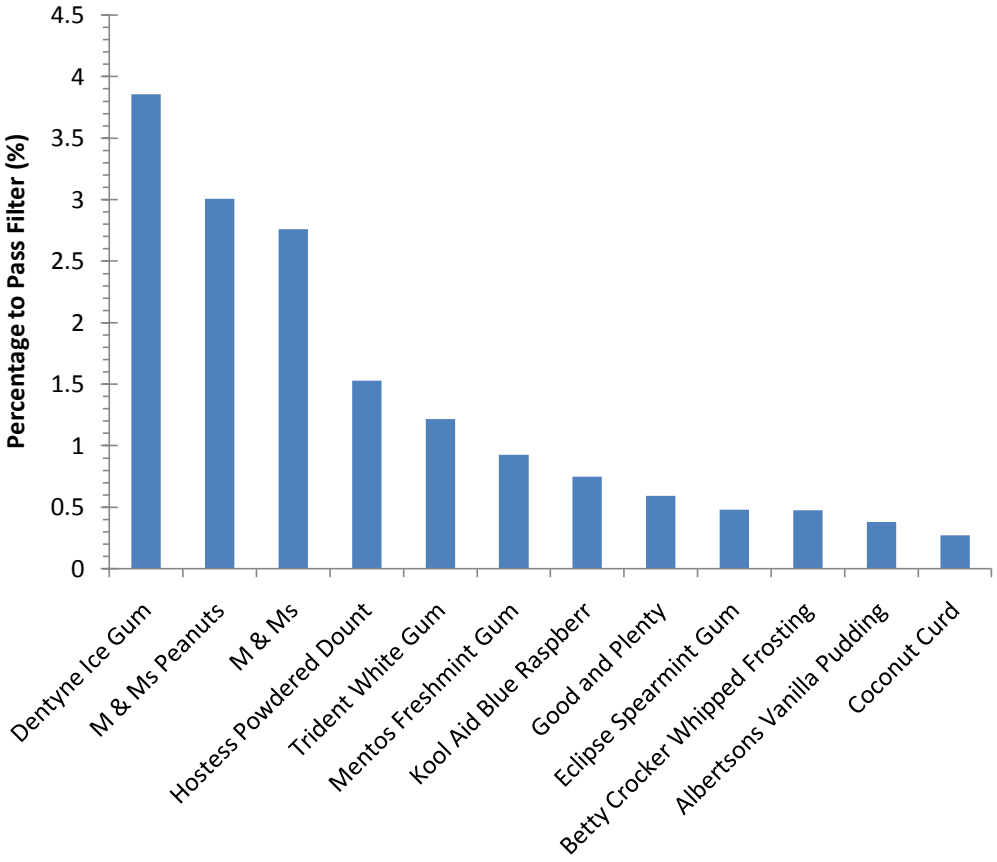

Figure 5.4. Percentage of total Ti in foods that passed a 0.45 µm filter.

5.5 DISCUSSION

All the results are expressed in Ti. This is because, once digested, TiO_2 dissolves into Ti ions, a necessary step for analysis by ICP-MS. However, since Ti is naturally present in foods at trace levels, Ti measured by digestion is almost totally included in food as TiO_2. There were high

levels of Ti even in samples that did not have TiO_2 listed as an ingredient. A person could ingest several hundred mg of TiO_2 each day by eating just a couple servings of the foods with large amounts of TiO_2. [108] The foods with the highest concentrations of Ti were gums, candies with hard shell coatings, and white confectionary products.

The fraction of Ti that passed a through the filter was largely dependent on the type of food that was digested. Though the white foods had large total quantities of Ti, generally less than 1% of it was able to pass through the filter. It is important to note that the filters used had a collection efficiency of 99% for particles larger than 0.45 µm. Thus, 1% passage may not mean that all the Ti that passed is actually nanosized, it could be larger particles. Foods with hard shells like the gum and the M&Ms had a significant amount of Ti (>1%) that was able to pass through the filter. It is important to realize that TiO_2 that passes through the filter is not necessarily all of the TiO_2 with a particle size smaller than 0.45 µm. From previous work (results not shown) particles with a smaller primary particle size may still be absorbed to the filter or they may form aggregates that are too large to pass through the filter. However, if some TiO_2 materials can pass the filter and can be shown to be in the nano size range, then that is relevant to ingestion studies and as a key source for environmental releases.

5.6 SUMMARY

- Foods that had the highest measured concentrations of TiO_2 were those that were bright white, or those with a candy shell. The highest concentration in any food was Dickinson's Coconut Curd at 3.59 µg/mg
- TiO_2 was found in foods at concentrations high enough that a person could ingest greater than 100 mg from a single serving. Hostess Powdered Donnettes had the highest mass from a single serving with 205 mg Ti.
- Many foods did not list TiO_2 as an ingredient, but still had relatively high concentrations of TIO_2.
- 3.9% of Ti particles were small enough to pass through a 0.45 µm filter for Dentyne Ice gum, with 5 different foods having greater than 1% passage.

CHAPTER 6: NANOSIZED TITANIUM DIOXIDE USED IN PERSONAL CARE PRODUCTS

6.1 INTRODUCTION

6.1.1 TiO_2 nanomaterials in personal care products. TiO_2 nanomaterials are increasingly being used in personal care products (PCPs). Their light dispersion properties make them ideal UV blockers for sunscreens and cosmetic products. Both TiO_2 and ZnO nanomaterials have been used to prevent damage to the skin by either absorbing or scattering the UV light. They are often coated with organic materials in order to trap hydroxyl radicals that can damage cells. TiO_2 has been recognized as a UV blocker for decades, but TiO_2 nanomaterials have become more popular lately because their size makes them transparent rather than a chalky white color. [9] In addition to being transparent, TiO_2 nanomaterials have been shown to have a higher sun protection factor (SPF) than larger TiO_2 particles. [127] TiO_2 and ZnO have an advantage over organic UV blockers because they are less like to cause an allergic reaction and have a higher photstability. [128]

TiO_2 nanomaterials typically exist as aggregates of particles with a primary particle diameter of 30-150 nm. The aggregates tend to be bounded so strongly that the force of application will not break them up. [129] The nanomaterials provided the best UV attenuation when they were less aggregated and more evenly distributed. [130] To increase

photostability and prevent aggregation, TiO_2 nanomaterials are commonly coated with aluminum, silicon, or polymers. [131] Silica coatings were found to be the most effective at stabilizing the particles and minimizing any negative effects. [132]

Dermatological and health authorities recommend the use of sunscreen before any sun exposure as a photoprotective strategy to prevent cell carcinoma. [128, 133] A recent survey showed that one third of people questioned observe the advice of health experts, saying they use sunscreen regularly. It is estimated that 33 million Americans use sunscreen every day and another 177 million use it occasionally. [9] Sunscreens and cosmetics are regulated by the FDA as over the counter drugs. TiO_2 nanomaterials are not considered to be a new additive, but rather a variation in particle size of an existing drug additive. [134] The only limitation stipulated by the FDA for sunscreens is that TiO_2 concentration be less than 25%. Most tend to have a lower concentration, between 2% and 15%. [9] With the wide prevalence of sunscreen use and the lack of a distinction between TiO_2 nanomaterials and larger sized particles, the general public is being exposed to nanomaterials of which they are largely ignorant.

6.1.2 Risk associated with TiO_2 used in PCPs. The risk from a substance depends on the hazard potential as well as external exposure likelihood. The application of sunscreens and cosmetics is one of the few times that the general public is intentionally exposed to nanomaterials.

The primary concern associated with the use of PCPs is dermal exposure, though they can be accidently ingested as well. [112] The reason there is concern is that uncoated TiO_2 nanomaterials can produce DNA damaging reactive oxygen species (ROS) and cause lipid peroxidation and protein tyrosine nitration which may cause cell death or lead to the onset or progression of diseases. [132, 135] Dermal studies tended to find anatase TiO_2 nanomaterials to be more toxic. [136]

For these toxic effects to be relevant, TiO_2 nanomaterials must be able to penetrate the epidermis and be distributed through the body. Dermal exposure is covered in more detail in Chapter 2. Most studies on translocation of TiO_2 nanomaterials through the epidermis found that they could not pass the stratum corneum or outermost layer of the epidermis and that the distribution appeared similar to that of larger TiO_2 particles. [129] The studies that did observe nanomaterials in the dermis found that it was only a tiny fraction of the dose, with no significant penetration. [137] A minority of researchers claim that TiO_2 nanoparticles do pose a significant threat from application to the skin. Wu [138] argues that while no penetration into the dermis was observed in porcine skin conducted *in vitro*, there was significant penetration and distribution of TiO_2 nanomaterials in an *in vivo* study of hairless mice. However, most literature reviews and studies claim that there is either no threat to human health or that the threat is negligible and the products can be considered safe. [129, 133]

6.1.3 Characterization of TiO_2 nanomaterials in PCPs. In order to better understand the potential benefits and hazards of TiO_2 nanomaterials in PCPs, one must better understand their size distribution. A study on microscopy of TiO_2 nanomaterials in PCPs found that transmission electron microscopy (TEM) and scanning electron microscopy (SEM) used together can provide an adequate characterization of the nanomaterials, and recommended using WetSEM as well to view the nanomaterials in the creams without having to dry them first. [18] Sedimentation field flow fractionation (FFF) has successfully been coupled with ICP-OES and ICP-MS for the size distribution characterization of both sunscreen and face cream. [19, 139] These methods can all be used to provide better data about primary particle size, aggregation size, and concentration of TiO_2 nanomaterials used in PCPs.

6.1.4 Environmental release and fate of TiO_2 nanomaterials from PCPs. Though it is generally agreed up that PCPs containing TiO_2 nanomaterials do not pose a significant health threat to humans, their safety does not mean their use is without consequence. As people bathe and laundry is washed, the sunscreen and cosmetics end up in wastewater. After treatment at WWTPs the water is returned to the environment. Organic UV filters used in sunscreens have already been found in surface waters in Switzerland. [140] In the United Kingdom, concentrations of Ti small enough to pass a 0.45 µm filter were found to be 11 times higher than the background directly downstream of a WWTP.

[48] Discharge from WWTPs is an indirect source of sunscreen to the environment. Sunscreen may also be introduced to the environment directly from recreational activities in lakes or pools. [9, 140]

As the sunscreen ages in the wastewater or surface water, TiO_2 nanomaterials can be released. One study showed that the aging of sunscreen in natural waters caused 30% of the total TiO_2 nanomaterials to be released. Once released they created a stable dispersion of sub-micron aggregates. [141] Another study observed similar results with TiO_2 nanomaterials forming a stable suspension of colloidal byproducts ranging in size from 50 nm to 700 nm. The presence of natural organic matter (NOM) was found to be a contributing factor to colloidal stability. [131]

6.2 PROBLEM STATEMENT

TiO_2 nanomaterials are specifically included in PCPs like sunscreen and cosmetics. The regular use and disposal of PCPs creates a large source of TIO_2 nanomaterial releases to the environment. This research project was intended to study a number of PCPs with and without TiO_2 listed as an ingredient to determine the mass concentration of TiO_2 in the consumer products. This provided an idea of how much TiO_2 a person may use from normal application of the PCPs. The smallest particles were isolated and quantified.

6.3 MATERIALS AND METHODOLOGY

6.3.1 Personal care products. Thirty two different PCPs were purchased in Arizona grocery stores in March 2011. Many different types of products were chosen including 3 deodorants, 1 lip balm, 6 shampoos, 1 shaving cream, 13 sunscreens, and 8 toothpastes. Different types of PCPs were selected including name brands and generic brands. Samples were transported to the laboratory and stored in a clean, dry cupboard. Information about the products, including whether or not TiO_2 was listed on the label was recorded.

6.3.2 Digestion. 500 mg of each product was weighed and added to a clean microwave digestion vessel. The products were then microwave digested with 2 mL HF and 8 mL HNO_3 to break down the organic matter and the TiO_2. This method is described in detail in Chapter 3. Some of the products with a large amount of organics were not totally broken down by the initial 2 mL of hydrogen peroxide added after digestion. As the liquid was evaporated, if it became apparent that there was organic material remaining in the sample, the sample was cooled and then 2 mL of hydrogen peroxide was added and the sample was heated again. It is important to note that samples with high concentrations of Ti will turn orange with the addition of peroxide in an acidic environment. [83] (See Appendix D, Photo D.8). Ti was quantified using the same ICP-MS analysis procedure detailed in Chapter 3. All samples with Ti concentrations outside of the calibration range were diluted and re-

analyzed. A study using a similar method of acid digestion for Ti quantification in sunscreens demonstrated a recovery of 95%. [85] A recovery evaluation for TiO_2 nanoparticles and microparticles was conducted in Chapter 5.

6.3.3 Separation method. In order to determine how much TiO_2 is in the nanosize range a separation method had to be created to separate smaller TiO_2 from larger TiO_2 and organic materials. 500 mg of a product sample was added to a beaker. The organic material from the sample was broken down by adding 10 mL of hydrogen peroxide and 0.5 mL of HNO_3 and heating on a hot plate at 110°C. When the volume of liquid remaining in the sample was less than 1 mL, the beakers were removed from the hot plate and allowed to cool. The beaker sides and bottom were then rinsed with approximately 20 mL of nanopure water. The sample was filtered with a 0.45 µm nylon filter and added to a microwave vessel. To determine the total TiO_2 that was able to pass the 0.45 µm filter the sample was then digested using the digestion method. The pH of the samples was determined before filtration to ensure that the nylon filter would not be damaged during filtration.

6.4 RESULTS

6.4.1 Total TiO_2 in PCPs. All 32 PCPs were digested and the concentration of TiO_2 (determined as Ti) in the product was determined. The highest concentration of Ti in any sunscreen was found in Neutrogena

Sensitive Skin Sunblock Lotion at 70.1 µg/mg. The highest concentration of Ti in any toothpaste was found in Sensodyne at 5.64 µg/mg. The three sunscreens with TiO_2 listed as an ingredient were the highest of any PCPs. The toothpastes all had TiO_2 listed as an ingredient and had a concentration one order of magnitude lower than the sunscreens made with TiO_2. The sunscreens without TiO_2 listed on the label had concentrations of TiO_2 that were three orders of magnitude lower than those with TiO_2 listed. The concentrations of TiO_2 in the shampoo, lip balm, shaving cream and deodorant were all much lower with the highest concentration of any being in Head and Shoulders 2 in 1 shampoo at 0.0056 µg/mg. The results for the total titanium concentration for all the PCPs can be seen in Figure 6.1. The values plotted in orange are the sunscreens that had TiO_2 listed as an ingredient. The values plotted in red are the toothpastes that had TiO_2 listed as an ingredient. All other products did not list TiO_2 as an ingredient.

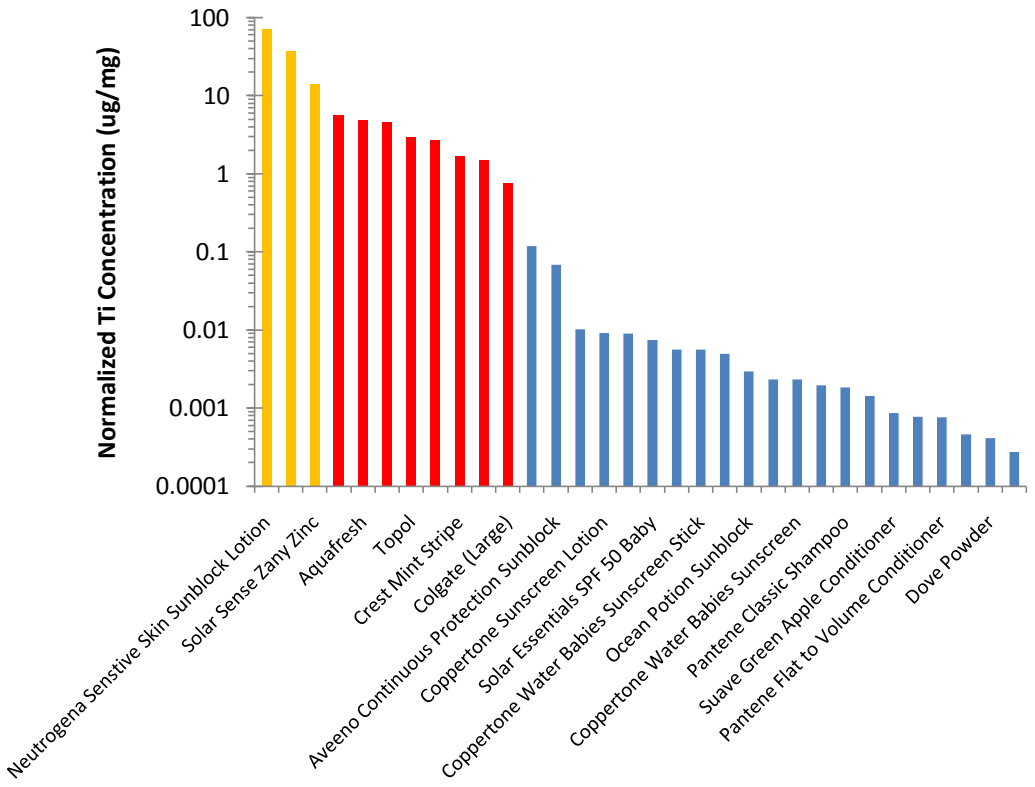

Figure 6.1. Total titanium concentration for PCPs.

6.4.2 TiO_2 fraction to pass a 0.45 µm filter. PCPs with the highest concentration of Ti were further examined by digesting the organics and filtering with a 0.45 µm filter. From preliminary experiments (data not shown here) it was known that only a small fraction of the total Ti can pass the filter so only the samples with a high concentration of Ti would have measurable concentrations after filtering. Two of the sunscreens and 3 toothpastes with high Ti concentrations were selected. 6.3% of the total Ti in the Neutrogena Pure and Free Baby sunscreen was able to pass through the filter which was the highest of any sample. The sunscreens had a higher percentage of Ti that was able to pass through

the filter compared to the toothpastes. Each of the toothpastes had less than 1% of the total Ti pass through the filter. The results are displayed in Figure 6.3.

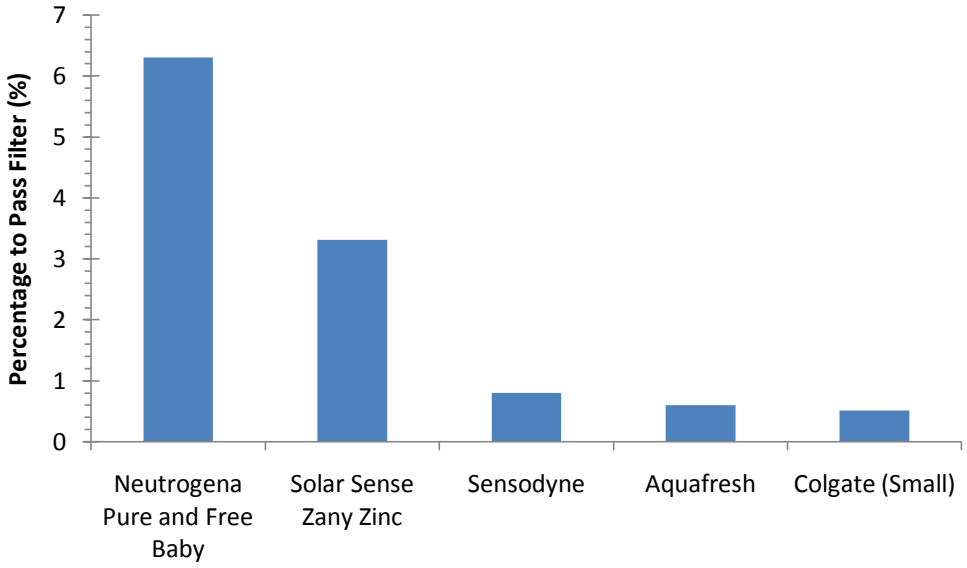

Figure 6.3. Ti percentage to pass through a 0.45 µm filter from sunscreens and toothpastes.

6.5 DISCUSSION

. The TiO_2 concentration in the consumer products tended to be more consistent than the wide range of concentrations seen in the food products. The 3 sunscreens that used TiO_2 as a UV blocker had TiO_2 concentrations on the same order of magnitude. TiO_2 in those sunscreens represented between 1.4% and 7% of the total mass which is similar to what was reported in the literature and listed on the ingredients. The 8 toothpastes all had TiO_2 concentration on the same order of magnitude.

All other PCPs did not have TiO_2 listed and had noticeably lower concentrations meaning that unlike the food products, having TiO_2 omitted on the label meant that there was likely a very low concentration of TiO_2.

The sunscreens had a significant amount (3-6%) of Ti that passed through the 0.45 µm filter, more so than any of the foods evaluated in Chapter 5. The toothpastes evaluated had less than 1% pass through the filter. Since the filter has a 99% efficiency, the percentage of the toothpastes to pass through a 0.45 µm filter was not significant and could have been larger particles. This means that the sunscreen had a larger fraction of small particles than the toothpastes indicating that the size distribution is closer to the nano range.

6.6 SUMMARY

- Sunscreens that had TiO_2 listed as an ingredient had the highest concentrations of Ti with Neutrogena Sensitive Skin Sunblock being the highest with 70.1 ug Ti/mg.
- All toothpastes had similar Ti concentrations, between 0.75 and 5.64 ug Ti/mg.
- PCPs that did not list TiO_2 as an ingredient had Ti concentrations that were several orders of magnitude lower than those products with TiO_2 listed as an ingredient with none being higher than 0.12 ug Ti/mg.

- 6.3% of the total Ti measured in Neutrogena Pure and Free Baby was able to pass through a 0.45 μm filter indicating a larger portion of small near-nanosized particles.
- Less than 1% of the total Ti in the toothpastes was able to pass through a 0.45 μm filter.

CHAPTER 7: NANOSIZED TITANIUM DIOXIDE USED IN PAINTS

7.1 INTRODUCTION

7.1.1 Nanoscale TiO_2 in paints. TiO_2 particles are used to whiten paints. Nearly 90% of the total titanium mineral production is used for pigments in paints. [90]. TiO_2 used in paints has a size distribution including some nanosized particles. The advantages of shifting TiO_2 production to a nanoformat mean that the size distribution is likely to shift even farther toward the nano range. [11] TiO_2 nanoparticles with a diameter of 20-300 nm have been observed in surface waters and traced back to exterior paint as a source. The TiO_2 nanoparticles had detached under normal weather conditions. [21] The eventual TiO_2 mass lost due to weathering from exterior paint is approximately 1.5 mg/m^2. Though this is a small portion of the total TiO_2 mass in the paint (25,000 mg/m^2), it can add up to a large source of TiO_2 to the environment when every painted façade is considered. [142]

7.1.2 TiO_2 nanomaterials used in coatings. TiO_2 nanomaterials are used specifically in coatings used in the automotive industry. TiO_2 nanoparticles incorporated into polyurethane coatings caused an increase in resistance to weathering and enhanced mechanical properties. [143] Over time the wearing of the coating on automobiles will also cause the release of TiO_2 nanomaterials. Though consumer products like paints and coatings don't have the same likelihood of exposure as PCPs meant to be

applied to the skin, they still have environmental implications, perhaps even more so because they are less likely to experience treatment from WWTPs.

7.2 PROBLEM STATEMENT

TiO_2 nanomaterials are specifically incorporated into coatings for automobiles. There is also likely a fraction of TiO_2 materials used as pigments in paints that are in the nano size range. The regular application of paints and their weathering creates a large source of TIO_2 nanomaterial releases to the environment. This research project was intended to study a number of paints to determine the mass concentration of TiO_2 in the paint. This provided an idea of how much TiO_2 might be applied during the painting of a surface.

7.3 MATERIALS AND METHODOLOGY

7.3.1 Paint products. Eight different paint type products were purchased in Arizona hardware stores in March and June 2011. Different types of paints were selected including 3 sealers, 2 base paints, 2 white paints, and 1 glue. White paint type products were chosen because they were expected to have higher TiO_2 concentrations. Samples were transported to the laboratory and stored in a clean, dry cupboard. Information about the products, including whether or not TiO_2 was listed on the label was recorded.

7.3.2 Digestion. 500 mg of each product was weighed and added to a clean microwave digestion vessel. The products were then microwave digested with 2 mL HF and 8 mL HNO_3 to break down the organic matter and the TiO_2. This method is described in detail in Chapter 3. It is important for the paint and sealer products that the products were not allowed to dry into the vessels before acid was added. Some of the products with a large amount of organics were not totally broken down by the initial 2 mL of hydrogen peroxide added after digestion. As the liquid was evaporated, if it became apparent that there was organic material remaining in the sample, the sample was cooled and then 2 mL of hydrogen peroxide was added and the sample was heated again. It is important to note that samples with high concentrations of Ti will turn orange with the addition of peroxide in an acidic environment. [83] (See Appendix D, Photo D.8). Ti was quantified using the same ICP-MS analysis procedure detailed in Chapter 3. All samples with Ti concentrations outside of the calibration range were diluted and re-analyzed. A study using a similar method of acid digestion for Ti quantification in sunscreens demonstrated a recovery of 95%. [85] A recovery evaluation for TiO_2 nanoparticles and microparticles was conducted in Chapter 5.

7.4 RESULTS

7**.4.1 Total TiO_2 in paints.** All 8 paint type products were digested and the concentration of TiO_2 (determined as Ti) in the products were

determined. Three of the products were digested in triplicate. The triplicates were in good agreement, all within 20%. The highest concentration of Ti in any product was found in the Benjamin Moore White paint at 114 µg/mg. The Ace brand paint had a similar concentration. All three sealant products had similar concentrations which were high, but an order of magnitude lower than the white paints. The two base paint samples and the glue had concentrations that were 2 orders of magnitude lower than then sealants. The results for the total titanium concentration for all the paint type products can be seen in Figure 7.1.

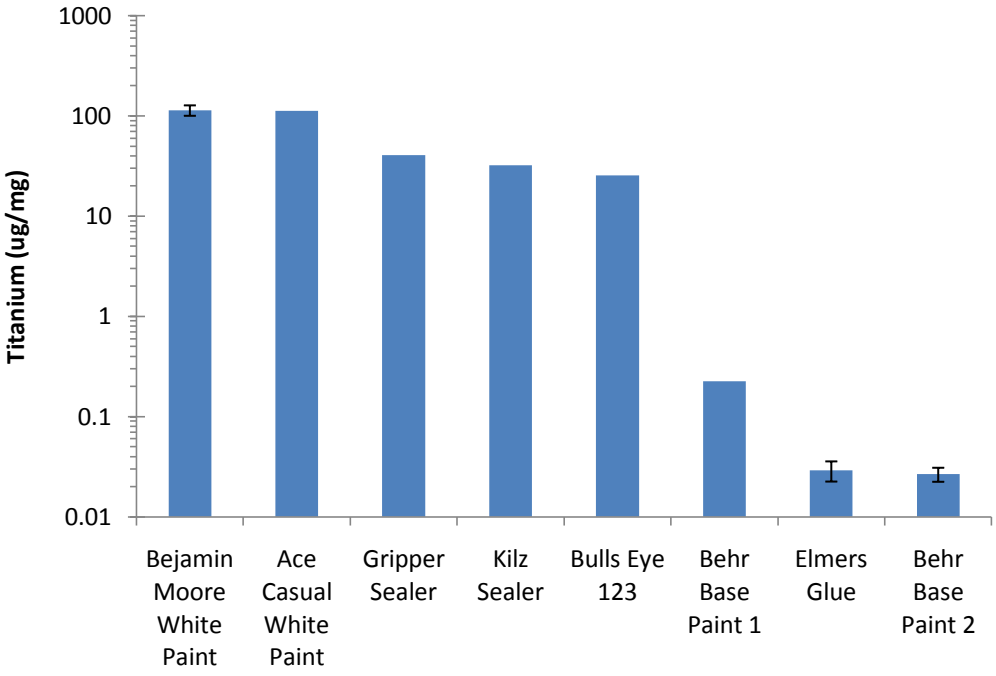

Figure 7.1. Total titanium concentration for paint type products. Error bars represent the standard deviation from samples digested in triplicate.

7.5 DISCUSSION

The TiO_2 concentration in the white paint products and the sealers was generally higher than the concentrations seen in foods and PCPs. This is because such a large amount of TiO_2 is added to the paints and sealers to create and maintain a bright white color after application. The base paints contained a lower concentration of TiO_2 because though they are white when they are purchased, they are intended to have other colors mixed into the paint. Therefore, there is less need to have TiO_2 to provide bright white coloring. Elmer's glue is white in the bottle, but is intended to dry clear, meaning there is less need for TiO_2 as a pigment.

7.6 SUMMARY

- White paints had the highest concentrations of Ti with Benjamin Moore being the highest at 113.7 µg Ti/mg.
- The Ti concentration in the sealer products was less than half of that in the white paints, with gripper sealer being the highest at 40.7 µg Ti/mg.
- The base paints and Elmer's glue had Ti concentrations greater than 2 orders of magnitude lower than the paints and sealers with one Behr base paint having the highest concentration at 0.22 µg Ti/mg.

CHAPTER 8: SYNTHESIS OF FINDINGS AND RECOMMENDATIONS

8.1 INTRODUCTION

As TiO_2 nanomaterial use has increased in recent years it is important to understand the implications of the nanomaterials on human health. The development of a pharmacokinetic model aids in the prediction of TiO_2 tissue concentrations resulting from different exposure methods and dosages. However, the resulting concentrations are only modeled. In order to verify the results, empirically, a method had to be developed that can digest tissue and recover the entirety of the TiO_2 in the tissue. Microwave digestion of samples with nitric and hydrofluoric acid proved to be an efficient method for rapid quantification of the TiO_2. The digestion method was then used to quantify the deposition of various TiO_2 nanomaterials instilled into rat lungs. The results of the instillation project provide more information for the model, specifically about deposition and clearance rates of different kinds of TiO_2 nanomaterials. The digestion method was also robust enough to be used to digest food products and consumer products. Digesting the foods allowed for measurement of the total TiO_2 in foods and PCPs as well as determination of the nano sized fraction of TiO_2. The data gained from those studies can be used to determine realistic dose inputs for exposure by ingestion.

TiO_2 nanomaterials not only have implications for human health, but for releases to the environment and their impacts. The excretion

information from the pharmacokinetic model can be used with the data from the TiO_2 food project to determine estimates of the mass of nano TiO_2 that can enter wastewater from human waste. The data from the TiO_2 PCP study can be used to determine estimate of the mass of nano TiO_2 that can enter wastewater from the use of products like sunscreen and toothpaste. The digestion method could also be applied for a study of TiO_2 nanomaterials in wastewater.

8.2 SUMMARY OF FINDINGS

8.2.1 Pharmacokinetic modeling of TiO_2 nanomaterials. It is the purpose of this project to develop a pharmacokinetic ADME model for TiO_2 nanomaterials that can predict tissue concentrations based on an exposure level.

- Inhalation is the most important exposure route for human health implications of TiO_2 nanomaterials.
- TiO_2 nanomaterials are more slowly cleared from the lungs than larger particles and have greater toxic effects with the half-life being as high as 501 days.
- TiO_2 nanomaterials may distribute to the lymphatic system, brain, kidneys, liver, and spleen. Modeled liver concentrations were generally highest, as much as 3.3 µg/g after inhalation.

- Primary particle size plays an important role in the ADME of particles as dose crystal structure, surface coating, and charge.
- Extremely small TiO_2 nanomaterials (< 5nm diameter) are excreted by the kidneys through the urine.
- Larger TiO_2 nanomaterials (~25 nm) are more likely to be excreted in bile from the liver.

8.2.2 TiO_2 quantification method development. The purpose of this project is to develop a quantification method consisting of a digestion procedure and analysis procedure capable of accurately measuring TiO_2 at widely varying concentrations.

- The digestion method degraded organic material enough that the samples could be analyzed by ICP without damaging the instruments.
- The digestion method had greater than 86% recovery of Ti.
- ICP-MS was the best choice for quantifying Ti because the detection limit of 164 ng/L was lower than ICP-OES detection limit.
- Ti isotope 49 m/z is the best isotope to monitor because it has the least interferences from other species like P-O and S-O complexes.
- The MDL for the digestion method was 1 µg TiO_2.

8.2.3 TiO_2 nanomaterial morphology effect on deposition and clearance in rat lungs. This project intended to study how three different morphologies of TiO_2 nanomaterials—anatase nanoparticles, rutile nanoparticles, and nanobelts—affected the deposition into the lungs of rats after intratracheal instillation, and the clearance rate of the particles 1 day and 1 week after instillation by collaborators at UC-Davis.

- Anatase TiO_2 nanoparticles deposited in rat lungs to a greater degree than rutile nanoparticles or nanobelts with an average of 41 µg of Ti found in caudal lobes 1 day after exposure to anatase TiO_2. This was 218% higher than the second highest average concentration.

- The anatase TiO_2 nanoparticles were also found at the highest concentration in the caudal lobes with 1236 ng Ti/mg dry tissue as the average.

- TiO_2 nanoparticles concentration were found to be 58% higher in caudal lobes than in the cranial lobes for anatase TiO_2. Similar trends were observed for all morphologies.

- There was no significant evidence that there was less TiO_2 material in the lung 7 days after instillation when compared to 1 day after instillation for all morphologies. The Ti concentration had increased beyond the 80% confidence interval level for nanobelts from day 1 to day 7.

- The Ti lung concentrations from the digestion of the lungs showed an R^2 agreement of 0.376 with cell inclusion counts conducted with microscopy.

8.2.4 Nanoscale fraction of TiO_2 used in food products. This research project intended to study a number of foods with and without TiO_2 listed as an ingredient to determine if TiO_2 is present. The total TiO_2 was quantified to understand the total TiO_2 mass a person may be exposed to from a normal diet. The smallest particles were isolated and quantified.

- Foods that had the highest measured concentrations of TiO_2 were those that were bright white, or those with a candy shell. The highest concentration in any food was Dickinson's Coconut Curd at 3.59 µg/mg

- TiO_2 was found in foods at concentrations high enough that a person could ingest greater than 100 mg from a single serving. Hostess Powdered Donnettes had the highest mass from a single serving with 205 mg Ti.

- Many foods did not list TiO_2 as an ingredient, but still had relatively high concentrations of TIO_2.

- 3.9% of Ti particles were small enough to pass through a 0.45 µm filter for Dentyne Ice gum, with 5 different foods having greater than 1% passage.

8.2.5 Nanosized TiO_2 used in PCPs. This research project intended to study a number of PCPs with and without TiO_2 listed as an ingredient to determine the mass concentration of TiO_2 in the consumer products. This gave an idea of how much TiO_2 a person may use from normal application of the PCPs. The smallest particles were isolated and quantified.

- Sunscreens that had TiO_2 listed as an ingredient had the highest concentrations of Ti with Neutrogena Sensitive Skin Sunblock being the highest with 70.1 ug Ti/mg.
- All toothpastes had similar Ti concentrations, between 0.75 and 5.64 ug Ti/mg.
- PCPs that did not list TiO_2 as an ingredient had Ti concentrations that were several orders of magnitude lower than those products with TiO_2 listed as an ingredient with none being higher than 0.12 ug Ti/mg.
- 6.3% of the total Ti measured in Neutrogena Pure and Free Baby was able to pass through a 0.45 µm filter indicating a larger portion of small near-nanosized particles.

- Less than 1% of the total Ti in the toothpastes was able to pass through a 0.45 µm filter.Less than 1% of the total Ti in the toothpastes was able to pass through a 0.45 µm filter.

8.2.6 Nanosized TiO2 used in paints. This research project intended to study a number of paints to determine the mass concentration of TiO_2 in the paint. This gave an idea of how much TiO_2 might be applied during the painting of a surface. The smallest particles were isolated and quantified.

- White paints had the highest concentrations of Ti with Benjamin Moore being the highest at 113.7 µg Ti/mg.

- The Ti concentration in the sealer products was less than half of that in the white paints, with gripper sealer being the highest at 40.7 µg Ti/mg.

- The base paints and Elmer's glue had Ti concentrations greater than 2 orders of magnitude lower than the paints and sealers with one Behr base paint having the highest concentration at 0.22 µg Ti/mg.

8.3 SYNTHESIS OF FINDINGS

8.3.1 Individual uptake. Since the mass of Ti from a single serving can approach 100 mg, a person could easily ingest 500 mg of TiO_2 in one day. If 2% of those TiO_2 particles are in the nano size range,

which is a reasonable assumption depending on the types of foods ingested, than a person may ingest 10 mg of TiO_2 nanosized particles per day. If a person ingested a larger amount of candies with hard shells like M&Ms and Good and Plenty, it is not unreasonable to assume that a person may ingest as much as 1 gram of TiO_2 per day. In candies with hard shells there is a greater fraction of nanosized TiO_2 particles. If 4% of the particles are in the nanosized range, then a person may ingest as much as 40 mg of nanosized TiO_2 per day. For a person weighing 70 kg, ingesting 40 mg of TiO_2 nanomaterials results in an ingestion dose of 0.57 mg/kg per day. By using this data as an input for the ADME model developed in Chapter 2, and assuming the particles have an average diameter of 25 nm, the resulting concentrations in the kidney, liver, and spleen 14 days after ingestion are 0.043, 0.012, and 0.066 ng TiO_2/g tissue respectively. These tissue concentrations are very low compared to the concentrations that may result from the inhalation of TiO_2 nanomaterials (See Chapter 2). In addition to the intentional ingestion of food, there may be accidental ingestion of PCPs such as sunscreen or toothpaste. If as little as 0.5 g of Sensodyne toothpaste is ingested by accident it can results in 2.8 mg of Ti ingestion. Ingesting 0.5 g of Neutrogena Sensitive Skin Sunblock would cause the ingestion of 35 mg Ti with 2.1 mg of the Ti particles being in the nanosized range.

Though only the lungs of the rats from Chapter 4 were analyzed for TiO_2, one can predict the TiO_2 concentration in the other tissues using the

ADME model from Chapter 2. The average concentration of anatase TiO_2 deposited into the caudal lobes after 1 day was selected as an input for the ADME model because it was the highest concentration found in any lung lobe leading to the highest concentrations in other tissues. Extrapolating the normalized concentration for the whole lung tissue, it can be expected that 0.3 mg of TiO_2 would deposit into the lungs. This leads to a TiO_2 concentration in the kidney, liver, and spleen 14 days after instillation of 0.001, 0.01 and 0.003 μg TiO_2/g tissue respectively. These concentrations are nearly an order of magnitude higher than those resulting from daily ingestion of food predicted above. The dermal absorption of sunscreen is unlikely to cause any relevant uptake of TiO_2.

8.3.2 Societal and environmental applications. Although ingestion of TiO_2 or dermal absorption did not cause widespread distribution throughout the body, the ingestion of foods and use of PCPs can still have important implications. It is recommended that 2 mg of sunblock per square inch of exposed skin be applied. However, a study of the application patterns of randomly selected individuals over 4.5 years showed that the median applied amount was 1.5 g/day. [144] Eventually this sunscreen is washed off and mixes with the wastewater. If the sunscreen used was a TiO_2 based sunscreen, 1.5 g/day of sunscreen would generate 105 mg TiO_2/day and 6.3 mg nanosized TiO_2/day as waste. It was described above how a typical person will ingest 10 mg nanosized TiO_2/day. Since little of this is absorbed and distributed

through the body, nearly all of it would pass through the digestive system and leave the body as waste. In this manner, from a typical diet and the use of sunscreen, an individual may be responsible for as much 16 mg of nanosized TiO_2/day in wastewater. Assuming an individual produces 120 gal sewage/day, the wastewater would have an average concentration of 13.8 µg/L of TiO_2 small enough to pass through a 0.45 µm filter. Though this sewage will go through treatment, as much as 4% of the total Ti in the influent is not removed and is released to the environment. [47] TiO_2 may also bypass WWTPs. This can occur when paint weathers and TiO_2 mixes with storm water or from PCPs washing off during recreational use and mixing with surface water.

8.4 CONCLUSIONS

8.4.1 Pharmacokinetics of TiO_2 nanomaterials. Pulmonary absorption is the most relevant exposure route for TiO_2 nanomaterials. Because of the enhanced toxicity of nanoscale TiO_2 materials, individuals who regularly work with TiO_2 nanomaterials in their workplace and are likely to inhale large quantities should be monitored for toxic effects or potentially for TiO_2 nanomaterials in the urine or blood.

8.4.2 TiO_2 digestion method. Microwave digestion with HF and HNO_3 provided good recovery of Ti materials. The method was robust enough to digest complex matrices and had low interferences allowing for the quantification of trace amounts of Ti. The method has the added

advantage of being capable of rapid digestion and analysis of samples. Other digestion methods using sulfuric acid or ICP-OES should be used sparingly.

8.4.3 TiO_2 nanomaterial morphology effects on deposition and clearance. When the enhanced toxicity of anatase TiO_2 nanomaterials is coupled with their apparent higher deposition rates, the threat to human health is far greater for airborne anatase TiO_2 nanomaterials. This is an important consideration for policy makers. The enhanced threat from the production of pure anatase TiO2 nanomaterials may cause anatase production processes to be regulated differently than rutile production processes.

8.4.4 Individual Uptake. An individual could ingest 10 mg of TiO_2 nanomaterials from a typical diet and even more if a person's diet consisted of candies or highly processed white foods. However, the uptake of these nanomaterials is minimal and not a large threat to human health. The exception is for those individuals with preexisting GI diseases such as Crohn's disease. A diet minimizing microparticles and nanoparticles is recommended for individuals with Crohn's disease. The results of this study have shown that the ingredient listings on foods are not always a good indicator of whether they include TiO_2.

8.4.5 Societal and Environmental Implications. The ingestion of foods and application of PCPs containing TiO_2 can result in 16 mg nano

TiO_2/day introduced to the wastewater for each individual. As the production and use of TiO_2 nanomaterials increases the amount of TiO_2 in the wastewater will increase. This will likely cause an increased concentration of TiO_2 nanomaterials in the biosolids from WWTPs that are land applied as well as the treated effluent waters, both of which allow a greater loading of TIO_2 nanomaterials to the environment.

8.5 FUTURE WORK RECOMMENDATIONS

The results derived from the ADME model could be further verified by a study monitoring the feces and/or urine to complete a mass balance based on inputs like inhalation and ingestion and excreted outputs. The model could also be expanded to other tissues in the body by using the digestion method detailed in this work. It would be beneficial to have more data for different sizes of nanoparticles to create a continuum of distributions based on nanoparticle diameter rather than only being able to model two TiO_2 nanoparticle sizes. More data on clearance rates for different types of TIO_2 nanomaterials could be garnered for the model from another morphology inhalation study that monitored the animals for a greater time after instillation and harvested other organs to generate tissue concentration data.

The synthesis of the findings had suggested a large amount of nanosized TiO_2 may be entering the wastewater. TiO2 nanomaterials in wastewater could be monitored to verify the findings by sampling

wastewater influents at different WWTPs and using the separation and digestion methods in this thesis. Furthermore, the digestion method could be modified to be used for other types of samples like biosolids or soil samples. Digesting biosolids could be used to monitor how the concentration of TiO_2 nanomaterials may be changing. Since biosolids are often land applied for agriculture, soil samples with biosolids applied could be compared to control soil samples to determine whether TiO_2 nanomaterials may be a relevant cause of concern for agricultural production. It would also be beneficial to study how TiO_2 nanosized particles from foods and PCPs change by aggregation or coating of the surface in wastewater or environmental matrices.

WORKS CITED

1. Oberdörster, G.; Maynard, A.; Donaldson, K.; Castranova, V.; Fitzpatrick, J.; Ausman, K.; Carter, J.; Karn, B.; Kreyling, W.; Lai, D.; Olin, S.; Monteiro-Riviere, N.; Warheit, D.; Hong, Y., Principles for characterizing the potential human health effects from exposure to nanomaterials: elements of a screening strategy. *Particle & Fibre Toxicology* **2005,** *2*, 8-35.

2. Grassian, V., *Nanoscience and Nanotechnology*. 1st ed.; Wiley and Sons, Inc.: Hoboken, NJ, 2008; p 469.

3. Theron, J.; Walker, J. A.; Cloete, T. E., Nanotechnology and water treatment: Applications and emerging opportunities. *Critical Reviews in Microbiology* **2008,** *34*, (1), 43-69.

4. Chang, C., The immune effects of naturally occurring and synthetic nanoparticles. *Journal of Autoimmunity* **2010,** *34*, (3), J234-J246.

5. Balzani, V.; Credi, A.; Venturi, M., Molecular machines working on surfaces and at interfaces. *Chemphyschem* **2008,** *9*, (2), 202-220.

6. Suh, W. H.; Suslick, K. S.; Stucky, G. D.; Suh, Y. H., Nanotechnology, nanotoxicology, and neuroscience. *Progress in Neurobiology* **2009,** *87*, (3), 133-170.

7. Warheit, D. B., Debunking Some Misconceptions about Nanotoxicology. *Nano Letters* **2010,** *10*, (12), 4777-4782.

8. Titanium Dioxide Uses and Market. (June 1st, 2011),

9. Davis, J.; Wang, A.; Shtakin, J. A., Nanomaterial Case Studies: Nanoscale Titanium Dioxide in Water Treatment and in Topical Sunscreen. In Draft ed.; Agency, E. P., Ed. Research Triangle Park, NC, 2009.

10. Landsiedel, R.; Ma-Hock, L.; Kroll, A.; Hahn, D.; Schnekenburger, J.; Wiench, K.; Wohlleben, W., Testing Metal-Oxide Nanomaterials for Human Safety. *Advanced Materials* **2010,** *22*, (24), 2601-2627.

11. Robichaud, C. O.; Uyar, A. E.; Darby, M. R.; Zucker, L. G.; Wiesner, M. R., Estimates of Upper Bounds and Trends in Nano-TiO2 Production As a Basis for Exposure Assessment. *Environmental Science & Technology* **2009,** *43*, (12), 4227-4233.

12. Macwan, D. P.; Dave, P. N.; Chaturvedi, S., A review on nano-TiO2 sol-gel type syntheses and its applications. *Journal of Materials Science* **2011,** *46*, (11), 3669-3686.

13. Mahshid, S.; Askari, M.; Ghamsari, M. S., Synthesis of TiO2 nanoparticles by hydrolysis and peptization of titanium isopropoxide solution. *Journal of Materials Processing Technology* **2007,** *189*, (1-3), 296-300.

14. Zhou, X. P.; Ni, S. Y.; Zhang, X.; Wang, X. Q.; Hu, X. H.; Zhou, Y., Controlling Shape and Size of TiO2 Nanoparticles with Sodium Acetate. *Current Nanoscience* **2008,** *4*, (4), 397-401.

15. Wu, J.; Bai, G.-R.; Eastman, J.; Zhou, G.; Vasudevan , V., Synthesis of TiO2 Nanoparticles Using Chemical Vapor Condensation. *Materials Research Society Symposia Proceedings* **2005,** *879*.

16. Daranyi, M.; Csesznok, T.; Kukovecz, A.; Konya, Z.; Kiricsi, I.; Ajayan, P. M.; Vajtai, R., Layer-by-layer assembly of TiO2 nanowire/carbon nanotube films and characterization of their photocatalytic activity. *Nanotechnology* **2011,** *22*, (19), 9.

17. Macak, J. M.; Tsuchiya, H.; Ghicov, A.; Yasuda, K.; Hahn, R.; Bauer, S.; Schmuki, P., TiO2 nanotubes: Self-organized electrochemical formation, properties and applications. *Current Opinion in Solid State & Materials Science* **2007,** *11*, (1-2), 3-18.

18. Lorenz, C.; Tiede, K.; Tear, S.; Boxall, A.; von Goetz, N.; Hungerbuhler, K., Imaging and Characterization of Engineered Nanoparticles in Sunscreens by Electron Microscopy, Under Wet and Dry Conditions. *International Journal of Occupational and Environmental Health* **2010,** *16*, (4), 406-428.

19. Contado, C.; Pagnoni, A., TiO2 nano- and micro-particles in commercial foundation creams: Field Flow-Fractionation techniques together with ICP-AES and SQW Voltammetry for their characterization. *Analytical Methods* **2010,** *2*, (8), 1112-1124.

20. Adams, L. K.; Lyon, D. Y.; Alvarez, P. J. J., Comparative eco-toxicity of nanoscale TiO2, SiO2, and ZnO water suspensions. *Water Research* **2006,** *40*, (19), 3527-3532.

21. Kaegi, R.; Ulrich, A.; Sinnet, B.; Vonbank, R.; Wichser, A.; Zuleeg, S.; Simmler, H.; Brunner, S.; Vonmont, H.; Burkhardt, M.; Boller, M., Synthetic TiO2 nanoparticle emission from exterior facades into the aquatic environment. *Environmental Pollution* **2008,** *156*, (2), 233-239.

22. Morimoto, Y.; Kobayashi, N.; Shinohara, N.; Myojo, T.; Tanaka, I.; Nakanshi, J., Hazard Assessments of Manufactured Nanomaterials. *Journal of Occupational Health* **2010,** *52*, (6), 325-334.

23. Zhang, R.; Niu, Y. J.; Li, Y. W.; Zhao, C. F.; Song, B.; Li, Y.; Zhou, Y. K., Acute toxicity study of the interaction between titanium dioxide nanoparticles and lead acetate in mice. *Environmental Toxicology and Pharmacology* **2010,** *30*, (1), 52-60.

24. Quetel, C. R.; Vassileva, E.; Petrov, I.; Chakarova, K.; Hadjiivanov, K. I., First results on Fe solid-phase extraction from coastal seawater using anatase TiO2 nano-particles. *Analytical and Bioanalytical Chemistry* **2010,** *396*, (6), 2349-2361.

25. Dastjerdi, R.; Montazer, M., A review on the application of inorganic nano-structured materials in the modification of textiles: Focus on anti-microbial properties. *Colloids and Surfaces B-Biointerfaces* **2010,** *79*, (1), 5-18.

26. Sung, W. P.; Tsai, T. T.; Wu, M. J.; Wang, H. J.; Surampalli, R. Y., Removal of Indoor Airborne Bacteria by Nano-Ag/TiO2 as Photocatalyst: Feasibility Study in Museum and Nursing Institutions. *Journal of Environmental Engineering-Asce* **2011,** *137*, (3), 163-170.

27. Wang, R. M.; Wang, B. Y.; He, Y. F.; Lv, W. H.; Wang, J. F., Preparation of composited Nano-TiO2 and its application on antimicrobial and self-cleaning coatings. *Polymers for Advanced Technologies* **2010,** *21*, (5), 331-336.

28. Yaghoubi, H.; Taghavinia, N.; Alamdari, E. K., Self cleaning TiO2 coating on polycarbonate: Surface treatment, photocatalytic and nanomechanical properties. *Surface & Coatings Technology* **2010,** *204*, (9-10), 1562-1568.

29. Liu, L.; Miao, P.; Xu, Y. Y.; Tian, Z. P.; Zou, Z. G.; Li, G. X., Study of Pt/TiO2 nanocomposite for cancer-cell treatment. *Journal of Photochemistry and Photobiology B-Biology* **2010,** *98*, (3), 207-210.

30. Roy, S. C.; Paulose, M.; Grimes, C. A., The effect of TiO2 nanotubes in the enhancement of blood clotting for the control of hemorrhage. *Biomaterials* **2007,** *28*, (31), 4667-4672.

31. Chen, Y.; Yan, L. D.; Yuan, T.; Zhang, Q. Y.; Fan, H. J., Asymmetric Polyurethane Membrane with In Situ-Generated Nano-TiO2 as Wound Dressing. *Journal of Applied Polymer Science* **2011,** *119*, (3), 1532-1541.

32. Ni, M.; Leung, M. K. H.; Leung, D. Y. C.; Sumathy, K., A review and recent developments in photocatalytic water-splitting using TiO2 for hydrogen production. *Renewable & Sustainable Energy Reviews* **2007,** *11*, (3), 401-425.

33. Wang, J. X.; Zhou, G. Q.; Chen, C. Y.; Yu, H. W.; Wang, T. C.; Ma, Y. M.; Jia, G.; Gao, Y. X.; Li, B.; Sun, J.; Li, Y. F.; Jiao, F.; Zhao, Y. L.; Chai, Z. F., Acute toxicity and biodistribution of different sized titanium dioxide particles in mice after oral administration. *Toxicology Letters* **2007,** *168*, (2), 176-185.

34. Warheit, D. B.; Sayes, C. M.; Reed, K. L.; Swain, K. A., Health effects related to nanoparticle exposures: Environmental, health and safety considerations for assessing hazards and risks. *Pharmacology & Therapeutics* **2008,** *120*, (1), 35-42.

35. Baan, R.; Straif, K.; Grosse, Y.; Secretan, W.; El Ghissassi, F.; Cogliano, V.; Agency, W. H. O. I., Carcinogenicity of carbon black, titanium dioxide, and talc. *Lancet Oncology* **2006,** *7*, (4), 295-296.

36. Fabian, E.; Landsiedel, R.; Ma-Hock, L.; Wiench, K.; Wohlleben, W.; Van Ravenzwaay, B., Tissue distribution and toxicity of intravenously administered titanium dioxide nanoparticles in rats. *Archives of Toxicology* **2008,** *82*, (3), 151-157.

37. Krug, H. F.; Wick, P., Nanotoxicology: An Interdisciplinary Challenge. *Angewandte Chemie-International Edition* **2011,** *50*, (6), 1260-1278.

38. Lockman, P. R.; Koziara, J. M.; Mumper, R. J.; Allen, D. D., Nanoparticle surface charges alter blood-brain barrier integrity and permeability. *Journal of Drug Targeting* **2004,** *12*, (9-10), 635-641.

39. Long, T. C.; Saleh, N.; Tilton, R. D.; Lowry, G. V.; Veronesi, B., Titanium dioxide (P25) produces reactive oxygen species in immortalized brain microglia (BV2): Implications for nanoparticle neurotoxicity. *Environmental Science & Technology* **2006,** *40*, (14), 4346-4352.

40. Liang, X. J.; Chen, C. Y.; Zhao, Y. L.; Jia, L.; Wang, P. C., Biopharmaceutics and Therapeutic Potential of Engineered Nanomaterials. *Current Drug Metabolism* **2008,** *9*, (8), 697-709.

41. Koeneman, B. A.; Zhang, Y.; Westerhoff, P.; Chen, Y. S.; Crittenden, J. C.; Capco, D. G., Toxicity and cellular responses of intestinal cells exposed to titanium dioxide. *Cell Biology and Toxicology* **2010,** *26*, (3), 225-238.

42. Frampton, M. W., Does Inhalation of Ultrafine Particles Cause Pulmonary Vasular Effects in Humans? *Inhalation Toxicology* **2007,** *19*, 75-79.

43. Kuempel, E. D.; Tran, C. L.; Castranova, V.; Bailer, A. J., Lung dosimetry and risk assessment of nanoparticles: Evaluating and extending current models in rats and humans. *Inhalation Toxicology* **2006,** *18*, (10), 717-724.

44. Shin, J. A.; Lee, E. J.; Seo, S. M.; Kim, H. S.; Kang, J. L.; Park, E. M., NANOSIZED TITANIUM DIOXIDE ENHANCED INFLAMMATORY RESPONSES IN THE SEPTIC BRAIN OF MOUSE. *Neuroscience* **2010,** *165*, (2), 445-454.

45. Vamanu, C. I.; Cimpan, M. R.; Hol, P. J.; Sornes, S.; Lie, S. A.; Gjerdet, N. R., Induction of cell death by TiO2 nanoparticles: Studies on a human monoblastoid cell line. *Toxicology in Vitro* **2008,** *22*, (7), 1689-1696.

46. Kiser, M. A.; Westerhoff, P.; Benn, T.; Wang, Y.; Perez-Rivera, J.; Hristovski, K., Titanium Nanomaterial Removal and Release from Wastewater Treatment Plants. *Environmental Science & Technology* **2009,** *43*, (17), 6757-6763.

47. Westerhoff, P.; Song, G. X.; Hristovski, K.; Kiser, M. A., Occurrence and removal of titanium at full scale wastewater treatment plants: implications for TiO2 nanomaterials. *Journal of Environmental Monitoring* **2011,** *13*, (5), 1195-1203.

48. Neal, C.; Jarvie, H.; Rowland, P.; Lawler, A.; Sleep, D.; Scholefield, P., Titanium in UK rural, agricultural and urban/industrial rivers: Geogenic and anthropogenic colloidal/sub-colloidal sources and the significance of within-river retention. *Science of the Total Environment* **2011,** *409*, (10), 1843-1853.

49. Gottschalk, F.; Nowack, B., The release of engineered nanomaterials to the environment. *Journal of Environmental Monitoring* **2011,** *13*, (5), 1145-1155.

50. Ma, X. M.; Geiser-Lee, J.; Deng, Y.; Kolmakov, A., Interactions between engineered nanoparticles (ENPs) and plants: Phytotoxicity, uptake and accumulation. *Science of the Total Environment* **2010,** *408*, (16), 3053-3061.

51. Johnston, B. D.; Scown, T. M.; Moger, J.; Cumberland, S. A.; Baalousha, M.; Linge, K.; van Aerle, R.; Jarvis, K.; Lead, J. R.; Tyler, C.

R., Bioavailability of Nanoscale Metal Oxides TiO2, CeO2, and ZnO to Fish. *Environmental Science & Technology* **2010,** *44*, (3), 1144-1151.

52. Menard, A.; Drobne, D.; Jemec, A., Ecotoxicity of nanosized TiO2. Review of in vivo data. *Environmental Pollution* **2011,** *159*, (3), 677-684.

53. Zhu, X. S.; Chang, Y.; Chen, Y. S., Toxicity and bioaccumulation of TiO2 nanoparticle aggregates in Daphnia magna. *Chemosphere* **2010,** *78*, (3), V-215.

54. Lu, M. G.; Al-Jamal, K. T.; Kostarelos, K.; Reineke, J., Physiologically Based Pharmacokinetic Modeling of Nanoparticles. *Acs Nano* **2010,** *4*, (11), 6303-6317.

55. Hämeri, K.; Lähde, T.; Hussein, T.; Koivisto, J.; Savolainen, K., Facing the key workplace challenge: Assessing and preventing exposure to nanoparticles at source. *Inhalation Toxicology* **2009,** *21*, (s1), 17-24.

56. Demou, E.; Stark, W. J.; Hellweg, S., Particle Emission and Exposure during Nanoparticle Synthesis in Research Laboratories. *Annals of Occupational Hygiene* **2009,** *53*, (8), 829-838.

57. Liao, C. M.; Chiang, Y. H.; Chio, C. P., Assessing the airborne titanium dioxide nanoparticle-related exposure hazard at workplace. *Journal of Hazardous Materials* **2009,** *162*, (1), 57-65.

58. Brouwer, D., Exposure to manufactured nanoparticles in different workplaces. *Toxicology* **2010,** *269*, (2-3), 120-127.

59. Osman, T. M., Environmental, health, and safety considerations for producing nanomaterials. *Jom* **2008,** *60*, (3), 14-17.

60. Seipenbusch, M.; Binder, A.; Kasper, G., Temporal Evolution of Nanoparticle Aerosols in Workplace Exposure. *Annals of Occupational Hygiene* **2008,** *52*, (8), 707-716.

61. Hagens, W. I.; Oomen, A. G.; de Jong, W. H.; Cassee, F. R.; Sips, A., What do we (need to) know about the kinetic properties of nanoparticles in the body? *Regulatory Toxicology and Pharmacology* **2007,** *49*, (3), 217-229.

62. Choi, H. S.; Ashitate, Y.; Lee, J. H.; Kim, S. H.; Matsui, A.; Insin, N.; Bawendi, M. G.; Semmler-Behnke, M.; Frangioni, J. V.; Tsuda, A., Rapid translocation of nanoparticles from the lung airspaces to the body. *Nat Biotech* **2010,** *28*, (12), 1300-1303.

63. Jani, P. U.; McCarthy, D. E.; Florence, A. T., TITANIUM-DIOXIDE (RUTILE) PARTICLE UPTAKE FROM THE RAT GI TRACT AND TRANSLOCATION TO SYSTEMIC ORGANS AFTER ORAL-ADMINISTRATION. *International Journal of Pharmaceutics* **1994,** *105*, (2), 157-168.

64. Crosera, M.; Bovenzi, M.; Maina, G.; Adami, G.; Zanette, C.; Florio, C.; Filon Larese, F., Nanoparticle dermal absorption and toxicity: a review of the literature. *International Archives of Occupational & Environmental Health* **2009,** *82*, (9), 1043-1055.

65. Takahashi, Y.; Mizuo, K.; Shinkai, Y.; Oshio, S.; Takeda, K., Prenatal exposure to titanium dioxide nanoparticles increases dopamine levels in the prefrontal cotex and neostriatum of mice. *Journal of Toxicological Sciences* **2010,** *35*, (5), 749-756.

66. O'Brien, N. J.; Cummins, E. J., A Risk Assessment Framework for Assessing Metallic Nanomaterials of Environmental Concern: Aquatic Exposure and Behavior. *Risk Analysis* **2010**, no-no.

67. Oberdorster, G.; Oberdorster, E.; Oberdorster, J., Nanotoxicology: An emerging discipline evolving from studies of ultrafine particles. *Environmental Health Perspectives* **2005,** *113*, (7), 823-839.

68. Geiser, M.; Rothen-Rutishauser, B.; Kapp, N.; Schurch, S.; Kreyling, W.; Schulz, H.; Semmler, M.; Hof, V. I.; Heyder, J.; Gehr, P., Ultrafine particles cross cellular membranes by nonphagocytic mechanisms in lungs and in cultured cells. *Environmental Health Perspectives* **2005,** *113*, (11), 1555-1560.

69. Meiring, J.; Borm, P.; Bagate, K.; Semmler, M.; Seitz, J.; Takenaka, S.; Kreyling, W., The influence of hydrogen peroxide and histamine on lung permeability and translocation of iridium nanoparticles in the isolated perfused rat lung. *Particle and Fibre Toxicology* **2005,** *2*, (1), 3.

70. Shimada, A.; Kawamura, N.; Okajima, M.; Kaewamatawong, T.; Inoue, H.; Morita, T., Translocation pathway of the intratracheally instilled ultrafine particles from the lung into the blood circulation in the mouse. *Toxicologic Pathology* **2006,** *34*, (7), 949-957.

71. Zhu, M. T.; Feng, W. Y.; Wang, Y.; Wang, B.; Wang, M.; Ouyang, H.; Zhao, Y. L.; Chai, Z. F., Particokinetics and Extrapulmonary Translocation of Intratracheally Instilled Ferric Oxide Nanoparticles in Rats and the Potential Health Risk Assessment. *Toxicological Sciences* **2009,** *107*, (2), 342-351.

72. Oberdorster, G.; Sharp, Z.; Atudorei, V.; Elder, A.; Gelein, R.; Kreyling, W.; Cox, C., Translocation of inhaled ultrafine particles to the brain. *Inhalation Toxicology* **2004,** *16*, (6-7), 437-445.

73. Wang, J. X.; Liu, Y.; Jiao, F.; Lao, F.; Li, W.; Gu, Y. Q.; Li, Y. F.; Ge, C. C.; Zhou, G. Q.; Li, B.; Zhao, Y. L.; Chai, Z. F.; Chen, C. Y., Time-dependent translocation and potential impairment on central nervous system by intranasally instilled TiO2 nanoparticles. *Toxicology* **2008,** *254*, (1-2), 82-90.

74. Mistry, A.; Glud, S. Z.; Kjems, J.; Randel, J.; Howard, K. A.; Stolnik, S.; Illum, L., Effect of physicochemical properties on intranasal nanoparticle transit into murine olfactory epithelium. *Journal of Drug Targeting* **2009,** *17*, (7), 543-552.

75. Edilberto, B.; James, B. M.; Brian, A. W.; Bahman, A.; Paul, M. H.; David, B. W.; Jeffrey, I. E., Pulmonary Responses of Mice, Rats, and Hamsters to Subchronic Inhalation of Ultrafine Titanium Dioxide Particles. *Toxicological Sciences* **2004,** *77*, (2), 347-357.

76. Sugibayashi, K.; Todo, H.; Kimura, E., Safety evaluation of titanium dioxide nanoparticles by their absorption and elimination profiles. *Journal of Toxicological Sciences* **2008,** *33*, (3), 293-298.

77. Hoet, P.; Bruske-Hohlfeld, I.; Salata, O., Nanoparticles - known and unknown health risks. *Journal of Nanobiotechnology* **2004,** *2*, (1), 12.

78. Semmler, M.; Seitz, J.; Erbe, F.; Mayer, P.; Heyder, J.; Oberdorster, G.; Kreyling, W. G., Long-term clearance kinetics of inhaled ultrafine insoluble iridium particles from the rat lung, including transient translocation into secondary organs. *Inhalation Toxicology* **2004,** *16*, (6-7), 453-459.

79. Oberdorster, G.; Ferin, J.; Lehnert, B. E., CORRELATION BETWEEN PARTICLE-SIZE, IN-VIVO PARTICLE PERSISTENCE, AND LUNG INJURY. *Environmental Health Perspectives* **1994,** *102*, 173-179.

80. Schmid, O.; Moller, W.; Semmler-Behnke, M.; Ferron, G. A.; Karg, E.; Lipka, J.; Schulz, H.; Kreyling, W. G.; Stoeger, T., Dosimetry and toxicology of inhaled ultrafine particles. *Biomarkers* **2009,** *14*, 67-73.

81. van Bussel, W.; Kerkhof, F.; van Kessel, T.; Lamers, H.; Nous, D.; Verdonk, H.; Verhoeven, B.; Boer, N.; Toonen, H., Accurate Determination of Titanium as Titanium Dioxide for Limited Sample Size Digestibility Studies of Feed and Food Matrices by Inductively Coupled Plasma Optical Emission Spectrometry With Real-Time Simultaneous Internal Standardization. *Atomic Spectroscopy* **2010,** *31*, (3), 81-88.

82. Shirin, K.; Naseem, S.; Sheikh, S. A.; Shafiq, S.; Latif, S., A comparative study of sample preparation methods for stream sediments analyses using ICP-AES. *Journal of the Chemical Society of Pakistan* **2005,** *27*, (5), 501-507.

83. Boguhn, J.; Baumgartel, T.; Dieckmann, A.; Rodehutscord, M., Determination of titanium dioxide supplements in different matrices using two methods involving photometer and inductively coupled plasma optical emission spectrometer measurements. *Archives of Animal Nutrition* **2009,** *63*, (4), 337-342.

84. Korn, M. D. A.; Ferreira, A. C.; Costa, A. C. S.; Nobrega, J. A.; Silva, C. R., Comparison of decomposition procedures for analysis of titanium dioxide using inductively coupled plasma optical emission spectrometry. *Microchemical Journal* **2002,** *71*, (1), 41-48.

85. Zachariadis, G. A.; Sahanidou, E., Multi-element method for determination of trace elements in sunscreens by ICP-AES. *Journal of Pharmaceutical and Biomedical Analysis* **2009,** *50*, (3), 342-348.

86. Clesceri, L.; Greenberg, A.; Eaton, A., *Standard Methods for the Examination of Water and Wastewater*. 20th ed.; American Public Health Association: Washington, DC, 1998.

87. Levine, K. E.; Fernando, R. A.; Lang, M.; Essader, A.; Wong, B. A., Development, and validation of a high-throughput method for the determination of titanium dioxide in rodent lung and lung-associated lymph node tissues. *Analytical Letters* **2003,** *36*, (3), 563-576.

88. El-Sheikh, A. H.; Sweileh, J. A., A rapid and simple microwave-assisted digestion procedure for spectrophotometric determination of titanium dioxide photocatalyst on activated carbon. *Talanta* **2007,** *71*, (5), 1867-1872.

89. Packer, A. P.; Lariviere, D.; Li, C. S.; Chen, M.; Fawcett, A.; Nielsen, K.; Mattson, K.; Chatt, A.; Scriver, C.; Erhardt, L. S., Validation of an inductively coupled plasma mass spectrometry (ICP-MS) method for the determination of cerium, strontium, and titanium in ceramic materials used in radiological dispersal devices (RDDs). *Analytica Chimica Acta* **2007,** *588*, (2), 166-172.

90. Tripathi, A.; Chattopadhyay, P., Digestion of titanium bearing geologic materials involving microwaves. *Annali Di Chimica* **2007,** *97*, (10), 1047-1064.

91. Zhang, S. C.; Nicol, M. J., Kinetics of the dissolution of ilmenite in sulfuric acid solutions under reducing conditions. *Hydrometallurgy* **2010,** *103*, (1-4), 196-204.

92. Sneddon, J.; Vincent, M. D., ICP-OES and ICP-MS for the determination of metals: Application to oysters. *Analytical Letters* **2008,** *41*, (8), 1291-1303.

93. Lienemann, C. P.; Dreyfus, S.; Pecheyran, C.; Donard, O. F. X., Trace metal analysis in petroleum products: Sample introduction evaluation in ICP-OES and comparison with an ICP-MS approach. *Oil & Gas Science and Technology-Revue De L Institut Francais Du Petrole* **2007,** *62*, (1), 69-77.

94. Beauchemin, D., Inductively Coupled Plasma Mass Spectrometry. *Analytical Chemistry* **2010,** *82*, (12), 4786-4810.

95. Heard, K.; Hill, R. E.; Cairns, C. B.; Dart, R. C., Calcium neutralizes fluoride bioavailability in a lethal model of fluoride poisoning. *Journal of Toxicology-Clinical Toxicology* **2001,** *39*, (4), 349-353.

96. Ohno, T.; Sarukawa, K.; Tokieda, K.; Matsumura, M., Morphology of a TiO2 photocatalyst (Degussa, P-25) consisting of anatase and rutile crystalline phases. *Journal of Catalysis* **2001,** *203*, (1), 82-86.

97. U.S. Code of Federal Regulations. In *Title 40: Protection of the Environment*, 1.11 ed.; Agency, E. P., Ed. Federal Register: Washington, DC, 2011; Vol. Part 136.

98. van Ravenzwaay, B.; Landsiedel, R.; Fabian, E.; Burkhardt, S.; Strauss, V.; Ma-Hock, L., Comparing fate and effects of three particles of different surface properties: Nano-TiO2, pigmentary TiO2 and quartz. *Toxicology Letters* **2009,** *186*, (3), 152-159.

99. Pauluhn, J., Poorly soluble particulates: Searching for a unifying denominator of nanoparticles and fine particles for DNEL estimation. *Toxicology* **2011,** *279*, (1-3), 176-188.

100. Kreyling, W. G.; Biswas, P.; Messing, M. E.; Gibson, N.; Geiser, M.; Wenk, A.; Sahu, M.; Deppert, K.; Cydzik, I.; Wigge, C.; Schmid, O.; Semmler-Behnke, M., Generation and characterization of stable, highly concentrated titanium dioxide nanoparticle aerosols for rodent inhalation studies. *Journal of Nanoparticle Research* **2011,** *13*, (2), 511-524.

101. Sager, T. M.; Kommineni, C.; Castranova, V., Pulmonary response to intratracheal instillation of ultrafine versus fine titanium dioxide: role of particle surface area. *Particle and Fibre Toxicology* **2008,** *5*, 15.

102. Andersson, P. O.; Lejon, C.; Ekstrand-Hammarstrom, B.; Akfur, C.; Ahlinder, L.; Bucht, A.; Osterlund, L., Polymorph- and Size-Dependent Uptake and Toxicity of TiO2 Nanoparticles in Living Lung Epithelial Cells. *Small* **2011,** *7*, (4), 514-523.

103. Warheit, D. B.; Webb, T. R.; Reed, K. L.; Frerichs, S.; Sayes, C. M., Pulmonary toxicity study in rats with three forms of ultrafine-TiO2 particles: Differential responses related to surface properties. *Toxicology* **2007,** *230*, (1), 90-104.

104. Li, N.; Ma, L.; Wang, J.; Zheng, L.; Liu, J.; Duan, Y.; Liu, H.; Zhao, X.; Wang, S.; Wang, H.; Hong, F.; Xie, Y., Interaction Between Nano-Anatase TiO₂ and Liver DNA from Mice In Vivo. *Nanoscale Research Letters* **2010,** *5*, (1), 108-115.

105. Hamilton, R. F.; Wu, N. Q.; Porter, D.; Buford, M.; Wolfarth, M.; Holian, A., Particle length-dependent titanium dioxide nanomaterials toxicity and bioactivity. *Particle and Fibre Toxicology* **2009,** *6*, 11.

106. Scotter, M. J., Methods for the determination of European Union-permitted added natural colours in foods: a review. *Food Additives and Contaminants Part a-Chemistry Analysis Control Exposure & Risk Assessment* **2011,** *28*, (5), 527-596.

107. Titanium Dioxide (E171).

108. Lomer, M. C. E.; Thompson, R. P. H.; Commisso, J.; Keen, C. L.; Powell, J. J., Determination of titanium dioxide in foods using inductively coupled plasma optical emission spectrometry. *Analyst* **2000,** *125*, (12), 2339-2343.

109. Lomer, M. C. E.; Hutchinson, C.; Volkert, S.; Greenfield, S. M.; Catterall, A.; Thompson, R. P. H.; Powell, J. J., Dietary sources of inorganic microparticles and their intake in healthy subjects and patients with Crohn's disease. *British Journal of Nutrition* **2004,** *92*, (6), 947-955.

110. Butler, M.; Boyle, J. J.; Powell, J. J.; Playford, R. J.; Ghosh, S., Dietary microparticles implicated in Crohn's disease can impair macrophage phagocytic activity and act as adjuvants in the presence of bacterial stimuli. *Inflammation Research* **2007,** *56*, (9), 353-361.

111. U.S. Code of Federal Regulations. In *Title 21: Food and Drugs*, Administration, F. a. D., Ed. Federal Register: Washington D.C., 2011; Vol. Part 73.

112. Abbott, L. C.; Maynard, A. D., Exposure Assessment Approaches for Engineered Nanomaterials. *Risk Analysis* **2010,** *30*, (11), 1634-1644.

113. Xu, L. G.; Liu, Y.; Bai, R.; Chen, C. Y., Applications and toxicological issues surrounding nanotechnology in the food industry. *Pure and Applied Chemistry* **2010,** *82*, (2), 349-372.

114. Kim, B.; Kim, D.; Cho, D.; Cho, S., Bactericidal effect of TiO2 photocatalyst on selected food-borne pathogenic bacteria. *Chemosphere* **2003,** *52*, (1), 277-281.

115. Kim, Y.; Choi, Y.; Kim, S.; Park, J.; Chung, M.; Bin Song, K.; Hwang, I.; Kwon, K., Disinfection of Iceberg Lettuce by Titanium Dioxide-UV Photocatalytic Reaction. *Journal of Food Protection* **2009,** *72*, (9), 1916-1922.

116. Diaz-Visurraga, J.; Melendrez, M. F.; Garcia, A.; Paulraj, M.; Cardenas, G., Semitransparent Chitosan-TiO2 Nanotubes Composite Film for Food Package Applications. *Journal of Applied Polymer Science* **2010,** *116*, (6), 3503-3515.

117. Chawengkijwanich, C.; Hayata, Y., Development of TiO2 powder-coated food packaging film and its ability to inactivate Escherichia coli in vitro and in actual tests. *International Journal of Food Microbiology* **2008,** *123*, (3), 288-292.

118. Ditta, I. B.; Steele, A.; Liptrot, C.; Tobin, J.; Tyler, H.; Yates, H. M.; Sheel, D. W.; Foster, H. A., Photocatalytic antimicrobial activity of thin surface films of TiO2, CuO and TiO2/CuO dual layers on Escherichia coli and bacteriophage T4. *Applied Microbiology and Biotechnology* **2008,** *79*, (1), 127-133.

119. Chorianopoulos, N. G.; Tsoukleris, D. S.; Panagou, E. Z.; Falaras, P.; Nychas, G. J. E., Use of titanium dioxide (TiO2) photocatalysts as alternative means for Listeria monocytogenes biofilm disinfection in food processing. *Food Microbiology* **2011,** *28*, (1), 164-170.

120. Rico, C. M.; Majumdar, S.; Duarte-Gardea, M.; Peralta-Videa, J. R.; Gardea-Torresdey, J. L., Interaction of Nanoparticles with Edible Plants and Their Possible Implications in the Food Chain. *Journal of Agricultural and Food Chemistry* **2011,** *59*, (8), 3485-3498.

121. Stratmeyer, M. E.; Goering, P. L.; Hitchins, V. M.; Umbreit, T. H., What we know and don't know about the bioeffects of nanoparticles: developing experimental approaches for safety assessment. *Biomedical Microdevices* **2010,** *12*, (4), 569-573.

122. Powell, J. J.; Ainley, C. C.; Harvey, R. S. J.; Mason, I. M.; Kendall, M. D.; Sankey, E. A.; Dhillon, A. P.; Thompson, R. P. H., Characterisation of inorganic microparticles in pigment cells of human gut associated lymphoid tissue. *Gut* **1996,** *38*, (3), 390-395.

123. Schneider, J. C., Can microparticles contribute to inflammatory bowel disease: Innocuous or inflammatory? *Experimental Biology and Medicine* **2007,** *232*, (1), 1-2.

124. Lomer, M. C. E.; Thompson, R. P. H.; Powell, J. J., Fine and ultrafine particles of the diet: influence on the mucosal immune response and association with Crohn's disease. *Proceedings of the Nutrition Society* **2002,** *61*, (1), 123-130.

125. Jemec, A.; Drobne, D.; Remskar, M.; Sepcic, K.; Tisler, T., Effects of ingested nano-sized titanium dioxide on terrestrial isopods (Porcellio scaber). *Environmental Toxicology and Chemistry* **2008,** *27*, (9), 1904-1914.

126. Drobne, D.; Jemec, A.; Tkalec, Z. P., In vivo screening to determine hazards of nanoparticles: Nanosized TiO2. *Environmental Pollution* **2009,** *157*, (4), 1157-1164.

127. Lin, C. C.; Lin, W. J., Sun Protection Factor Analysis of Sunscreens Containing Titanium Dioxide Nanoparticles. *Journal of Food and Drug Analysis* **2011,** *19*, (1), 1-8.

128. Burnett, M. E.; Wang, S. Q., Current sunscreen controversies: a critical review. *Photodermatology Photoimmunology & Photomedicine* **2011,** *27*, (2), 58-67.

129. Schilling, K.; Bradford, B.; Castelli, D.; Dufour, E.; Nash, J. F.; Pape, W.; Schulte, S.; Tooley, I.; van den Bosch, J.; Schellauf, F., Human safety review of "nano" titanium dioxide and zinc oxide. *Photochemical & Photobiological Sciences* **2010,** *9*, (4), 495-509.

130. Tyner, K. M.; Wokovich, A. M.; Godar, D. E.; Doub, W. H.; Sadrieh, N., The state of nano-sized titanium dioxide (TiO2) may affect sunscreen performance. *International Journal of Cosmetic Science* **2011,** *33*, (3), 234-244.

131. Labille, J.; Feng, J. H.; Botta, C.; Borschneck, D.; Sammut, M.; Cabie, M.; Auffan, M.; Rose, J.; Bottero, J. Y., Aging of TiO2 nanocomposites used in sunscreen. Dispersion and fate of the degradation products in aqueous environment. *Environmental Pollution* **2010,** *158*, (12), 3482-3489.

132. Carlotti, M. E.; Ugazio, E.; Sapino, S.; Fenoglio, I.; Greco, G.; Fubini, B., Role of particle coating in controlling skin damage photoinduced by titania nanoparticles. *Free Radical Research* **2009,** *43*, (3), 312-322.

133. Nohynek, G. J.; Lademann, J.; Ribaud, C.; Roberts, M. S., Grey goo on the skin? Nanotechnology, cosmetic and sunscreen safety. *Critical Reviews in Toxicology* **2007,** *37*, (3), 251-277.

134. Hexsel, C. L.; Bangert, S. D.; Hebert, A. A.; Lim, H. W., Current sunscreen issues: 2007 Food and Drug Administration sunscreen labelling recommendations and combination sunscreen/insect repellent products. *Journal of the American Academy of Dermatology* **2008,** *59*, (2), 316-323.

135. Lu, N. H.; Zhu, Z. N.; Zhao, X. Q.; Tao, R.; Yang, X. L.; Gao, Z. H., Nano titanium dioxide photocatalytic protein tyrosine nitration: A potential hazard of TiO2 on skin. *Biochemical and Biophysical Research Communications* **2008,** *370*, (4), 675-680.

136. Braydich-Stolle, L. K.; Schaeublin, N. M.; Murdock, R. C.; Jiang, J.; Biswas, P.; Schlager, J. J.; Hussain, S. M., Crystal structure mediates mode of cell death in TiO2 nanotoxicity. *Journal of Nanoparticle Research* **2009,** *11*, (6), 1361-1374.

137. Sadrieh, N.; Wokovich, A. M.; Gopee, N. V.; Zheng, J. W.; Haines, D.; Parmiter, D.; Siitonen, P. H.; Cozart, C. R.; Patri, A. K.; McNeil, S. E.; Howard, P. C.; Doub, W. H.; Buhse, L. F., Lack of Significant Dermal Penetration of Titanium Dioxide from Sunscreen Formulations Containing Nano- and Submicron-Size TiO2 Particles. *Toxicological Sciences* **2010,** *115*, (1), 156-166.

138. Wu, J. H.; Liu, W.; Xue, C. B.; Zhou, S. C.; Lan, F. L.; Bi, L.; Xu, H. B.; Yang, X. L.; Zeng, F. D., Toxicity and penetration of TiO2 nanoparticles in hairless mice and porcine skin after subchronic dermal exposure. *Toxicology Letters* **2009,** *191*, (1), 1-8.

139. Samontha, A.; Shiowatana, J.; Siripinyanond, A., Particle size characterization of titanium dioxide in sunscreen products using sedimentation field-flow fractionation-inductively coupled plasma-mass

spectrometry. *Analytical and Bioanalytical Chemistry* **2011,** *399*, (2), 973-978.

140. Balmer, M. E.; Buser, H. R.; Muller, M. D.; Poiger, T., Occurrence of some organic UV filters in wastewater, in surface waters, and in fish from Swiss lakes. *Environmental Science & Technology* **2005,** *39*, (4), 953-962.

141. Botta, C.; Labille, J.; Auffan, M.; Borschneck, D.; Miche, H.; Cabie, M.; Masion, A.; Rose, J.; Bottero, J. Y., TiO2-based nanoparticles released in water from commercialized sunscreens in a life-cycle perspective: Structures and quantities. *Environmental Pollution* **2011,** *159*, (6), 1543-1548.

142. Kaegi, R.; Sinnet, B.; Zuleeg, S.; Hagendorfer, H.; Mueller, E.; Vonbank, R.; Boller, M.; Burkhardt, M., Release of silver nanoparticles from outdoor facades. *Environmental Pollution* **2010,** *158*, (9), 2900-2905.

143. Mirabedini, S. M.; Sabzi, M.; Zohuriaan-Mehr, J.; Atai, M.; Behzadnasab, M., Weathering performance of the polyurethane nanocomposite coatings containing silane treated TiO2 nanoparticles. *Applied Surface Science* **2011,** *257*, (9), 4196-4203.

144. Neale, R.; Williams, G.; Green, A., Application patterns among participants randomized to daily sunscreen use in a skin cancer prevention trial. *Archives of Dermatology* **2002,** *138*, (10), 1319-1325.

APPENDIX A

SUPPLEMENTARY INFORMATION

Table A.1

Digestion Reagent Concentrations

Reagent	Concentration	Titanium
Nitric Acid	70% by weight	< 10 pg/g
Hydrofluoric Acid	50% by weight	< 5 pg/g
Hydrogen Peroxide	30% by weight	

Table A.2

Passing Performance Report Requirements

Sensitivity and Stability Results				
Species	7 Li	115 In	220 Bkg	238 U
Mean CPS	> 60,000	> 400,000	< 3	> 800,000
% RSD	< 2.0 %	< 2.0 %	N/A	< 2.0 %
Ratio Results				
Ratio	137 Ba++/137 Ba	115 In/220 Bkg	156 CeO/140 Ce	
Limit	< 0.0300	< 800,000	< 0.0200	

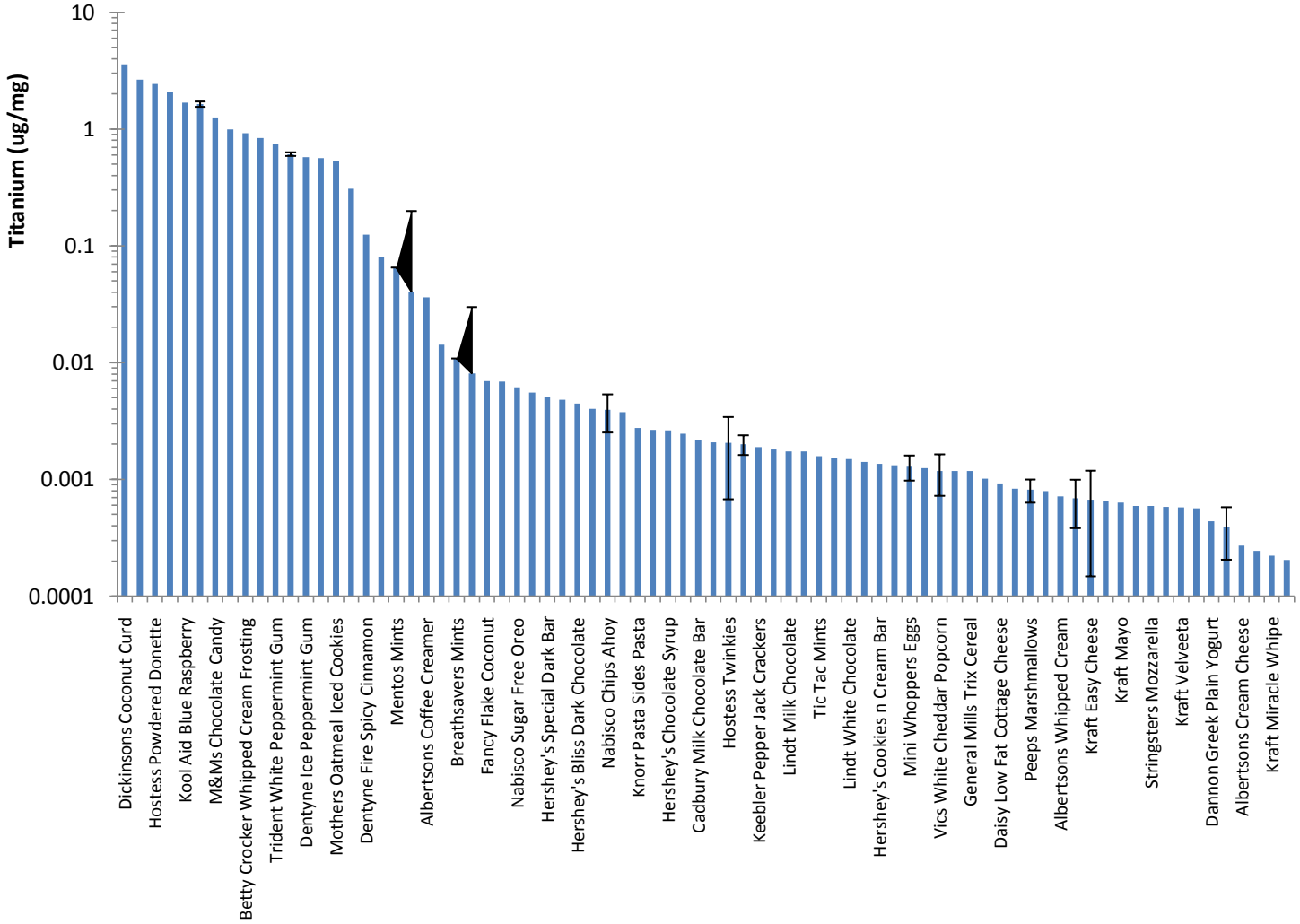

Figure A.1. Normalized titanium concentration for all foods.

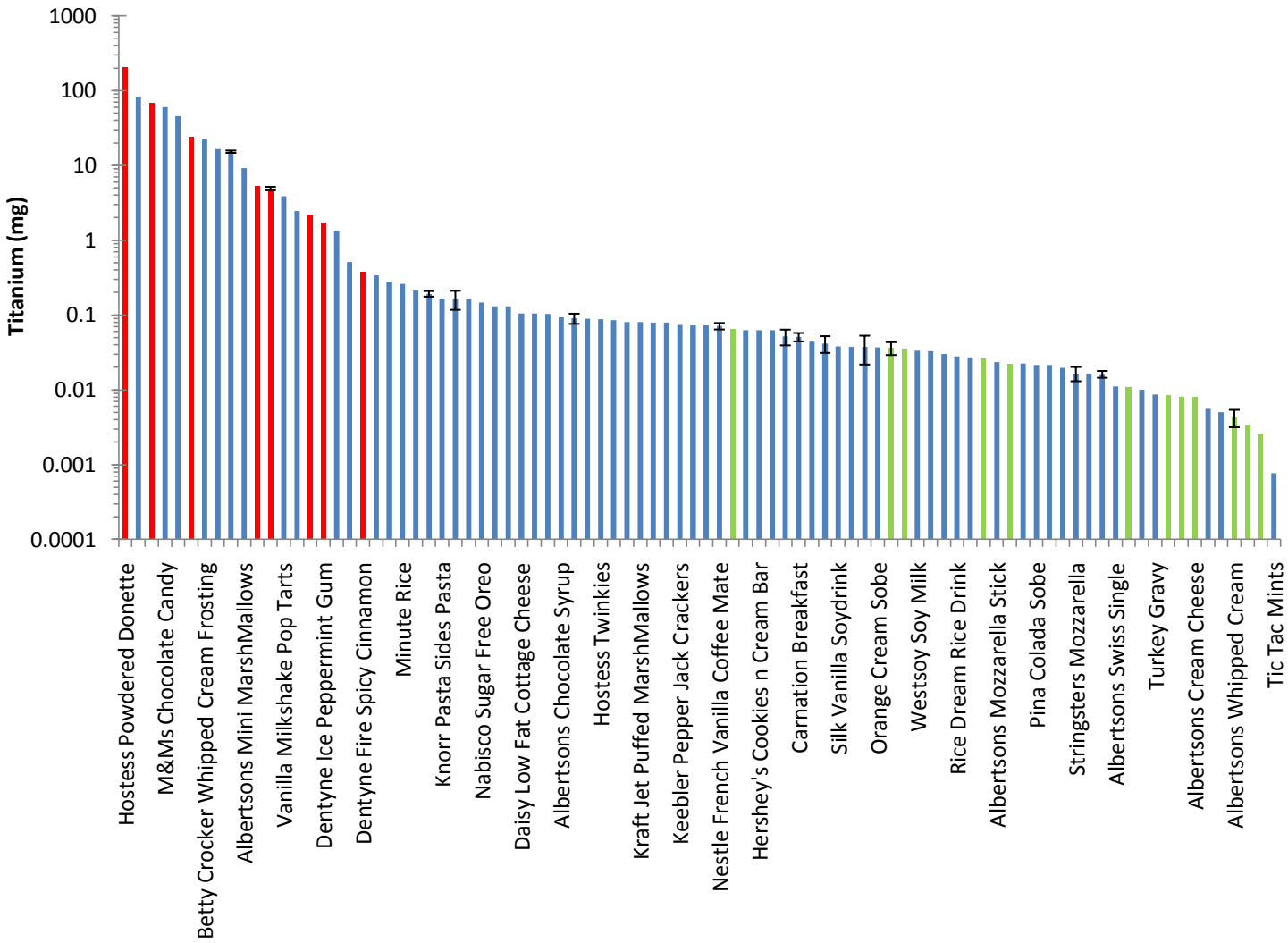

Figure A.2. Mass titanium per serving of food. Red bars indicate TiO2 was listed as an ingredient. Green bars indicate foods were below the detection limit.

APPENDIX B

STANDARD OPERATING PROCEDURES

B.1 TiO_2 Nanoparticle Stock Preparation

1. Add .6 grams of TiO_2 nanoparticle (NP) powder to 600 mL of nanopure water.
2. Sonicate the NP solution for 30 min at 100% amplitude (30 sec on and 5 sec off).
    a. Add ice around the beaker while sonicating to prevent overheating.
    b. Watch the power reading on the instrument. At 100% amplitude it should read approximately 120 W. This provides 200W/L of power.
3. Add 50 mL of the sonicated NP solution to each of eight 50 mL centrifuge vials.
4. Centrifuge the sonicated NP solution for 30 min at 3000 RCF.
5. Carefully remove the vials from the centrifuge and pipette off the top 30 mL of the solution from each vial without disturbing the bottom.
    a. Any solution remaining in the centrifuge vials can be combined and re-sonicated.
6. Run phase analysis light scattering (PALS) on the centrifuged NP solution to determine particle size. (For P25 TiO_2 NPs, the effective diameter should be ~50 nm)
7. If the particle size is not sufficiently small, centrifuge again and run PALS again.

B.2 TiO_2 Microwave Digestion in Tissues and other Organic Matrices

- Hydrofluoric acid will be used in this method, make sure you are properly trained and have all required notifications posted near your workspace.
- All work using acids should be done in the hood.
- All digestion vessels, Teflon, and glassware should be sonicated in an acid bath for at least 10 minutes to clean.

1. Add tissue or sample volume to microwave digestion vessel.

   Note: No more than 0.5 g of organics can be digested at a time.
2. If tissues must be dried first, weigh the empty vessel, dry the tissue at 80°C till weight loss no longer occurs (12-18 hours) and record the new weight.
3. Add 8 mL nitric acid and 2 mL of HF to each vessel.
4. Replace the stopper and tighten the lids as tight as possible!
5. Place the vessels in the microwave digestor carousel.
6. Place the carousel in the microwave and choose the proper method then press start/run.
7. Allow >20 min after the method has finished for the vessels to cool.
8. Remove the vessels from the carousel.
9. Carefully unscrew the lids from each vessel. Pressure will have built up causing a small burst of gas to escape upon opening.

10. Rinse each vessel with 2% nitric acid 3 or 4 times into a Teflon beaker. (About 30 mL of rinse)
11. Heat the beakers on a hotplate at 180°C for approximately 3-4 hours.

    Note: Do not heat the Teflon beakers over 220°C.

12. Continue heating until the remaining liquid is between 0.1-0.5 mL.
13. Remove from heat and allow the beaker to cool.
14. Rinse the beaker 3 or 4 times into a 25 mL volumetric flask with a 2% nitric acid rinse.
15. Continue filling the flask until it is to the 25 mL mark.
16. Transfer the solution to a clean 50 mL centrifuge vial until ICP analysis can be done.

B.3 TiO_2 Hotplate Digestion in Tissues and other Organic Matrices

1. Tare each Teflon vessel individually and add the tissue sample recording the weight.
2. Add 4 mL of concentrated ultrapure nitric acid and 8 mL of hydrogen peroxide.
3. Cap with a ribbed watch glass and place on hot plate.
4. Heat for 4 hrs at 120°C to degrade organics and evaporate acid. Do not go to total dryness.
5. Cool and add 2 mL of ultrapure hydrofluoric acid.
6. Heat at 80°C until remaining solution is between 0.1-0.5 mL.
7. Remove from heat and cool solution.
8. Add 2% nitric acid in nanopure and rinse the vessel 3+ times into a 25mL acid-washed volumetric flask.

APPENDIX C

MODEL DATA

Table C.1

Exposure Scenario #1 Model

INHALATION				
Input	**Value**	**Unit**	**Calculation**	**Source**
Air Concentration	2	mg/m3	2	
Exposure Time	20	days	20	
Volume Inhaled/Day	9.6	m3/day	9.6	
Total Air Volume	192	m3	=D5*D4	
Particle Mass Inhaled	384	mg	=D6*D3	
Mass Deposited in Alveoli	128	mg	=D7/3	EPA
Subject Mass	70	kg	70	
Inhalation Dose	1.8	mg/kg	=D8/D9	
Mass Absorbed to Blood (10 min)	35.8	mg	=D8*0.28	Choi
Mass Absorbed to Blood Total	64	mg	=D8*0.5	Choi
Blood Volume	5	L	5	
Maximum Blood Concentration	12.8	ug/mL	=D12/D13	
Lymph Node Conc. (10 min)	0.72	mg/g	=D11*0.02	Choi
Lymph Node Conc. (30 min)	1.28	mg/g	=D12*0.02	Choi
Mass Cleared by Urine	9.28	mg	=D12*0.145	Choi
Maximum Kidney Concentration	66.29	ug/g	=D17/140*1000	
Brain Concentration	Negligible	ug/g	Negligible	Wang
Liver Concentration	Negligible	ug/g	Negligible	Choi
Spleen Concentration	Negligible	ug/g	Negligible	Choi
Days Post Exposure	132	days	132	
Mass Remaining in Lungs	64	mg	=D8*(1/2) ^(D22/132)	Berm-udez

Table C.2

Exposure Scenario #2 Model for Inhalation

INHALATION				
Input	**Value**	**Unit**	**Calculation**	**Source**
Air Concentration	2.5	mg/m3	2.5	
Exposure Time	3	days	3	
Volume Inhaled/Work Day	9.6	m3/day	9.6	
Total Air Volume	28.8	m3	=D5*D4	
Particle Mass Inhaled	72	mg	=D6*D3	
Mass Deposited in Alveoli	36	mg	=D7/2	EPA
Subject Mass	70	kg	70	
Inhalation Dose	0.5	mg/kg	=D8/D9	
Mass Absorbed to Blood	8.64	mg	=D8*0.24	Geiser
Blood Volume	5	L	5	
Maximum Blood Concentration	1.7	ug/mL	=D11/D12	
Mass in Lymphatic System (100 days)	1.1	mg	=5/170*D8	Oberdorster
Kidney Concentration (1 day)	0.02	ug/g	=D10/5*0.24*0.67	Fabian
Kidney Concentration (14 days)	0.00	ug/g	=D10/5*0.24*0.2	Fabian
Kidney Concentration (28 days)	0.00	ug/g	=D10/5*0.24*0.2	Fabian
Liver Concentration (1 day)	3.3	ug/g	=133.8*0.24*D10/5	Fabian
Liver Concentration (14 days)	2.5	ug/g	=99.5*0.24*D10/5	Fabian
Liver Concentration (28 days)	2.7	ug/g	=111.3*0.24*D10/5	Fabian
Spleen Concentration (1 day)	1.9	ug/g	=78.7*0.24*D10/5	Fabian
Spleen Concentration (14 days)	1.2	ug/g	=48.8*0.24*D10/5	Fabian
Spleen Concentration (28 days)	0.8	ug/g	=33.3*0.24*D10/5	Fabian
Brain Concentration (1 day)	1.23	ng/g	=D10/50*120	Wang 2008
Days Post Exposure	501	days	501	
Mass Remaining in Lungs	18	mg	=D8*(1/2)^ (D25/501)	Oberdorster

Table C.3

Exposure Scenario #2 Model for Ingestion and Inhalation

INGESTION				
Input	**Value**	**Unit**	**Calculation**	**Source**
Subject Mass	70	kg	70	
Ingestion Dose	5.0	mg/kg	5.0	
Mass Absorbed to Blood	2.8	mg	=D3*I4*0.008	Wang
Blood Volume	5	L	5	
Maximum Blood Concentration	0.6	ug/mL	=I5/I6	
Kidney Concentration (14 days)	0.375	ng/g	=D4/5000*375	Wang
Liver Concentration (14 days)	0.107	ng/g	=D4/5000*106.7	Wang
Spleen Concentration (14 days)	0.580	ng/g	=D4/5000*580	Wang
Brain Concentration (1 day)	0.15	ng/g	=I4/5000*150	Wang

INJECTION				
Input	**Value**	**Unit**	**Calcualtion**	**Source**
Subject Mass	70	kg	70	
Injection Dose	5.0	mg/kg	5.0	
Mass Absorbed to Blood	350	mg	=M3*M4	
Blood Volume	5	L	5	
Maximum Blood Concentration	70.0	ug/mL	=M5/M6	
Kidney Concentration (1 day)	0.67	ug/g	=M4/5*0.67	Fabian
Kidney Concentration (14 days)	0.20	ug/g	=M4/5*0.2	Fabian
Kidney Concentration (28 days)	0.20	ug/g	=M4/5*0.2	Fabian
Liver Concentration (1 day)	133.8	ug/g	=133.8*M4/5	Fabian
Liver Concentration (14 days)	99.5	ug/g	=99.5*M4/5	Fabian
Liver Concentration (28 days)	111.3	ug/g	=111.3*M4/5	Fabian
Spleen Concentration (1 day)	78.7	ug/g	=78.7*M4/5	Fabian
Spleen Concentration (14 days)	48.8	ug/g	=48.8*M4/5	Fabian
Spleen Concentration (28 days)	33.3	ug/g	=33.3*M4/5	Fabian
Brain Concentration (1 day)	0.10	ng/g	=M4/5000*100	Zhang

APPENDIX D

PHOTOGRAPHS

D.1 Rat Lung Photographs

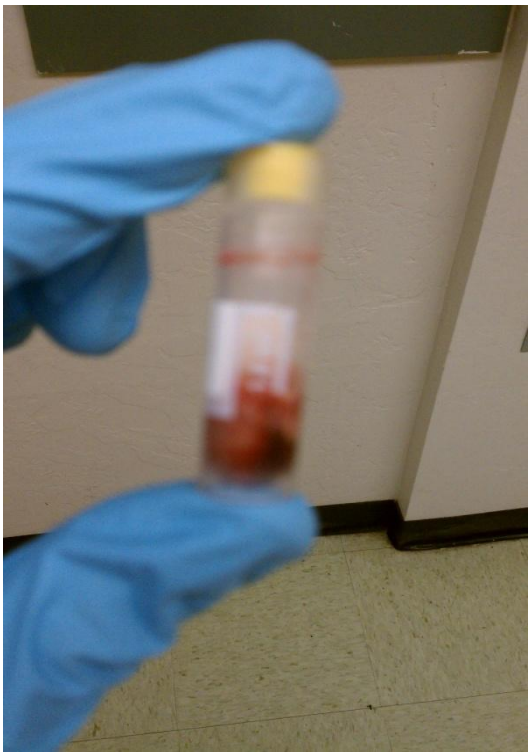

Figure D.1. Caudal lobe sample.

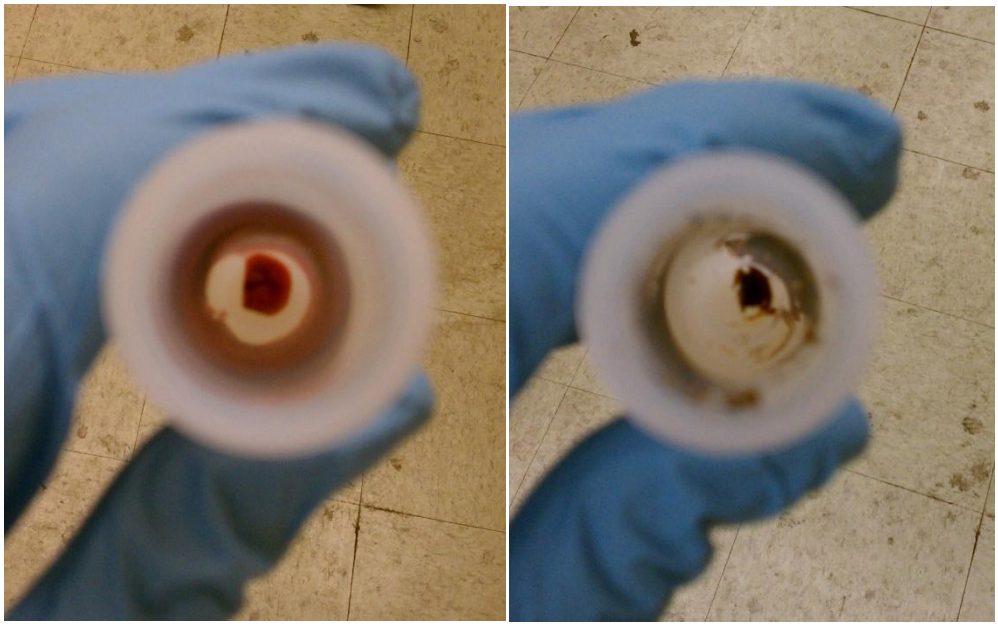

Figure D.2. Caudal lobe in a microwave digestion vessel before drying (left) and after drying (right).

Figure D.3. MARS Express microwave digestor.

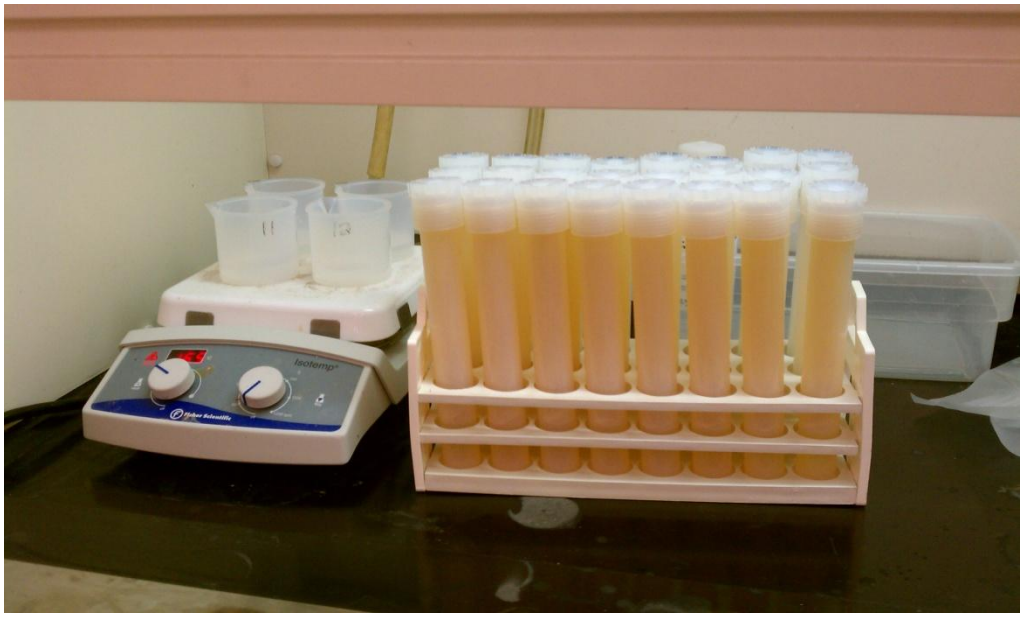

Figure D.4. Microwave vessels and Teflon beakers on a hotplate.

Figure D.5. Rat lung sample after digestion and evaporation

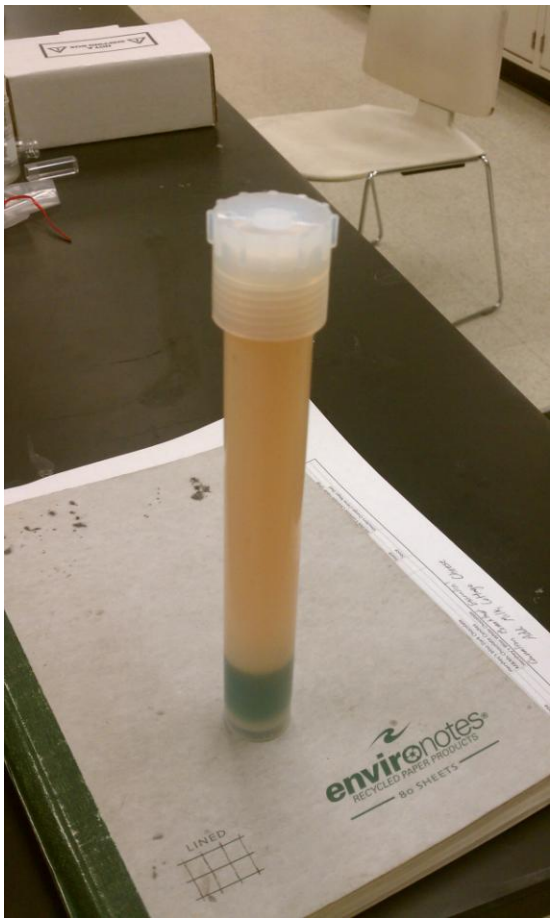

Figure D.6. Microwave vessel after digestion of dairy product.

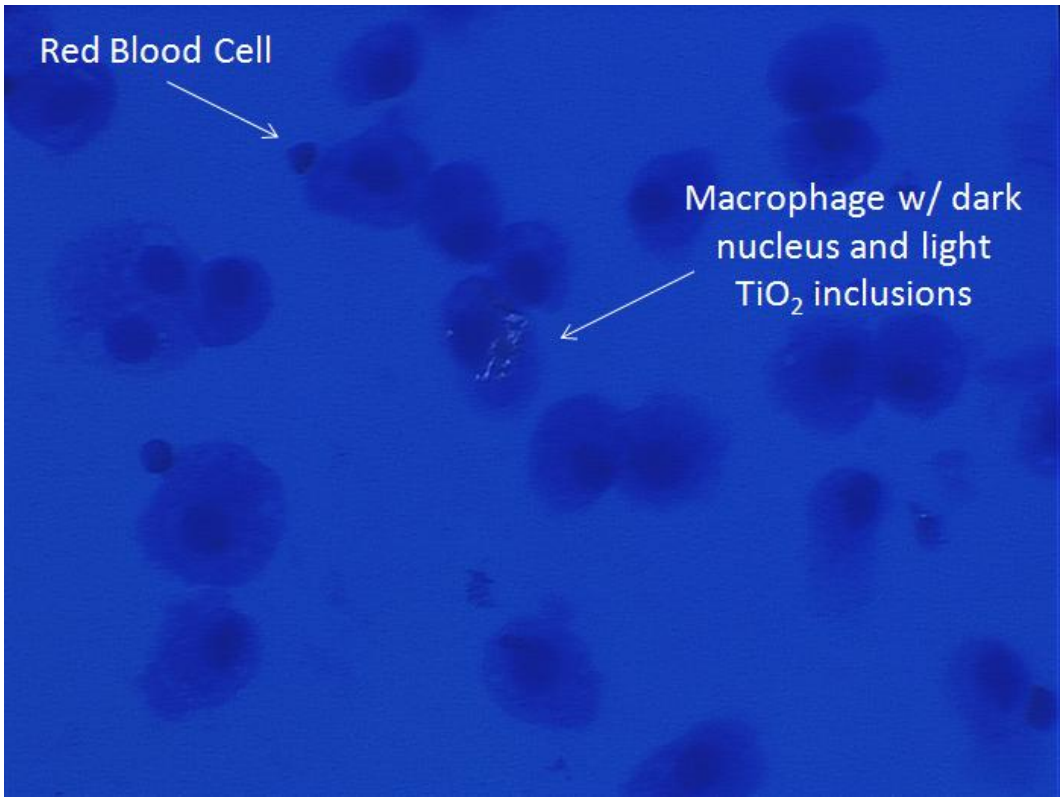

Figure D.7. Animal P1221 broncoalveloar lavage cells with TiO_2 nanobelt inclusions. Shown at 40x.

D.2 Food Product Photographs

Figure D.8. 0.45 µm nylon filter after filtering organics from a food sample.

D.3 Consumer Products Photographs

Figure D.9. Digested sunscreen.

APPENDIX E

METHOD DETECTION LIMITS

E.1 Purpose

Several tests were done to determine how digestion, matrix effects, and analysis instrument choice affect the recovery of nanoparticle solutions. Instrument detection limits (IDLs) for the ICP-OES and ICP-MS instruments were determined for Ti, Zn, and gold (Au). More on the IDL for Ti can be found in Chapter 3. Then solutions of TiO_2 and ZnO nanoparticles were prepared at magnitudes ranging from 10 µg/L (ppb) to 100 mg/L (ppm) in various environmentally and biologically relevant matrices. The solutions were then analyzed with and without digestion by both ICP-OES and ICP-MS. The digestion method used was a hot plate digestion utilizing nitric and sulfuric acid rather than the microwave digestion with HF as described in Chapter 3.

E.2 Instrument Detection Limit

Test Concentration	ICP-MS	ICP-OES
Titanium (2 µg/L)	81 ng/L	562 ng/L
Titanium (5 µg/L)	164 ng/L	491 ng/L
Zinc (2 µg/L)	414 ng/L	1950 ng/L
Zinc (5 µg/L)	616 ng/L	3690 ng/L
Gold (2 µg/L)	97 ng/L	N/A
Gold (5 µg/L)	349 ng/L	N/A

E.3 ICP-MS Ti Instrument Detection Limit Data

Test concentration = 0.002 mg/L

Sample #	C (ppb)
1	2.080
2	2.099
3	2.059
4	2.074
5	2.045
6	2.090
7	2.103
8	2.115
9	2.133
10	2.127

n	10
Average	2.09238
Variance	0.00082
StDev	0.02867
t (n-1, 0.01)	2.821

t value for 99% at n (from Table)

MDL (ppb) 0.081

t value * StDev

	X^2/df	(X^2/df) (MDL)
LCL	0.300	0.024
UCL	2.114	0.171

Average MDL 0.122

LCL 0.037

UCL 0.259

Test concentration = 0.005 mg/L

Sample #	C (ppb)
1	5.479
2	5.456
3	5.427
4	5.551
5	5.533
6	5.515
7	5.587
8	5.538
9	5.611
10	5.567

n	10
Average	5.52640
Variance	0.00338
StDev	0.05816
t (n-1, 0.01)	2.821

t value for 99% at n (from Table)

MDL (ppb) 0.164

t value * StDev

	X^2/df	(X^2/df) (MDL)
LCL	0.300	0.049
UCL	2.114	0.347

E.4 ICP-OES Ti Instrument Detection Limit Data

Test concentration = 0.002 mg/L

Sample #	C (ppb)
1	1.821
2	1.872
3	2.164
4	1.814
5	2.158
6	1.940
7	2.021
8	1.967
9	1.658
10	1.544

n	10
Average	1.89582
Variance	0.03967
StDev	0.19917
t (n-1, 0.01)	2.821

t value for 99% at n (from Table)

MDL (ppb) 0.562

t value * StDev

	X^2/df	(X^2/df) (MDL)
LCL	0.300	0.169
UCL	2.114	1.188

Test concentration = 0.005 mg/L

Sample #	C (ppb)
1	4.869
2	5.079
3	5.143
4	5.259
5	4.993
6	4.958
7	5.119
8	5.296
9	4.794
10	4.834

n	10
Average	5.03428
Variance	0.03031
StDev	0.17411
t (n-1, 0.01)	2.821

t value for 99% at n (from Table)

MDL (ppb) 0.491

t value * StDev

	X^2/df	(X^2/df) (MDL)
LCL	0.300	0.147
UCL	2.114	1.038

E.5 ICP-MS Zn Instrument Detection Limit Data

Test concentration = 0.002 mg/L

Sample #	C (ppb)
1	2.917
2	2.887
3	2.883
4	2.890
5	3.028
6	3.257
7	3.140
8	3.023
9	3.215
10	3.181

n	10
Average	3.04204
Variance	0.02158
StDev	0.14690
t (n-1, 0.01)	2.821

t value for 99% at n (from Table)

MDL (ppb) 0.414

t value * StDev

	X^2/df	(X^2/df) (MDL)
LCL	0.300	0.124
UCL	2.114	0.876

Average MDL 0.515
LCL 0.155
UCL 1.089

Test concentration = 0.005 mg/L

Sample #	C (ppb)
1	3.583
2	3.810
3	4.219
4	4.135
5	4.243
6	4.155
7	4.247
8	4.148
9	4.131
10	4.221

n	10
Average	4.08918
Variance	0.04764
StDev	0.21827
t (n-1, 0.01)	2.821

t value for 99% at n (from Table)

MDL (ppb) 0.616

t value * StDev

	X^2/df	(X^2/df) (MDL)
LCL	0.300	0.185
UCL	2.114	1.301

E.6 ICP-OES Zn Instrument Detection Limit Data

Test concentration = 0.002 mg/L

Sample #	C (ppb)
1	1.755
2	2.371
3	3.704
4	2.792
5	2.842
6	1.990
7	1.933
8	1.696
9	1.357
10	2.213

n	10
Average	2.26538
Variance	0.47689
StDev	0.69057
t (n-1, 0.01)	2.821

t value for 99% at n (from Table)

MDL (ppb) 1.948

t value * StDev

	X^2/df	(X^2/df) (MDL)
LCL	0.300	0.584
UCL	2.114	4.117

Test concentration = 0.005 mg/L

Sample #	C (ppb)
1	6.626
2	4.240
3	4.803
4	5.710
5	2.509
6	5.918
7	4.208
8	5.097
9	5.029
10	2.800

n	10
Average	4.69395
Variance	1.70603
StDev	1.30615
t (n-1, 0.01)	2.821

t value for 99% at n (from Table)

MDL (ppb) 3.685

t value * StDev

	X^2/df	(X^2/df) (MDL)
LCL	0.300	1.105
UCL	2.114	7.788

E.7 ICP-MS Au Instrument Detection Limit Data

Test concentration = 0.002 mg/L

Sample #	C (ppb)
1	1.927
2	1.997
3	2.028
4	2.035
5	2.035
6	2.037
7	2.021
8	2.023
9	2.031
10	2.042

n	10
Average	2.01754
Variance	0.00118
StDev	0.03429
t (n-1, 0.01)	2.821

t value for 99% at n (from Table)

MDL (ppb) 0.097
t value * StDev

	X^2/df	(X^2/df) (MDL)
LCL	0.300	0.029
UCL	2.114	0.204

Test concentration = 0.005 mg/L

Sample #	C (ppb)
1	4.776
2	4.849
3	4.895
4	4.977
5	5.111
6	5.101
7	5.116
8	5.110
9	5.065
10	5.038

n	10
Average	5.00383
Variance	0.01533
StDev	0.12383
t (n-1, 0.01)	2.821

t value for 99% at n (from Table)

MDL (ppb) 0.349
t value * StDev

	X^2/df	(X^2/df) (MDL)
LCL	0.300	0.105
UCL	2.114	0.738

E.8 Nitric/Sulfuric Acid Digestion of TiO_2 and ZnO in Nanopure

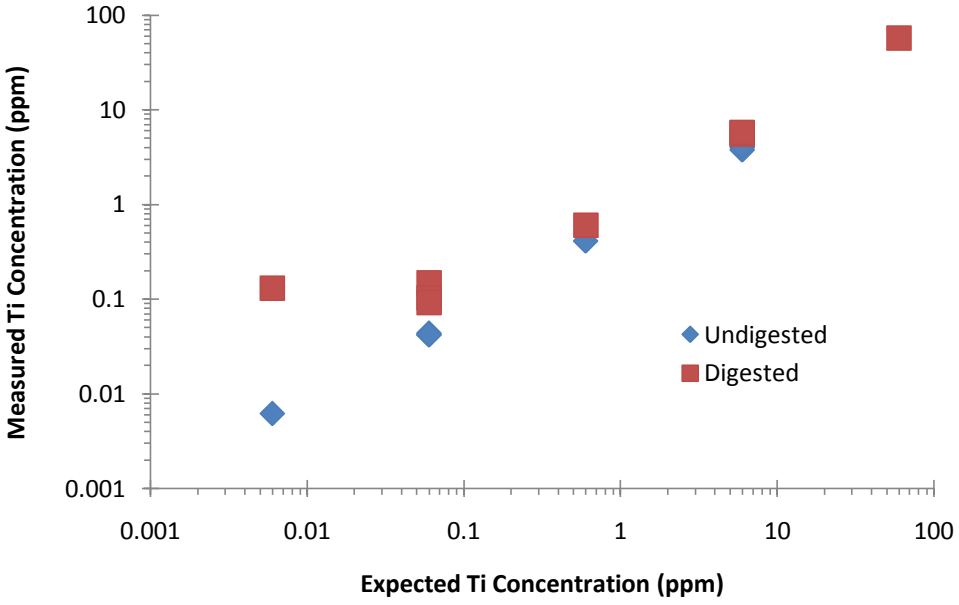

Figure E.1. TiO_2 analyzed by ICP-OES in a nanopure water matrix.

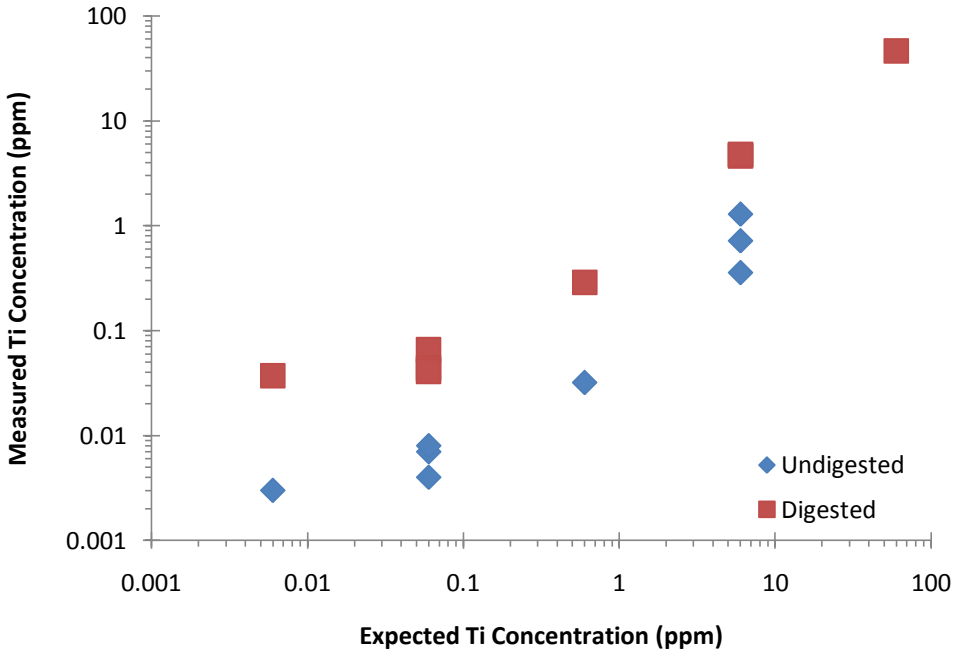

Figure E.2. TiO_2 analyzed by ICP-MS in a nanopure water matrix.

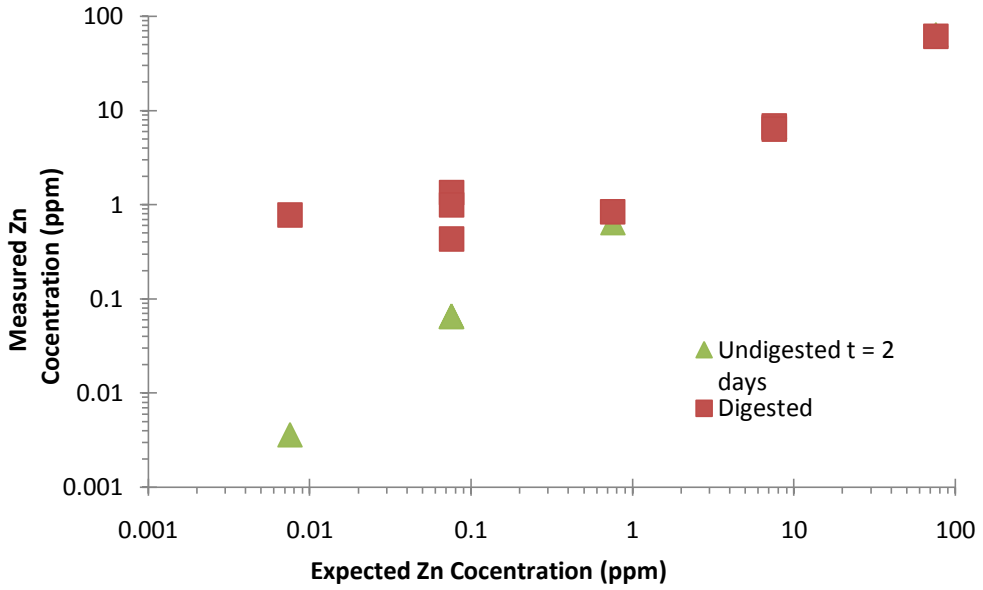

Figure E.3. ZnO analyzed by ICP-OES in a nanopure water matrix.

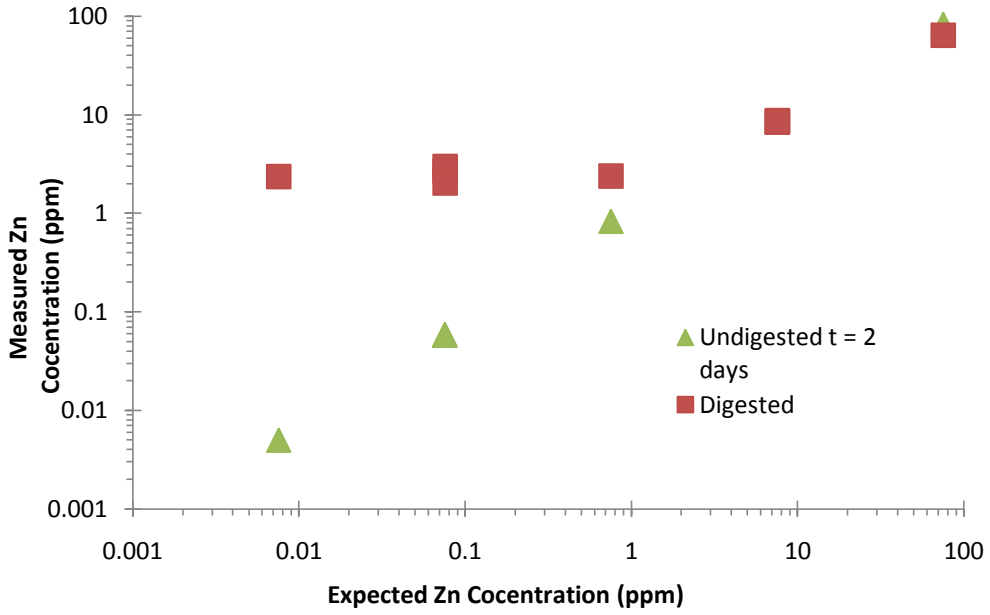

Figure E.4. ZnO analyzed by ICP-MS in a nanopure water matrix.

E.8.1 Nanopure Summary.

TiO_2 samples analyzed by ICP-OES had similar results at higher concentrations regardless of whether the samples were digested or not. However, TiO_2 samples analyzed by ICP-MS without digestion had a much lower measured concentration than expected when compared to those that were digested. This is likely because a smaller fraction of the nebulized sample reaches the plasma in the ICP-MS compared to the ICP-OES, and larger, undigested nanoparticles or aggregates would be less likely to pass through the spray chamber to the plasma. However, on both instruments, the digestion caused the measured concentration of the lowest sample to be nearly an order of magnitude higher. This is because of interferences caused by the sulfuric acid matrix in the samples post-digestion. Thus, digestion is likely necessary to determine an accurate quantification, but another digestion method would be preferred.

There was little difference in the measured concentration of ZnO samples with or without digestion for more concentrated samples. This is likely because ZnO will dissolve faster than titanium so digestion is not as necessary. However, for the more dilute samples the digestion caused the measured concentration to be much higher than the expected concentration. The 3 most dilute samples had nearly the same measured concentration regardless of the expected concentration. This is because the sulfuric acid matrix caused interferences resulting in higher readings. These trends were observed for both instruments.

E.9 Nitric/Sulfuric Acid Digestion of TiO_2 and ZnO in Moderately Hard Water

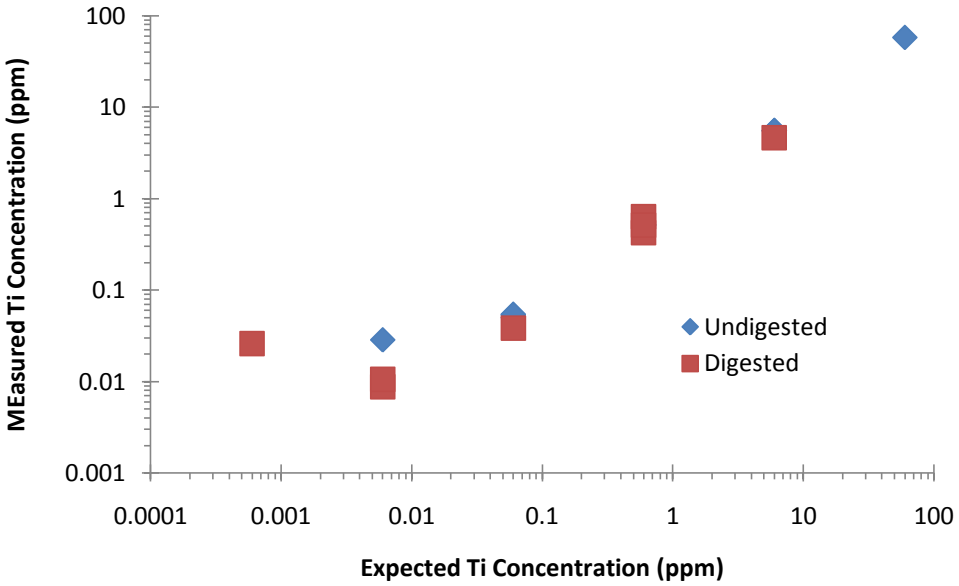

Figure E.5. TiO_2 analyzed by ICP-OES in a moderately hard water matrix**.**

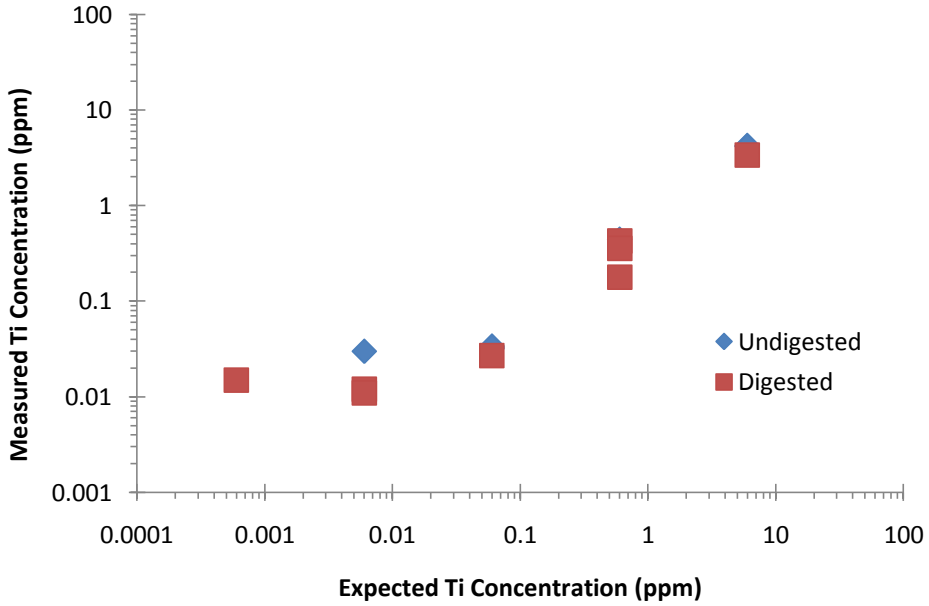

Figure E.6. TiO_2 analyzed by ICP-MS in a moderately hard water matrix.

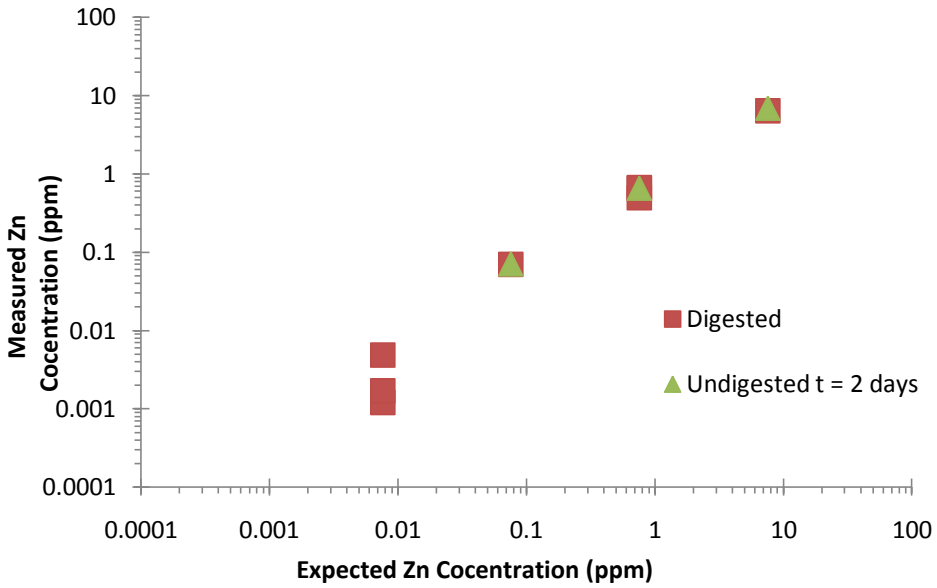

Figure E.7. ZnO analyzed by ICP-OES in a moderately hard water matrix**.**

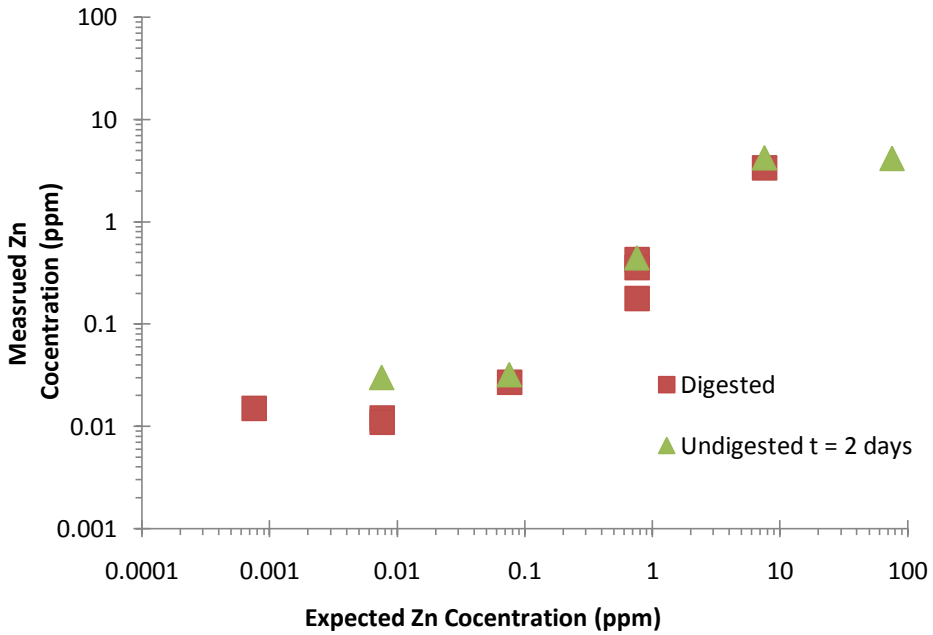

Figure E.8. ZnO analyzed by ICP-MS in a moderately hard water matrix**.**

E.9.1 Moderately Hard Summary

The analysis of TiO_2 in moderately hard water showed less of a need for digestion when compared to nanopure water. This could be because aggregates were more likely to form in nanopure than in the moderately hard water. If the aggregation was less in the moderately hard water then the sample might be fully ionized in the plasma even without digestion. A similar trend was observed to the nanopure water that the digestion technique caused false high readings for the most dilute samples.

Like the nanopure matrix, digestion seems to be less necessary for the ZnO in moderately hard water. The one exception this time was that the most concentrated sample had a much lower recovery than expected on the ICP-MS. When the ZnO samples were analyzed by ICP-MS there appeared to be an interference for the two most dilute samples. Because the higher measured concentrations were observed for both the digested and undigested samples, the interference was probably caused by the matrix effect of the moderately hard water or the moderately hard water and the sulfuric acid rather than just the sulfuric acid.

E.10 Nitric/Sulfuric Acid Digestion of TiO_2 and ZnO in Synthetic Urine

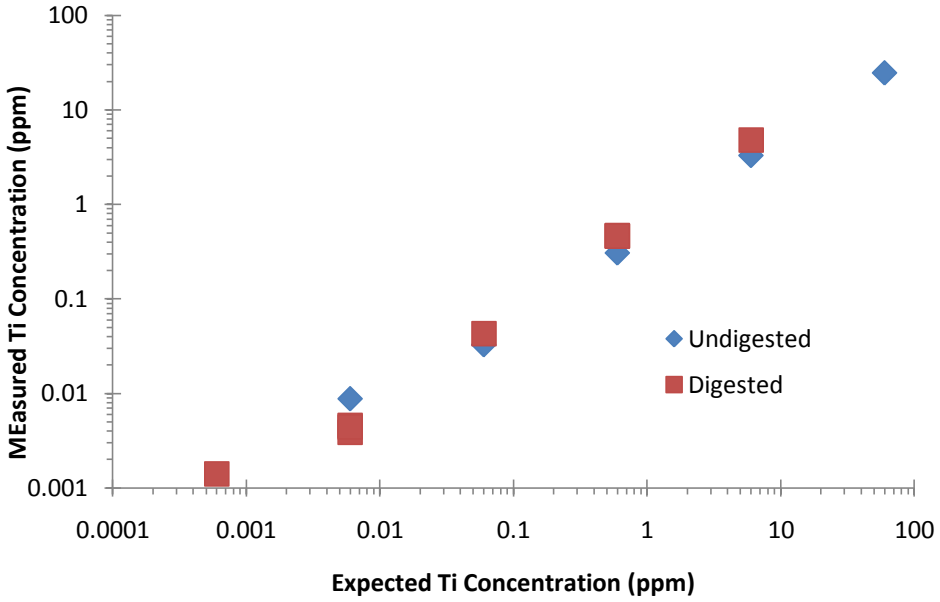

Figure E.9. TiO_2 analyzed by ICP-OES in a synthetic urine matrix.

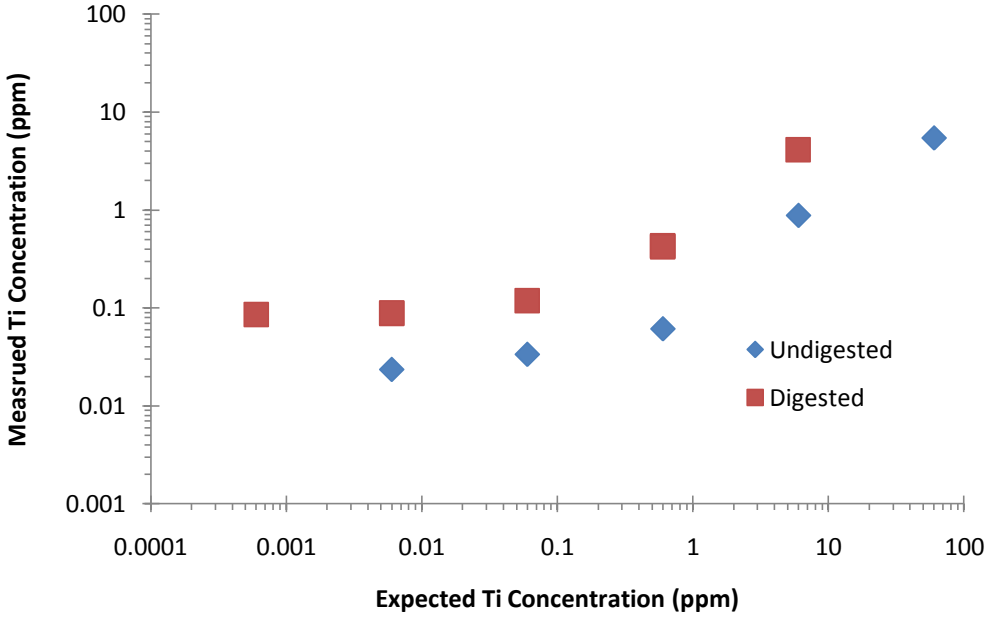

Figure E.10. TiO_2 analyzed by ICP-MS in a synthetic urine matrix.

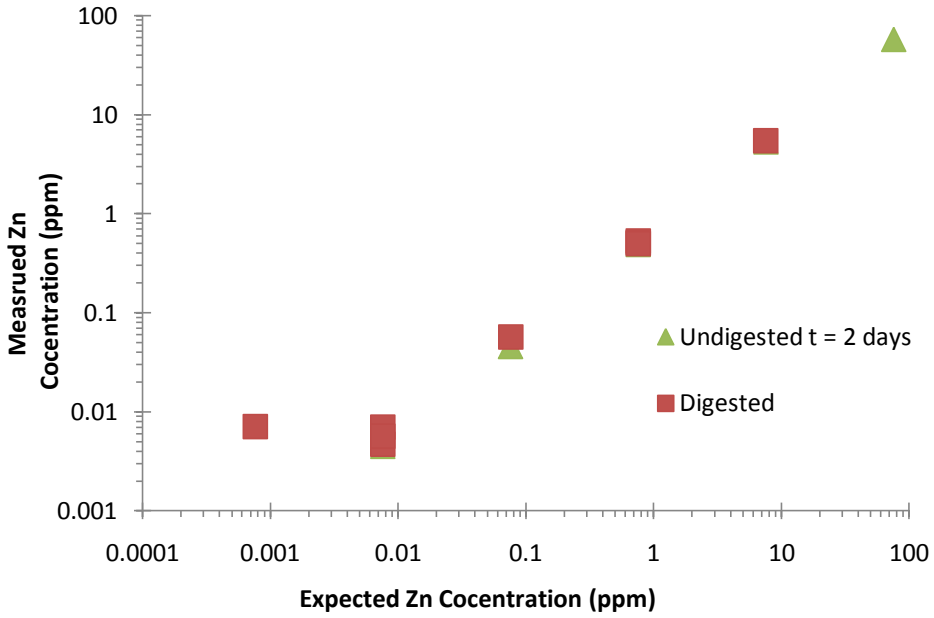

Figure E.11. ZnO analyzed by ICP-OES in a synthetic urine matrix.

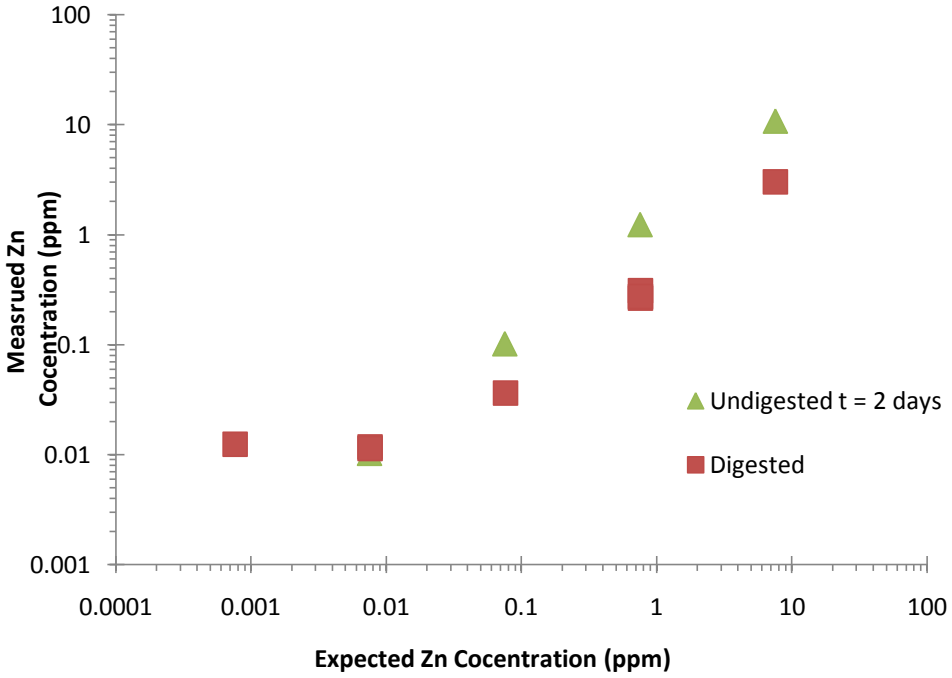

Figure E.12. ZnO analyzed by ICP-MS in a synthetic urine matrix.

E.10.1 Synthetic Urine Summary

The analysis of TiO_2 using ICP-OES again showed that digestion may not be necessary, the measured concentrations were similar and near the expected concentration. Surprisingly, the most dilute samples did not have a noticeable interference from the acid digestion matrix. This could be because the sulfate from the acid interacted with something in the synthetic urine and fell out of solution. When using ICP-MS it is apparent that digestion is needed to get an accurate measurement of more concentrated samples. However, for more dilute samples, both digested and undigested samples were measured higher than expected, with the digested samples more so. This is probably because both the synthetic urine and sulfuric acid matrix are causing interferences.

During analysis of ZnO the digested and undigested samples were in good agreement when analyzed by ICP-OES and the undigested samples had a higher measured concentration than the digested samples. The most dilute digested sample measured higher than expected on the ICP-OES cause of the sulfuric acid matrix. The two most dilute samples (digested and undigested) were higher than expected likely because of interferences with the Zn mass isotope from the synthetic urine matrix.

E.11 Detection Limit Summary

Digestion is not necessary for ZnO solutions unless at high concentrations. However, digestion is necessary for TiO_2 solutions

especially if analysis is being completed by ICP-MS which has lower detection limits. The sulfuric acid matrix of the digested caused interferences at lower concentrations. This was especially apparent when analysis was carried out by ICP-MS. A different digestion method could minimize the interferences for both instruments. However, there were interferences that arose from the moderately hard water and synthetic urine matrix even without any digestion. These interferences cause a higher reading than the actual concentration. Thus, it is important for any complex matrix to digest blanks in order to understand what interferences may arise.